Memoir of the Fukui Prefectural Dinosaur Museum 24: 41–76 (2025)

ARTICLE

ZIRCON U–PB DATING OF THE ASUWA GROUP, SUGO FORMATION, AND HINOSAN MESOZOIC FORMATION IN FUKUI PREFECTURE, CENTRAL JAPAN

Sachiho KOIZUMI[1, 2] and Shigeru OTOH[3*]

[1]Graduate School of Science and Engineering, University of Toyama, 3190 Gofuku, Toyama 930-8555, Japan
[2]Fukui Prefectural Dinosaur Museum, 51-11 Terao, Muroko, Katsuyama, Fukui 911-8601, Japan
[3]Faculty of Sustainable Design, Academic Assembly, University of Toyama, 3190 Gofuku, Toyama 930-8555, Japan
*Present Address: Sanwa Boring Co. Ltd., 464-2 Horikawa-machi, Toyama 939-8072, Japan

ABSTRACT

We conducted zircon U–Pb dating of the Asuwa Group, which contains Late Cretaceous plant and pollen fossils, as well as the age-unknown Sugo Formation and Hinosan Mesozoic Formation in Fukui Prefecture, central Japan. For each sample, we identified the youngest date cluster consisting of three or more $^{206}Pb/^{238}U$ dates that overlap within 2σ uncertainty and conservatively used its weighted mean of this cluster (YC2σ) to constrain the depositional age. The results are as follows: (1) A sample of felsic welded tuff (DS08) from the Doai Tuff Member, which constitutes the lower part of the Asuwa Formation within the Asuwa Group, yielded a probable formation age of 71.8 ± 0.87 Ma (2σ). (2) Two sandstone samples (DS102-1 and DS20) from the Sarao Alternation Member of the upper Asuwa Formation yielded maximum depositional dates (MDDs) of 70.20 ± 0.74 Ma and 69.05 ± 0.66 Ma, respectively. (3) A sandstone sample (KM01) from the Subara Formation, which is included in the Asuwa Formation, yielded an MDD of 68.32 ± 0.81 Ma. (4) Two sandstone samples (UM01-2 and SG05) from the Sugo Formation yielded MDDs of 174.7 ± 2.7 Ma and 109.3 ± 1.7 Ma, respectively. (5) A sample (KD01) from the undated Hinosan Mesozoic Formation yielded an MDD of 162.7 ± 2.6 Ma. By integrating these results with previous studies on fossils and the overlying strata, we interpret that most of the Asuwa Formation corresponds to the Maastrichtian Stage of the Upper Cretaceous, whereas part of the Sugo Formation correlates with the Lower Cretaceous Albian to the Upper Cretaceous Maastrichtian.

Key words: Cretaceous, Maastrichtian, zircon, U–Pb dating, LA-ICPMS, Asuwa Formation, Sugo Formation, central Japan

小泉早千穂・大藤　茂（2025）中部日本，福井県に分布する足羽層群，菅生層，および日野山中生層のジルコン U–Pb 年代測定．福井県立恐竜博物館紀要 24: 41–76.

中部日本，福井県に分布する上部白亜系を含む足羽層群，時代未詳の菅生層および日野山中生層のジルコン U–Pb 年代測定を実施した．各試料について，得られた $^{206}Pb/^{238}U$ 年代から互いの不確かさ 2σ の範囲が重なる 3 つ以上の年代からなる最も若い年代集団を選び出し，その加重平均から保守的に堆積年代を拘束した：(1) 足羽層群足羽層下部，土合凝灰岩部層の珪長質凝灰岩（試料 DS08）の形成年代は 71.8 ± 0.87 Ma．(2) 足羽層上部，皿尾互層部層の砂岩 2 試料（DS102-1 と DS20）の堆積年代上限値（MDD）は，それぞれ 70.20 ± 0.74 Ma（2σ）と 69.05 ± 0.66 Ma．(3) 足羽層群巣原層の砂岩試料（KM01）の MDD は 68.32 ± 0.81 Ma．(4) 菅生層の砂岩 2 試料（UM01-2 と SG05）の MDD は 174.7 ± 2.7 Ma と 109.3 ± 1.7 Ma．(5) 時代未詳の日野山中生層（KD01）の MDD は 162.7 ± 2.6 Ma であった．先行研究による産出化石や被覆層の情報を総合すると，足羽層の大部分は上部白亜系 Maastrichtian 階に，菅生層の一部は下部白亜系アルビアン階～上部白亜系 Maastrichtian 階に対比される．

INTRODUCTION

The Sea of Japan side of central Japan is divided into several geologic belts, including the Hida Belt, Hida Gaien Belt, Renge Belt, Akiyoshi Belt, Maizuru Belt, Ultra-Tamba Belt, and Mino Belt (e.g., Moreno et al., 2016). In the Reihoku district of Fukui Prefecture, which is the focus of this study (Fig. 1A), rocks representative of the Hida, Hida Gaien, Renge, Ultra-Tamba, and Mino Belts are exposed. In addition, Cretaceous and younger strata and rocks occur across these belts. Among these, fossiliferous Paleozoic to Triassic strata of the Hida Gaien Belt (e.g., Tsukada et al., 1997), the Permian accretionary complex of the Higashimata Formation in the Ultra-Tamba Belt (Umeda et al., 1996; Nakae, 2012), and the Kuzuryu and Tetori Groups

Received July 4, 2025. Accepted September 25, 2025.
Corresponding author—Sachiho KOIZUMI
E-mail: s-koizumi@dinosaur.pref.fukui.jp

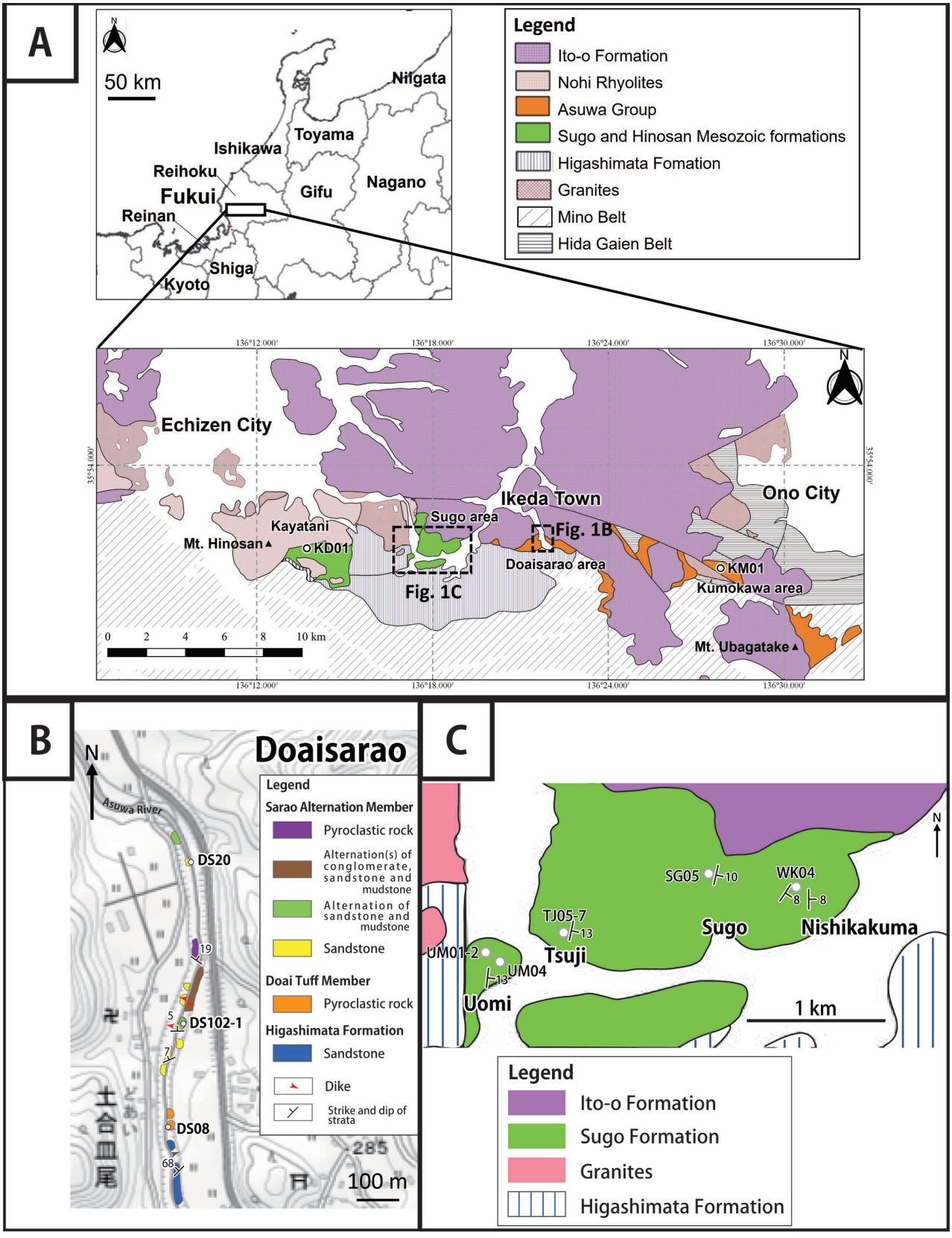

FIGURE 1. **A**, Geological map of the southern part of the Reihoku district in Fukui Prefecture modified from Geological Map of Gifu (Wakita et al., 1992). **B**, Route map in the Doaisarao area along Asuwa River. **C**, Sampling spots in the Sugo area.

distributed across the Hida and Hida Gaien Belts (e.g., Maeda, 1961; Yamada and Sano, 2018) have been extensively studied. In addition, felsic volcanic and volcaniclastic rocks dated to around 70 Ma, which are widespread from the Hida to the Mino Belts (e.g., Tanase et al., 2007; Hoshi et al., 2016), as well as Paleogene to Neogene strata related to the opening of the Sea of Japan (e.g., Kano et al., 2007), have also been the subject of numerous studies.

The Lower Cretaceous Tetori Group, which is widely exposed in the eastern Reihoku district, has been extensively studied in terms of stratigraphy, paleontology of intercalated marine beds, and geochronology (Maeda, 1961; Sano, 2015; Nagata et al., 2018; Sakai et al., 2018; Yamada and Sano, 2018). In particular, geochronological studies have constrained the maximum depositional age of the Itsuki Formation (Kawagoe et al., 2012) and dated the overlying Hayashidani Andesite to 109.3 ± 1.7 Ma (Nagata et al., 2018). The age of the Hayashidani Andesite is consistent with the age of garnet-bearing dacite (109.2 ± 0.8 Ma), from the Oyashirazu Formation in the Tomari area of Toyama Prefecture (Takeuchi et al., 2017), indicating vigorous igneous activity across the Hokuriku region toward the end of the Early Cretaceous. However, the recent synthesis of Cretaceous to Paleogene igneous activity in Japan by Yamaoka and Wallis (2023) does not discuss Early Cretaceous igneous activity in the Hokuriku region.

On the other hand, in central Japan, felsic pyroclastic rocks and volcanic rocks dating to around 70 Ma are widely distributed, indicating that magmatic activity was extremely vigorous at the end of the Cretaceous (e.g., Hoshi et al., 2016; Kaneko et al., 2019). These correspond to Nohi Rhyolites (*sensu stricto*) and Okumino Acid Igneous Complex (e.g., Tanase et al., 2007) and are collectively referred to as Nohi Rhyolites (*sensu lato*) in this paper. Hoshi et al. (2016) proposed that the Nohi Rhyolites (*s.s.*) formed rapidly at around 70 Ma, constituting one of the largest caldera-forming volcanic complexes on Earth. Fukui Prefecture, part of central Japan, also preserves records of volcanic activity around 70 million years ago. Specifically, in the eastern part of northeastern Fukui Prefecture (the Reihoku region), the Nohi Rhyolites (*s.l.*) are widely distributed, while in the southern part, the distribution is more limited and scattered. Contemporaneous Late Cretaceous clastic strata containing volcanic components of this age are also recognized. The Futomiyama Group in Toyama Prefecture (Kaneko et al., 2019) and the Oamamiyama Group in northern Gifu Prefecture (Nagata et al., 2025) are examples.

The Asuwa Group, which is sporadically distributed in the Reihoku district (e.g., Kawai, 1964), consists of strata intercalated with felsic pyroclastic and volcanic rocks. The name "Asuwa" originates from the Asuwa River, which flows through the type locality, the Doaisarao area, located in central Ikeda Town. The Asuwa Formation in the Doaisarao area (Tsukano and Miura, 1959), the Heikedake, Ubagatake, and Subara Formations in Ono City in the southeastern Reihoku district (Kobayashi, 1954; Kawai, 1956), and their correlatives are collectively referred to as the Asuwa Group (e.g., Kawai, 1964; Tsukano, 1969). Despite abundant exposures, the age of the Asuwa Group has thus far been constrained only by fossil evidence from the Asuwa Formation (Sazawa et al., 2020), and no numerical age determinations have been reported.

In the western Reihoku district, other Mesozoic strata besides the Asuwa Group are also sporadically distributed. For example, approximately 2 km west of the Doaisarao area, the Sugo Formation (Omura, 1972) unconformably overlies the Permian accretionary complex of the Higashimata Formation (Umeda et al., 1996; Nakae, 2012) and is itself unconformably overlain by felsic pyroclastic rocks. In addition, in the eastern part of Mt. Hinosan, sedimentary rocks intercalated with felsic pyroclastic rocks unconformably overlie the Higashimata Formation; in this study, we refer to these strata as the Hinosan Mesozoic Formation. These strata have been previously correlated with a part of the Tetori Group (Tsukano, 1969), or with the Asuwa Group or the Asuwa Formation (e.g., Wakita et al., 1992), but no definitive evidence has been presented to support these correlations.

Against this background, this study aims to constrain the depositional ages and stratigraphic affinities of the Asuwa Group, Sugo Formation and Hinosan Mesozoic Formation through zircon U–Pb geochronology and lithofacies analysis, thereby contributing to a better understanding of the Mesozoic geologic history of central Japan.

GEOLOGIC SETTING

The Asuwa Group

The Asuwa Group occurs sporadically in several small areas in the Reihoku district. Late Cretaceous plant fossils were first reported from the Doaisarao area in Ikeda Town, the type locality (Fig. 1A), by Matsuo and Kida (1953), who named the fossil assemblage the Asuwa Flora. Subsequent studies revealed that fossils such as *Nelumbium orientalis* from the Asuwa Flora are Late Cretaceous in age and indicate freshwater environments (e.g., Matsuo, 1954, 1962, 1970). Matsuo (1954) also proposed the term Asuwa Group for the strata containing this flora. In addition to the Asuwa Formation at the type locality, the following strata are included in the Asuwa Group (e.g., Kawai, 1964; Tsukano, 1969): (1) the Subara, Ubagatake, Saruzuka Conglomerate, and Heikedake Formations, which are distributed sequentially from east to west in Ono City, east of the Doaisarao area; and (2) the Iritani Alternation and the Mobara Formation, which are distributed from east to west in Echizen City, west of the Doaisarao area (Tsukano, 1969). Based on plant fossils and stratigraphic relationships with surrounding units, the Asuwa Group is considered to belong to the Upper Cretaceous. However, detailed lithological descriptions and numerical age constraints have not yet been published. In this study, we focus on the Asuwa and Subara Formations.

The Asuwa Formation

The Asuwa Formation in the Doaisarao area overlies the Permian Higashimata Formation of the Ultra-Tamba Belt (e.g., Omura, 1972; Umeda et al. 1996), and is overlain by the Miocene Ito-o Formation consisting of andesitic rocks (e.g., Nakajima et al., 1990). The Asuwa Formation is well exposed along the Asuwa River in the Doaisarao area. However, due to the lack of suitable outcrops, the boundary between the Higashimata and Asuwa Formations is poorly exposed. The contact likely represents either an unconformity or a fault, as suggested by the marked difference in dip angles. The Higashimata Formation dips steeply (68°–78°), while the Asuwa Formation dips gently to moderately (5°–19°), both with an approximately E–W strike.

The Asuwa Formation is divided into two members, the Doai Tuff and the Sarao Alternation Members in ascending order (Tsukano and Miura, 1959). The Doai Tuff Member is approximately 30 m thick and mainly consists of felsic pyroclastic rocks containing coarse quartz grains approximately 5–8 mm in diameter. The Sarao Alternation Member is 170 m thick at the type locality and comprises, in ascending order: (1) alternating layers of grayish very fine sandstone to siltstone and yellowish coarse sandstone to fine conglomerate and (2) fine sandstone with grayish tuff intruded by rhyolitic dikes. Some very fine sandstones are parallelly laminated. The conglomerate is matrix-supported and contains subangular clasts. Some coarse sandstone layers exhibit current ripples. Sazawa et al. (2020) reported Maastrichtian pollen fossils from mudstone in the Sarao Alternation Member.

The Subara Formation

The Subara Formation is distributed in the Kumokawa area in western Ono City, where it is bounded by faults against Paleozoic strata of the Hida Gaien Belt to the north and south. It yields Late Cretaceous specimens of the Asuwa Flora (e.g., *Osmunda asuwensis*) and is considered part of the Asuwa Group (Tsukano, 1969). The formation consists mainly of sandstone, siltstone, conglomerate, and tuff, and dips 10°–20° to the southwest. The sandstone is reddish-gray, medium to coarse grained, poorly sorted, and contains very fine gravels. The conglomerate is matrix-supported and includes well-rounded pebbles of rhyolite and chert.

The Sugo Formation

The Sugo Formation (Omura, 1972) is a sedimentary unit distributed in the Sugo area of western Ikeda Town (Fig. 1A, 1C). According to the geological map by Hattori (2012), the Sugo Formation apparently overlies the Higashimata Formation along either a fault contact or an unconformity. At the eastern margin of its distribution, in the Sadakata area, the Sugo Formation is reported to be conformably overlain by strata of the Asuwa Group (Omura, 1972). Omura (1972) noted that the Sugo Formation differs from the Asuwa Group in the characteristics of its clasts and matrix. Hattori (2012) suggested that although the Sugo Formation is lithologically similar to the Subara Formation of the Asuwa Group, it differs in several aspects from the Sarao Alternation Member.

The Sugo Formation generally strikes N–S and dips eastward at moderate angles (8°–20°), indicating that the eastern layers are stratigraphically higher. It consists of sandstone, siltstone, shale, conglomerate, and their interbeds. The sandstone is typically dark brown or beige, well sorted, medium grained, and contains fine rounded pebbles. The siltstone is greenish gray, and the shale is beige; these frequently form alternating sequences with sandstone or conglomerate. The conglomerate is mainly matrix-supported and contains angular clasts of chert, siltstone, and sandstone. In Nishikakuma in the Sugo area (Fig. 1C), outcrops of reddish very fine bedded sandstone in the upper part of the Sugo Formation are observed, with the thickness ranging from 10 to 30 cm. Fragmentary plant fossils have been recovered from the siltstone, but none are suitable for precise age determination.

The Hinosan Mesozoic Formation

In the eastern part of Mt. Hinosan, sedimentary strata are exposed that lie stratigraphically between the Upper Permian and Upper Cretaceous. Omura (1972) divided the non-Paleozoic strata of Mt. Hinosan into two units: the Kayatani Formation, distributed in a small area centered around Kayatani, and the Hino-San Formation, distributed along the hiking trail from Nakahirabuki to the summit of Mt. Hinosan. The Kayatani Formation unconformably overlies the Higashimata Formation of the Ultra-Tamba Belt and is itself unconformably overlain by the Nohi Rhyolites (*s.l.*) (Fig. 1A). According to Omura (1972), the Kayatani Formation consists mainly of white granular acidic tuff, along with tuffaceous sandstone and shale.

In this study, we collectively refer to the Hinosan Formation and the Kayatani Formation, which unconformably overlie Paleozoic strata, as the “Hinosan Mesozoic Formation.” We collected an ivory-colored siltstone sample (Sample KD01 described later) from the Kayatani area. We identified only one exposure of the Hinosan Mesozoic Formation during this study. Although its lithology does not closely match previous descriptions of the Kayatani Formation, the exposure lies within the mapped distribution of that formation (Omura, 1972). We therefore consider sample KD01 to be representative of the Hinosan Mesozoic Formation.

SAMPLE DESCRIPTIONS

We studied the following ten samples: (1) one tuff sample from the Doai Tuff Member (DS08), (2) two sandstone samples from the Sarao Alternation Member (DS102-1, DS20), (3) one sandstone sample from the Subara Formation (KM01), (4) five sandstone samples from the Sugo Formation (UM01-2, UM04, TJ05-7, SG05, WK04), and (5) one siltstone sample from the Hinosan Mesozoic Formation (KD01). Additionally,

TABLE 1. The data of modal composition of the sandstones.

Formation	Area	Sample No.	Modal composition (vol.%)				Ratio excluding matrix (vol.%)			Rock type
			Quartz	Feldspar	Rock fragments	Matrix	Quartz	Feldspar	Rock fragments	
Sarao A. M.	Doaisarao	DS20	36.6	8.9	38.6	16.0	43.5	10.6	45.9	lithic wacke
		DS102-1	25.0	7.4	52.2	15.4	29.6	8.7	61.7	lithic wacke
Subara F.	Kumokawa	KM01	33.4	3.2	39.0	24.4	44.2	4.2	51.6	lithic wacke
Sugo F.	Nishikakuma	WK04	42.2	22.2	23.8	11.8	47.8	25.2	27.0	lithic arenite
	Sugo	SG05	41.4	11.0	25.8	21.8	52.9	14.1	33.0	lithic wacke
	Tsuji	TJ05-7	50.2	25.0	17.2	7.6	54.3	27.1	18.6	feldspathic arenite
	Uomi	UM01-2	40.1	23.2	28.4	8.3	43.7	25.3	31.0	lithic arenite
		UM04	44.6	26.0	26.8	2.6	45.8	26.7	27.5	lithic arenite
Hinosan Meso. F.	Mt. Hinosan	KD01(silt.)	25.0	17.4	45.2	12.4	28.5	19.9	51.6	lithic

we determined the modal composition of the sandstone samples using a petrographic microscope and an automatic point counter. We counted five hundred points per thin section for each sandstone sample to calculate the percentages of quartz, feldspar, rock fragments, and matrix (Table 1). The sandstone samples were classified into rock facies by the ratios of quartz, feldspar, and rock fragments based on Okada (1968, 1971) (Fig. 3). Furthermore, we separated zircons from samples DS08, DS102-1, DS20, KM01, UM01-2, SG05, and KD01, and conducted U–Pb dating. The methodology and results of the U–Pb dating are described in the following sections.

The Asuwa Formation

Felsic weakly-welded lapilli tuff from the Doai Tuff Member (Sample DS08; 35° 51'48.15'' N 136° 21'41.52'' E; Fig. 2A)

Sample DS08 was collected from the basal part of the Doai Tuff Member in an outcrop along the Asuwa River in the Doaisarao area. The sample is white to yellow felsic weakly-welded lapilli tuff containing coarse β-quartz grains. It consists of quartz, feldspar, opaque minerals, and alteration minerals such as chlorite as well as fragments of “chert” (microcrystalline quartz aggregate) and volcanic ejecta such as devitrified pumice.

Sandstone of the lower part of the Sarao Alternation Member (Sample DS102-1; 35° 51'55.19'' N, 136° 21'43.00'' E; Fig. 2B)

Sample DS102-1 was collected from an outcrop of alternating layers of very fine and coarse sandstone along the Asuwa River in the Doaisarao area. The sandstone is gray, very fine grained, poorly sorted, and subangular lithic wacke, consisting of quartz (25.0%), feldspar (7.4%), rock fragments (52.2%), and matrix (15.4%). The rock fragments are mostly volcanic rocks such as andesite and mudstone, with chert.

Sandstone of the upper part of the Sarao Alternation Member (Sample DS20; 35° 52'06.21'' N, 136° 21'43.15'' E; Fig. 2C)

Sample DS20 was collected from an outcrop of fine to medium grained sandstone along the Asuwa River in the Doaisarao area, located approximately 70 m above the sampling horizon of DS102-1. The sandstone is yellowish white, medium grained, poorly sorted, and subangular lithic wacke consisting of quartz (36.6%), feldspar (8.9%), rock fragments (38.6%), and matrix (16.0%). The rock fragments are mostly andesite and mudstone, with chert.

The Subara Formation

Sandstone of the Subara Formation (Sample KM01; 35° 51'06.97'' N, 136° 27'48.40'' E; Fig. 2D)

A sandstone sample, KM01, was collected from an outcrop of alternating layers of very fine sandstone, coarse sandstone, and conglomerate along the Mana River in the Kumokawa area, Ono City. The sandstone is reddish-gray, medium to coarse grained, poorly sorted, and subangular lithic wacke consisting of quartz (33.4%), feldspar (3.2%), rock fragments (39.0%), and matrix (24.4%). The rock fragments are mostly andesite, chert, and shale that contains parallel-aligned mica.

The Sugo Formation

Sandstone of the lower part of the Sugo Formation at Uomi in the Sugo area (Sample UM01-2; 35° 51'35.20'' N, 136° 17'11.91'' E; Fig. 2E)

A sandstone sample, UM01-2, was collected from an outcrop of alternating layers of medium-grained sandstone, conglomerate-bearing sandstone, conglomerate, and siltstone along a forest road in the Uomi area, Ikeda Town. This sandstone is white, medium grained, poorly sorted, and subangular lithic arenite consisting of quartz (40.1%), feldspar (23.2%), rock fragments (28.4%), and matrix (8.3%). The rock fragments are mostly andesite, chert, and mudstone.

Sandstone of the lower part of the Sugo Formation at Uomi in the Sugo area (Sample UM04; 35° 51'31.29'' N, 136° 17'17.05'' E; Fig. 2F)

A sandstone sample, UM04, was collected from an outcrop of alternating layers of medium-grained sandstone and siltstone along a forest road in the Uomi area, located approximately 25 m above the sampling horizon of UM01-2. The sandstone is brown, medium grained, moderately sorted, and subangular

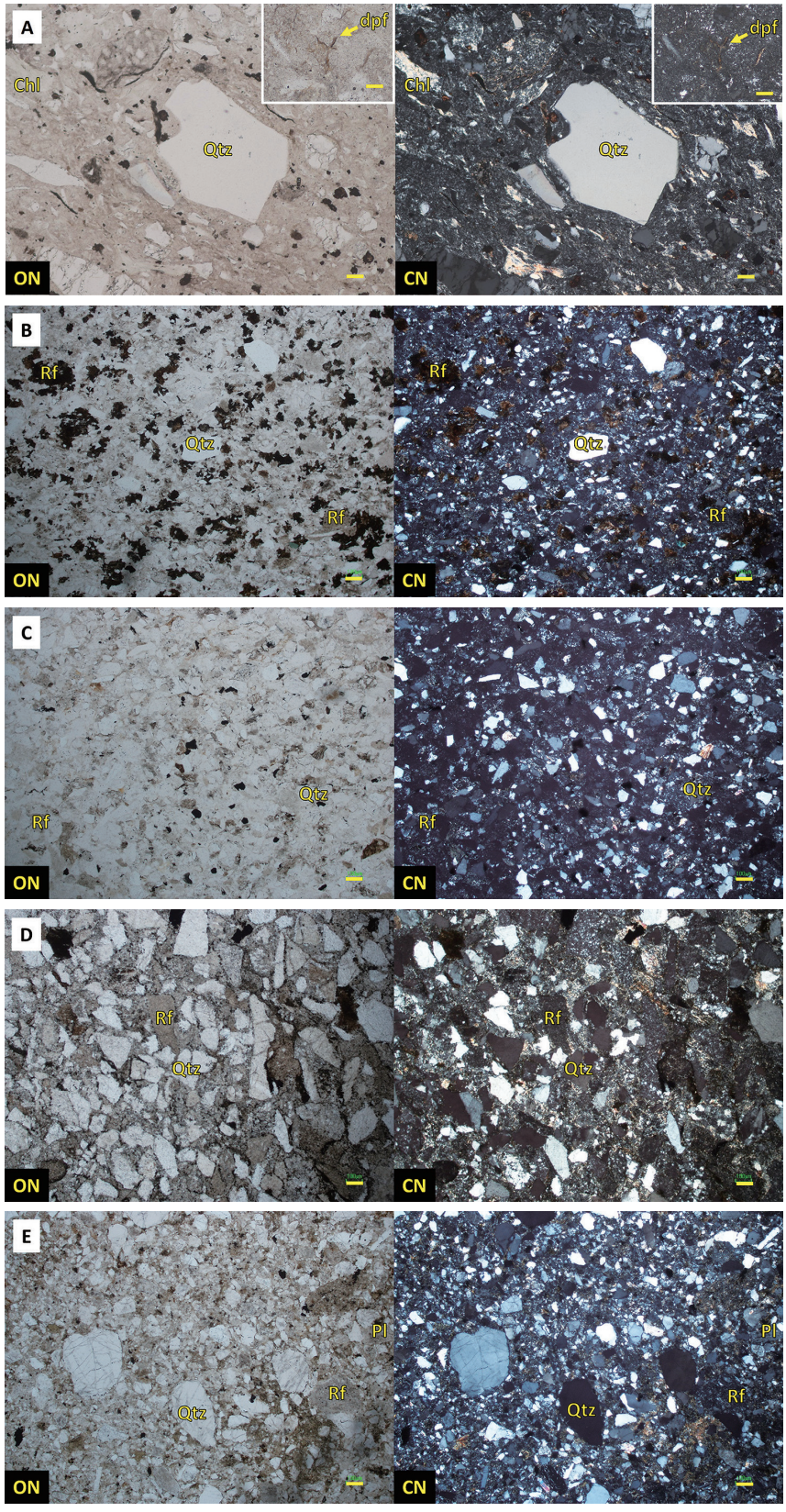

FIGURE 2. Photomicrographs of studied samples (yellow scale bar = 100 μm). **A**, Felsic tuff of the Doai Tuff Member (sample DS08). **B**, Very fine sandstone of the lower part of the Sarao Alternation Member (sample DS102-1). **C**, Medium sandstone of the upper part of the Sarao Alternation Member (sample DS20). **D**, Coarse sandstone of the Subara Formation (sample KM01). **E**, Fine to very fine sandstone of the lower part of the Sugo Formation (sample UM01-2).

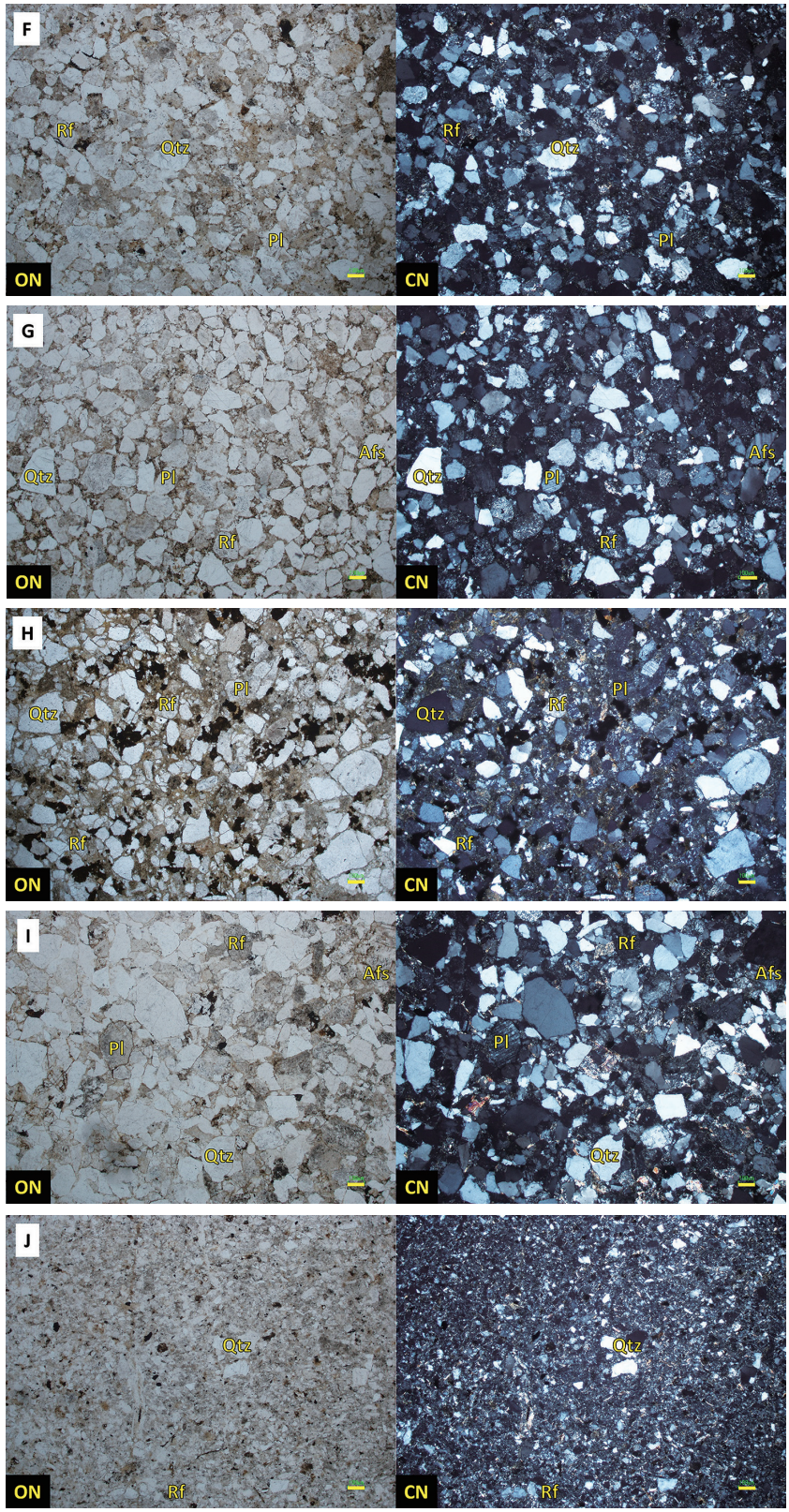

F, Fine sandstone of the lower part of the Sugo Formation (sample UM04). **G**, Medium sandstone of the lower part of the Sugo Formation (sample TJ05-7). **H**, Medium sandstone of the upper part of the Sugo Formation (sample SG05). **I**, Medium sandstone of the upper part of the Sugo Formation (sample WK04). **J**, Siltstone of the Hinosan Mesozoic Formation (sample KD01). Qtz: quartz, Pl: plagioclase, Afs: alkali feldspar, Rf: rock fragments, Chl: chlorite, dpf: devitrified pumice fragments.

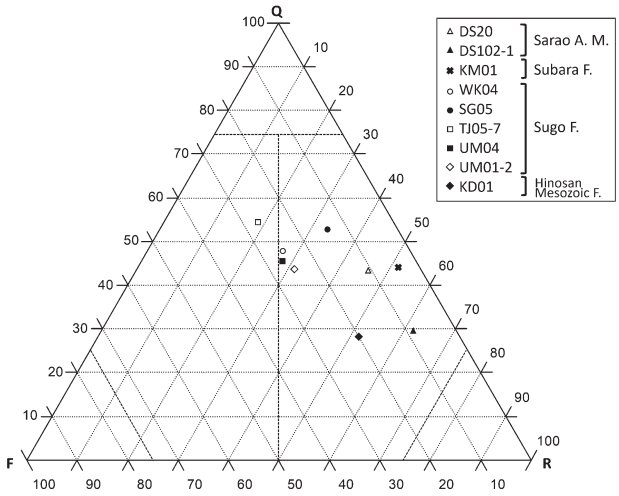

FIGURE 3. QFR diagram showing the grain compositions of sandstone and siltstone samples from the Sarao Alternation Member (sample DS102-1, DS20), the Subara Formation (sample KM01), and the Sugo Formation (sample UM01-2, UM04, TJ05-7, SG05, WK04). Q: quartz, F: feldspar, R: rock fragments.

lithic arenite consisting of quartz (44.6%), feldspar (26.0%), rock fragments (26.8%), and matrix (2.6%). The rock fragments are mostly andesite, chert, and mudstone.

Sandstone of the lower part of the Sugo Formation at Tsuji in the Sugo area (Sample TJ05-7; 35° 51'33.89'' N, 136° 17'30.16'' E; Fig. 2G)

A sandstone sample, TJ05-7, was collected from an outcrop of alternating layers of medium-grained sandstone, conglomerate, and siltstone along a forest road in the Tsuji area, about 100 m to the east of the Uomi area. The sandstone is brown, medium grained, moderately sorted, and subangular feldspathic arenite consisting of quartz (50.2%), feldspar (25.0%), rock fragments (17.2%), and matrix (7.6%). The rock fragments are mostly andesite.

Sandstone of the upper part of the Sugo Formation in the Sugo area (Sample SG05; 35° 51'50.78'' N, 136° 18'14.25'' E; Fig. 2H)

Sample SG05 was collected from an outcrop of medium-grained sandstone containing fine conglomerate and siltstone along a forest road in the Sugo area, about 1 km to the east of the Tsuji area. The sandstone, containing fine conglomerate, is beige, medium grained, poorly sorted, and subangular to sub-rounded lithic arenite consisting of quartz (41.4%), feldspar (11.0%), rock fragments (25.8%), and matrix (21.8%). The rock fragments are andesite, chert, and mudstone.

Sandstone of the upper part of the Sugo Formation at Nishikakuma in the Sugo area (Sample WK04; 35° 51'55.10'' N, 136° 18'42.23'' E; Fig. 2I)

Sample WK04 was collected from an outcrop of medium-grained sandstone containing fine conglomerate and siltstone along a forest road in the Nishikakuma area, about 500 m to the east of the Sugo area. The sandstone, containing fine conglomerate, is beige, medium grained, moderately sorted, and sub-rounded lithic arenite consisting of quartz (42.2%), feldspar (22.2%), rock fragments (23.8%), and matrix (11.8%). The rock fragments are mostly andesite, rhyolite, and chert.

The Hinosan Mesozoic Formation

Siltstone of the Hinosan Mesozoic Formation (Sample KD01; 35° 51'42.36'' N, 136° 13'41.09'' E; Fig. 2J)

Sample KD01 was collected from an outcrop in the riverbed of a stream in the Kayatani area of the northeast foot of Mt. Hinosan. This siltstone is ivory, poorly sorted, subangular, and lithic siltstone consisting of quartz (25.0%), feldspar (17.4%), rock fragments (45.2%), and matrix (12.4%). The rock fragments are mostly andesite and mudstone.

ANALYTICAL METHOD

The zircon samples for analyses were prepared following the procedures described in Kawagoe et al. (2012) and Nagata et al. (2018). The measurements were carried out using laser ablation inductively coupled plasma mass spectrometry (LA-ICPMS) installed at the Graduate School of Environmental Studies, Nagoya University. The ICPMS instrument was an Agilent 7700x quadrupole-based system connected to a New Wave Research NWR-213-type LA system, which used a frequency quintupled Nd:YAG laser with a 213-nm wavelength. The measurement conditions, optimized to reduce matrix effects, were as follows: energy density of 5.7 J/cm^2, repetition rate of 10 Hz, pre-ablation time of 8 s, ablation time of 10 s, and the ablation pit size of 25 μm (Kouchi et al., 2015). The analyses were carried out in peak-jumping mode, and the peaks of the following isotopes were monitored: ^{202}Hg, ^{204}(Hg+Pb), ^{206}Pb, ^{207}Pb, ^{232}Th, and ^{238}U. Data were acquired in a sequence of 28 analyses, consisting of 5 gas blank measurements, 4 analyses of the NIST (National Institute of Standards and Technology, U.S.A.) SRM 610 glass standard (recommended ^{206}Pb/^{238}U value of 0.2236), one analysis of the Nancy 91500 zircon (^{206}Pb/^{238}U age of 1062.4 ± 0.8 Ma; 2σ: Wiedenbeck et al., 1995), one analysis of OD-3 (^{206}Pb/^{238}U age of 33.04 ± 0.1 Ma; 2σ: Iwano et al., 2013), 8 analyses of unknown zircons, 4 analyses of SRM 610 standard, and 5 gas blank measurements.

After the analyses, we rejected the following analytical data: (1) data from spots containing inclusions or cracks, (2) data from zircon grains that moved during laser ablation, and (3) data with common lead (^{206}PbC; Stacey and Kramers, 1975) content of 5% or more. We plotted all the remaining data on a concordia diagram using Isoplot 4.15 (Ludwig, 2012). We subsequently chose concordant spots, defined as those whose 2σ uncertainty ellipse derived from ^{206}Pb/ ^{238}U and ^{207}Pb/ ^{235}U data sets overlaps the concordia curve, and adopted the ^{206}Pb/ ^{238}U ages from the concordant data sets for the following discussion. The age assignments to the geologic time scale in this study follow Cohen et al. (2024).

TABLE 2. U–Pb isotopes and dates of zircons from sample DS08. Abbreviations: C: concordant data, D: discordant data.

Spot No.	Th/U	$^{207}Pb/^{206}Pb$	Uncertainty 2SD	$^{207}Pb/^{235}U$	Uncertainty 2SD	$^{206}Pb/^{238}U$	Uncertainty 2SD	^{206}Pb–^{207}Pb (Ma)	Uncertainty 2SD	^{235}U–^{207}Pb (Ma)	Uncertainty 2SD	^{238}U–^{206}Pb (Ma)	Uncertainty 2SD	Memo
DS08-01	0.84	0.0591	0.0131	0.0914	0.0209	0.01122	0.00060			88.8	20.3	71.9	3.9	C
DS08-02	0.65	0.0525	0.0125	0.0848	0.0208	0.01171	0.00063			82.7	20.2	75.1	4.0	C
DS08-03	1.07	0.0543	0.0071	0.0845	0.0114	0.01127	0.00040			82.3	11.2	72.3	2.5	C
DS08-04	0.57	0.0506	0.0125	0.0782	0.0199	0.01122	0.00061			76.5	19.4	71.9	3.9	C
DS08-05	0.85	0.1858	0.0224	0.3753	0.0491	0.01465	0.00075			323.6	42.3	93.8	4.8	D
DS08-06	0.73	0.0282	0.0069	0.0829	0.0207	0.02134	0.00106			80.9	20.1	136.1	6.7	D
DS08-07	0.90	0.0572	0.0155	0.0928	0.0260	0.01176	0.00079			90.1	25.2	75.4	5.1	C
DS08-08	0.95	0.0825	0.0239	0.1409	0.0424	0.01238	0.00102			133.8	40.3	79.3	6.5	D
DS08-09	0.79	0.0573	0.0122	0.0853	0.0188	0.01080	0.00062			83.1	18.4	69.2	4.0	C
DS08-10	0.58	0.0468	0.0135	0.0716	0.0211	0.01108	0.00072			70.2	20.7	71.1	4.6	C
DS08-11	0.53	0.0553	0.0119	0.0902	0.0200	0.01183	0.00067			87.7	19.5	75.8	4.3	C
DS08-12	0.67	0.0694	0.0238	0.1104	0.0391	0.01155	0.00100			106.4	37.7	74.0	6.4	C
DS08-13	0.86	0.0562	0.0108	0.0863	0.0171	0.01115	0.00058			84.1	16.7	71.5	3.7	C
DS08-14	0.83	0.0498	0.0061	0.0748	0.0096	0.01088	0.00042			73.2	9.4	69.8	2.7	C
DS08-15	0.56	0.0456	0.0188	0.0692	0.0291	0.01099	0.00091			67.9	28.6	70.5	5.8	C
DS08-16	0.97	0.0631	0.0098	0.0985	0.0159	0.01132	0.00053			95.4	15.4	72.5	3.4	D
DS08-17	0.90	0.0460	0.0165	0.0661	0.0240	0.01042	0.00065			65.0	23.6	66.8	4.2	C
DS08-18	0.74	0.0489	0.0206	0.0893	0.0381	0.01324	0.00094			86.8	37.0	84.8	6.0	C
DS08-19	0.82	0.0422	0.0164	0.0672	0.0264	0.01156	0.00073			66.1	26.0	74.1	4.7	C
DS08-20	0.74	0.0731	0.0199	0.1048	0.0293	0.01040	0.00066			101.2	28.3	66.7	4.3	D
DS08-21	0.85	0.0441	0.0179	0.0656	0.0270	0.01080	0.00072			64.5	26.6	69.3	4.6	C
DS08-22	0.58	0.0617	0.0269	0.0951	0.0422	0.01118	0.00090			92.2	41.0	71.7	5.8	C
DS08-23	0.90	0.0476	0.0137	0.0771	0.0227	0.01175	0.00069			75.4	22.2	75.3	4.4	C
DS08-24	0.69	0.0832	0.0172	0.1304	0.0278	0.01136	0.00062			124.5	26.6	72.8	4.0	D
DS08-25	0.56	0.0495	0.0162	0.0815	0.0272	0.01194	0.00081			79.5	26.6	76.5	5.2	C
DS08-26	0.91	0.0472	0.0106	0.0733	0.0169	0.01127	0.00052			71.8	16.5	72.2	3.3	C
DS08-27	0.90	0.0439	0.0074	0.0677	0.0117	0.01118	0.00037			66.5	11.5	71.6	2.4	C
DS08-28	0.75	0.0614	0.0149	0.0990	0.0247	0.01169	0.00066			95.8	23.9	74.9	4.2	C
DS08-29	0.70	0.0752	0.0232	0.1192	0.0380	0.01150	0.00091			114.4	36.5	73.7	5.8	D
91500-01	0.35	0.0770	0.0054	1.8680	0.1422	0.17602	0.00497	1121.0	79.3	1069.8	81.4	1045.2	29.5	C
91500-02	0.35	0.0703	0.0050	1.7410	0.1385	0.17959	0.00658	938.0	66.2	1023.8	81.5	1064.7	39.0	C
91500-03	0.34	0.0759	0.0052	1.8658	0.1426	0.17822	0.00605	1094.0	74.9	1069.0	81.7	1057.3	35.9	C
91500-04	0.34	0.0773	0.0056	1.8700	0.1463	0.17553	0.00523	1129.0	81.7	1070.5	83.8	1042.5	31.0	C
91500-05	0.35	0.0730	0.0064	1.7800	0.1589	0.17693	0.00328	1013.0	88.5	1038.1	92.7	1050.2	19.5	C
OD3-01	1.07	0.0489	0.0097	0.0359	0.0073	0.00531	0.00024			35.8	7.3	34.2	1.6	C
OD3-02	1.09	0.0408	0.0089	0.0289	0.0065	0.00513	0.00027			28.9	6.5	33.0	1.7	C
OD3-03	1.04	0.0409	0.0110	0.0293	0.0080	0.00518	0.00030			29.3	8.0	33.3	1.9	C
OD3-04	0.57	0.0493	0.0312	0.0362	0.0231	0.00532	0.00049			36.1	23.1	34.2	3.1	C
OD3-05	0.58	0.0398	0.0167	0.0277	0.0118	0.00506	0.00039			27.8	11.9	32.5	2.5	C

RESULTS

In this study, we conducted U–Pb dating of zircons from one tuff sample, five sandstone samples, and one siltstone sample. To estimate the maximum depositional dates (MDDs) of the sandstone and siltstone samples, we employed the following four measures based on the $^{206}Pb/^{238}U$ dates; (1) the youngest single grain date (YSG), (2) the weighted mean of the youngest two or more grain dates that overlap within uncertainty at 1σ (YC1σ; Dickinson and Gehrels, 2009), (3) the weighted mean of the youngest three or more grain dates that overlap within uncertainty at 2σ (YC2σ; Dickinson and Gehrels, 2009), and (4) the maximum likelihood age (MLA; Vermeesch, 2021). We used Isoplot 4.15 (Ludwig, 2012) to calculate YC1σ and YC2σ and IsoplotR (Vermeesch, 2018) to calculate the MLA (2σ). The U–Pb dating results are presented below.

The Asuwa Formation of the Asuwa Group

Felsic weakly-welded lapilli tuff of the Doai Tuff Member (sample DS08)

The zircons from sample DS08 were mostly euhedral (Fig. 4A). Most zircons were colorless and exhibited oscillatory, sector, or no zoning in CL images. We obtained 29 U–Pb analytical data sets from 29 zircon grains collected from this sample. Alongside DS08, two secondary standards, 91500 and OD-3 zircons, were analyzed. The weighted mean of the $^{206}Pb/^{238}U$ dates for secondary standards were 1050 ± 13 Ma and 33.48 ± 0.88 Ma (both at 2σ), respectively, and both overlap with the range of the recommended age of the standards within 2σ uncertainty. Of the zircon grains analyzed from DS08, 22 yielded concordant dates (Table 2; Fig. 4B). The $^{206}Pb/^{238}U$ dates from the concordant grains range from 66 and 84 Ma (Fig. 4C), with the youngest concordant date being 66.8 ± 4.2 Ma. A cluster of 19 grains with overlapping $^{206}Pb/^{238}U$ dates within 2σ uncertainty yielded a weighted mean date of 71.8 ± 0.87 Ma (2σ; MSWD = 1.2, probability = 0.23) (Fig. 4D), whereas the MLA was 72.0 ± 1 Ma (Fig. 4E).

Sandstone of the lower part of the Sarao Alternation Member (sample DS102-1)

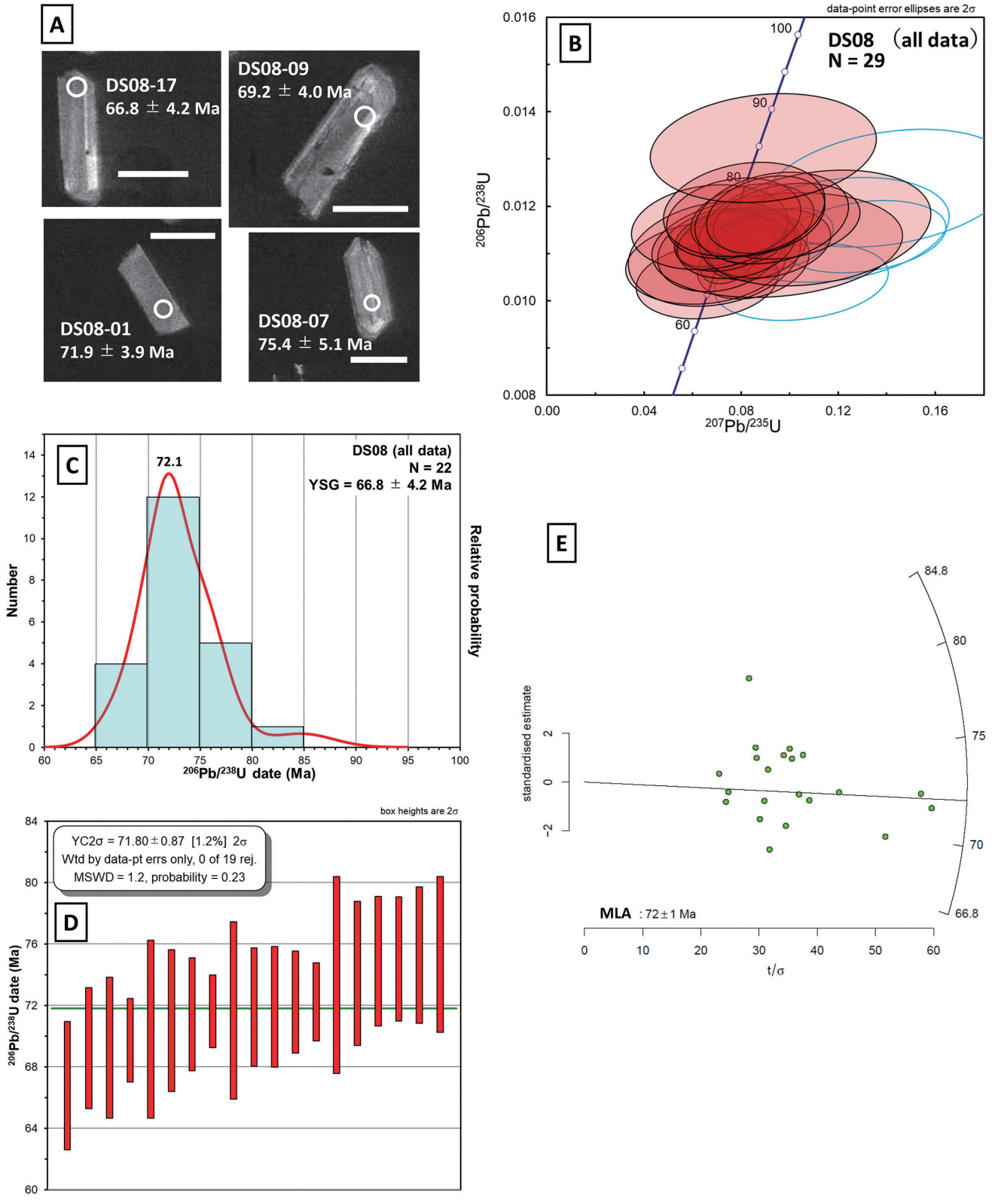

FIGURE 4. Analytical data of detrital zircons from tuff of the Doai Tuff Member (sample DS08). **A**, Cathodoluminescence images of zircons (white scale bar = 100 μm). **B**, Concordia diagram for all data. **C**, Probability density plot with a histogram for all $^{206}Pb/^{238}U$ dates from concordant grains. **D**, The mean date of the youngest three or more grains that overlap in date at 2σ (YC2σ). **E**, Radial plots and the maximum likelihood age (MLA) estimates. Blue open circles in the concordia diagrams from Fig.4 to Fig.10 show the analytical data for discordant grains. N: total number, %Pc: percentage of Precambrian zircons.

The zircons from sample DS102-1 were euhedral, with some grains showing abraded subhedral crystal faces (Table 3; Fig. 5A). Most grains were colorless and exhibited oscillatory, sector, or no zoning in CL images. We obtained 92 U–Pb data sets from 92 zircon grains collected from this sample. The weighted mean of $^{206}Pb/^{238}U$ dates for the 91500 zircon, analyzed alongside this sample, was 1067.2 ± 6.2 Ma (2σ) and overlaps the recommended age of this standard within 2σ uncertainty. By contrast, the weighted mean of $^{206}Pb/^{238}U$ dates for the OD-3 zircon was 31.52 ± 0.31 Ma (2σ), with the best estimate being approximately 4.6% younger than that of the recommended age. Of the zircon grains analyzed from DS102-1, 38 grains yielded concordant results (Fig. 5B). Three date groups of concordant detrital zircons were identified: 65–80 Ma (19 grains; 50.0% of 38 concordant grains), 162–266 Ma (44.7%), 2100–2231 Ma (5.3%) (Fig. 5C, 5D). The percentage of Precambrian zircons (%Pc) was 5.3. The YSG was 65.3 ± 1.6 Ma, YC1σ (2 dates) was 68.6 ± 0.7 Ma (1σ). YC2σ (7 dates) was 70.20 ± 0.74 Ma (2σ; MSWD = 2.0, probability = 0.063) (Fig. 5E), and the MLA was 65.3 ± 2.1 Ma (2σ) (Fig. 5F).

Sandstone of the upper part of the Sarao Alternation Member (sample DS20)

The zircons from sample DS20 were euhedral, with some grains showing abraded subhedral crystal faces (Fig. 6A). Most grains were colorless and exhibited oscillatory, sector, or no zoning in CL images. We obtained 71 U–Pb data sets from 71 zircon grains collected from this sample. The weighted mean of the $^{206}Pb/^{238}U$ dates for 91500 and OD-3 zircons, analyzed alongside this sample, were 1054.9 ± 6.8 Ma and 32.53 ± 0.46 Ma (2σ), respectively. Both overlap with the range of the recommended age of these standards within 2σ uncertainty. Of the zircon grains analyzed from DS20, 55 grains yielded concordant results (Table 4; Fig. 6B). Most concordant dates ranged from 65 to 80 Ma (43 grains; 78.2% of 55 concordant grains), with additional dates at 141 Ma (1.8%), 180–184 Ma (7.3%), 196 Ma (1.8%), 222–223 Ma (5.5%), 246 Ma (1.8%), 260 Ma (1.8%), and 1952 Ma (1.8%) (Fig. 6C, 6D). %Pc was 1.8. The YSG was 65.1 ± 6.3 Ma, YC1σ (10 dates) was 67.46 ± 0.47 Ma (1σ). YC2σ (20 dates) was 69.05 ± 0.66 Ma (2σ; MSWD = 1.5, probability = 0.083; Fig. 6E), and the MLA was 70.33 ± 0.61 Ma (2σ) (Fig. 6F).

The Subara Formation of the Asuwa Group

Sandstone of the Subara Formation (sample KM01)

The zircons from sample KM01 were euhedral, with some grains showing abraded subhedral crystal faces (Fig.7A). Most grains were colorless and exhibited oscillatory, sector, or no zoning in CL images. We obtained 101 U–Pb data sets from 101 zircon grains collected from this sample. The weighted mean of $^{206}Pb/^{238}U$ dates of 91500 zircon, analyzed alongside this sample, was 1058.4 ± 6.6 Ma (2σ), and overlaps with the range of the recommended age of this standard within 2σ uncertainty. On the other hand, the weighted mean of $^{206}Pb/^{238}U$ dates for OD-3 zircon was 31.93 ± 0.46 Ma (2σ), with the best estimate being approximately 3.4% younger than that of the recommended age. Of the zircon grains analyzed from KM01, 76 grains yielded concordant results (Table 5; Fig. 7B). The $^{206}Pb/^{238}U$ dates obtained from concordant data sets formed three main date groups and three single dates: 65–86 Ma (40 grains; 52.7% of 76 concordant grains), 152–281 Ma (34.2%), 383 Ma (1.3%), 773 Ma (1.3%), 1763–1886 Ma (9.2%), and 2076 Ma (1.3%) (Fig. 7C, 7D). %Pc was 10.5. The YSG was 65.6 ± 4.2 Ma, YC1σ (4 dates) was 66.3 ± 0.7 Ma (1σ). YC2σ (12 dates) was 68.32 ± 0.81 Ma (2σ; MSWD = 1.3, probability = 0.19; Fig. 7E), and the MLA was 70.78 ± 0.73 Ma (2σ) (Fig. 7F).

The Sugo Formation

Sandstone of the lower part of the Sugo Formation (sample UM01-2)

The zircons from sample UM01-2 were commonly abraded and had anhedral to subhedral shapes (Fig. 8A). Most grains were colorless and exhibited oscillatory, sector, or irregular zoning in CL images. We obtained 111 U–Pb data sets from 111 zircon grains collected from this sample. The weighted mean of $^{206}Pb/^{238}U$ dates for 91500 zircon, analyzed alongside this sample, was 1052.94 ± 8.0 Ma (2σ), with the best estimate being approximately 0.89% younger than that of the recommended age. On the other hand, the weighted mean of $^{206}Pb/^{238}U$ dates for OD-3 zircon was 32.57 ± 0.5 Ma (2σ) and overlaps with the range of the recommended age of this standard within 2σ uncertainty. Of the zircon grains analyzed from UM01-2, 76 grains yielded concordant results (Table 6; Fig. 8B). The $^{206}Pb/^{238}U$ dates obtained from concordant data sets formed four date groups and three single dates: 159 Ma (single grain; 1.3% of 76 concordant grains), 171–202 Ma (19.8%), 213–279 Ma (34.2%), 299–308 Ma (2.6%), 343 Ma (1.3%), 451 Ma (1.3%), and 1770–2287 Ma (39.5%) (Fig. 8C, 8D). %Pc was 39.5. The YSG was 159.3 ± 2.7 Ma, YC1σ (2 dates) was 172.5 ± 1.6 Ma (1σ). YC2σ (3 dates) was 174.7 ± 2.7 Ma (2σ; MSWD = 3.2, probability = 0.041; Fig. 8E), and the MLA was 159.3 ± 3.5 Ma (2σ) (Fig. 8F).

Sandstone of the upper part of the Sugo Formation (sample SG05)

The zircons from sample SG05 were commonly abraded and had anhedral to subhedral shapes (Fig. 9A). Most grains were colorless and exhibited oscillatory or sector zoning, and one grain showed a metamorphic rim in CL images. We obtained 113 U–Pb data sets from 113 zircon grains collected from this sample. The weighted mean of the $^{206}Pb/^{238}U$ dates for 91500 and OD-3 zircons, analyzed alongside this sample, were 1061.8 ± 6.6 Ma and 32.74 ± 0.34 Ma (2σ), respectively. The recommended age of 91500 zircon falls within the 2σ uncertainty range of the former date, while the latter overlaps the recommended age of OD-3 zircon within 2σ uncertainty. Of the zircon grains analyzed from SG05, 84 grains yielded concordant results (Table 7; Fig. 9B). The $^{206}Pb/^{238}U$ dates obtained from concordant data sets formed several date groups and single dates: 106–112 Ma (3 grains; 3.6% of 84 concordant grains), 139

TABLE 3. U–Pb isotopes and dates of zircons from sample DS102-1. Abbreviations: C: concordant data, D: discordant data.

Spot No.	Th/U	$^{207}Pb/^{206}Pb$	Uncertainty 2SD	$^{207}Pb/^{235}U$	Uncertainty 2SD	$^{206}Pb/^{238}U$	Uncertainty 2SD	^{206}Pb-^{207}Pb (Ma)	Uncertainty 2SD	^{235}U-^{207}Pb (Ma)	Uncertainty 2SD	^{238}U-^{206}Pb (Ma)	Uncertainty 2SD	Memo
DS102-1-01	0.86	0.0530	0.0040	0.1864	0.0154	0.02549	0.00086			173.5	14.3	162.2	5.4	C
DS102-1-02	0.87	0.0646	0.0101	0.1022	0.0167	0.01147	0.00053			98.8	16.2	73.5	3.4	D
DS102-1-03	1.13	0.0504	0.0083	0.0788	0.0134	0.01132	0.00050			77.0	13.1	72.6	3.2	C
DS102-1-04	0.65	0.1336	0.0043	7.0945	0.3185	0.38515	0.01195	2146.0	69.6	2123.3	95.3	2100.3	65.2	C
DS102-1-05	0.75	0.0578	0.0078	0.0925	0.0130	0.01160	0.00049			89.8	12.6	74.3	3.1	D
DS102-1-06	0.91	0.0479	0.0043	0.2224	0.0206	0.03364	0.00084			203.9	18.9	213.3	5.3	C
DS102-1-07	0.52	0.0543	0.0039	0.2136	0.0162	0.02854	0.00066			196.6	14.9	181.4	4.2	C
DS102-1-08	0.46	0.0669	0.0046	0.1018	0.0074	0.01104	0.00026			98.5	7.2	70.8	1.7	D
DS102-1-09	0.95	0.0518	0.0043	0.2107	0.0182	0.02950	0.00072			194.1	16.8	187.4	4.6	C
DS102-1-10	0.53	0.0528	0.0034	0.2524	0.0171	0.03470	0.00075			228.5	15.5	219.9	4.8	C
DS102-1-11	0.80	0.0653	0.0082	0.1039	0.0135	0.01154	0.00040			100.3	13.1	74.0	2.6	D
DS102-1-12	0.85	0.0478	0.0096	0.0766	0.0158	0.01162	0.00051			75.0	15.4	74.5	3.2	C
DS102-1-13	0.56	0.0575	0.0044	0.0947	0.0076	0.01195	0.00030			91.9	7.3	76.6	1.9	D
DS102-1-14	0.69	0.0511	0.0064	0.0863	0.0111	0.01224	0.00039			84.0	10.8	78.4	2.5	C
DS102-1-15	1.05	0.0550	0.0060	0.0860	0.0098	0.01133	0.00034			83.8	9.5	72.6	2.2	D
DS102-1-16	0.83	0.0609	0.0071	0.2276	0.0277	0.02709	0.00088			208.2	25.3	172.3	5.6	D
DS102-1-17	0.81	0.0553	0.0041	0.2050	0.0158	0.02690	0.00056			189.4	14.6	171.1	3.6	D
DS102-1-18	0.42	0.0577	0.0031	0.0867	0.0049	0.01091	0.00019			84.5	4.8	69.9	1.2	D
DS102-1-19	1.15	0.0586	0.0034	0.0899	0.0055	0.01112	0.00020			87.4	5.3	71.3	1.3	D
DS102-1-20	0.66	0.0476	0.0045	0.1966	0.0192	0.02997	0.00070			182.3	17.8	190.3	4.4	C
DS102-1-21	0.70	0.0642	0.0073	0.1061	0.0124	0.01198	0.00035			102.4	12.0	76.8	2.3	D
DS102-1-22	1.21	0.0525	0.0052	0.0769	0.0079	0.01064	0.00026			75.3	7.7	68.2	1.7	C
DS102-1-23	0.67	0.0795	0.0073	0.4079	0.0390	0.03722	0.00101	1185.0	108.7	347.3	33.2	235.5	6.4	D
DS102-1-24	0.66	0.0519	0.0054	0.0842	0.0091	0.01176	0.00030			82.1	8.9	75.4	1.9	C
DS102-1-25	0.49	0.1406	0.0040	8.6196	0.3017	0.44473	0.00891	2235.0	64.2	2298.5	80.5	2371.8	47.5	D
DS102-1-26	0.46	0.0486	0.0044	0.2648	0.0248	0.03948	0.00102			238.5	22.4	249.6	6.5	C
DS102-1-27	0.43	0.0488	0.0040	0.0846	0.0073	0.01257	0.00031			82.5	7.1	80.5	2.0	C
DS102-1-28	0.55	0.0538	0.0061	0.2599	0.0306	0.03504	0.00107			234.6	27.6	222.0	6.8	C
DS102-1-29	0.92	0.0463	0.0061	0.0765	0.0104	0.01197	0.00039			74.8	10.2	76.7	2.5	C
DS102-1-30	0.38	0.0603	0.0035	0.4814	0.0297	0.05794	0.00128			399.0	24.6	363.1	8.0	D
DS102-1-31	0.75	0.0640	0.0102	0.1012	0.0167	0.01147	0.00048			97.8	16.2	73.5	3.1	D
DS102-1-32	0.57	0.0601	0.0091	0.1157	0.0181	0.01396	0.00053			111.1	17.4	89.4	3.4	D
DS102-1-33	0.65	0.0510	0.0031	0.2464	0.0159	0.03502	0.00073			223.6	14.4	221.9	4.6	C
DS102-1-34	0.78	0.0782	0.0127	0.1173	0.0198	0.01088	0.00049			112.6	19.0	69.8	3.1	D
DS102-1-35	0.47	0.0545	0.0034	0.2327	0.0152	0.03097	0.00065			212.4	13.8	196.6	4.2	D
DS102-1-36	0.89	0.0572	0.0084	0.0892	0.0136	0.01131	0.00041			86.7	13.2	72.5	2.7	C
DS102-1-37	0.69	0.1094	0.0223	0.1742	0.0373	0.01155	0.00074			163.0	34.9	74.0	4.8	D
DS102-1-38	1.00	0.0680	0.0097	0.0970	0.0144	0.01035	0.00041			94.0	13.9	66.4	2.6	D
DS102-1-39	0.64	0.0499	0.0034	0.2067	0.0147	0.03002	0.00068			190.7	13.6	190.6	4.3	C
DS102-1-40	1.21	0.0825	0.0080	0.1310	0.0134	0.01152	0.00036			125.0	12.8	73.8	2.3	D
DS102-1-41	0.56	0.0588	0.0058	0.0894	0.0093	0.01102	0.00032			86.9	9.0	70.6	2.0	D
DS102-1-42	0.34	0.0548	0.0033	0.0753	0.0049	0.00996	0.00022			73.7	4.8	63.9	1.4	D
DS102-1-43	0.50	0.0506	0.0042	0.2642	0.0231	0.03790	0.00095			238.0	20.8	239.8	6.0	C
DS102-1-44	0.70	0.0988	0.0050	0.5615	0.0303	0.04123	0.00080			452.5	24.4	260.4	5.1	D
DS102-1-45	0.86	0.1336	0.0029	5.8406	0.1506	0.31714	0.00446	2146.0	46.4	1952.4	50.3	1775.8	25.0	D
DS102-1-46	0.84	0.0586	0.0092	0.0927	0.0150	0.01147	0.00044			90.0	14.6	73.5	2.8	C
DS102-1-47	0.70	0.0509	0.0034	0.2197	0.0152	0.03128	0.00061			201.6	13.9	198.6	3.9	C
DS102-1-48	0.63	0.0532	0.0083	0.0837	0.0133	0.01140	0.00042			81.6	13.0	73.1	2.7	C
DS102-1-49	0.63	0.0486	0.0030	0.0735	0.0047	0.01097	0.00020			72.0	4.6	70.3	1.3	C
DS102-1-50	0.60	0.0781	0.0121	0.1169	0.0187	0.01085	0.00047			112.2	18.0	69.6	3.0	D
DS102-1-51	0.77	0.0456	0.0072	0.0763	0.0123	0.01215	0.00045			74.7	12.1	77.9	2.9	C
DS102-1-52	0.83	0.0638	0.0089	0.1012	0.0147	0.01150	0.00044			97.9	14.2	73.7	2.8	D
DS102-1-53	1.05	0.0469	0.0060	0.0699	0.0092	0.01081	0.00036			68.6	9.0	69.3	2.3	C
DS102-1-54	0.64	0.0665	0.0108	0.1047	0.0176	0.01142	0.00050			101.1	17.0	73.2	3.2	D
DS102-1-55	0.43	0.0537	0.0033	0.0789	0.0053	0.01064	0.00026			77.1	5.1	68.2	1.7	D
DS102-1-56	1.10	0.0596	0.0035	0.2014	0.0128	0.02453	0.00060			186.3	11.9	156.2	3.8	D
DS102-1-57	0.69	0.0558	0.0034	0.3015	0.0197	0.03919	0.00096			267.5	17.5	247.8	6.1	D
DS102-1-58	0.76	0.0508	0.0076	0.0792	0.0122	0.01131	0.00038			77.4	11.9	72.5	2.4	C
DS102-1-59	0.65	0.0564	0.0032	0.3369	0.0202	0.04334	0.00072			294.8	17.7	273.5	4.5	D
DS102-1-60	0.35	0.1295	0.0027	6.5496	0.1587	0.36687	0.00446	2091.0	43.8	2052.5	49.7	2014.6	24.5	D
DS102-1-61	0.76	0.1151	0.0030	5.6102	0.1616	0.35359	0.00458	1882.0	48.4	1917.6	55.2	1951.7	25.3	D
DS102-1-62	0.70	0.0874	0.0105	0.1398	0.0175	0.01160	0.00040			132.8	16.6	74.3	2.6	D
DS102-1-63	1.87	0.0867	0.0037	0.4279	0.0193	0.03580	0.00055			361.7	16.3	226.8	3.5	D
DS102-1-64	1.10	0.09	0.0060	0.1400	0.0103	0.01187	0.00026			133.1	9.8	76.0	1.6	D
DS102-1-65	0.62	0.06	0.0090	0.0973	0.0147	0.01153	0.00041			94.3	14.3	73.9	2.7	D
DS102-1-66	0.59	0.06	0.0111	0.0988	0.0182	0.01162	0.00050			95.7	17.7	74.4	3.2	D

continued on next page

Spot No.	Th/U	$^{207}Pb/^{206}Pb$	Uncertainty 2SD	$^{207}Pb/^{235}U$	Uncertainty 2SD	$^{206}Pb/^{238}U$	Uncertainty 2SD	^{206}Pb-^{207}Pb (Ma)	Uncertainty 2SD	^{235}U-^{207}Pb (Ma)	Uncertainty 2SD	^{238}U-^{206}Pb (Ma)	Uncertainty 2SD	Memo
DS102-1-67	0.39	0.10	0.0077	0.1795	0.0141	0.01265	0.00031			167.7	13.2	81.0	2.0	D
DS102-1-68	0.46	0.05	0.0062	0.0891	0.0106	0.01203	0.00033			86.6	10.3	77.1	2.1	C
DS102-1-69	0.54	0.05	0.0050	0.0709	0.0077	0.01099	0.00026			69.5	7.6	70.5	1.7	C
DS102-1-70	0.29	0.05	0.0028	0.2727	0.0156	0.03871	0.00060			244.9	14.0	244.8	3.8	C
DS102-1-71	0.87	0.05	0.0075	0.0735	0.0119	0.01111	0.00044			72.1	11.6	71.2	2.8	C
DS102-1-72	0.79	0.07	0.0095	0.1030	0.0148	0.01081	0.00044			99.5	14.3	69.3	2.9	D
DS102-1-73	0.82	0.06	0.0050	0.3031	0.0273	0.03718	0.00112			268.8	24.2	235.3	7.1	D
DS102-1-74	1.22	0.05	0.0039	0.2152	0.0180	0.03125	0.00089			197.9	16.6	198.3	5.6	C
DS102-1-75	0.81	0.14	0.0056	7.9476	0.3865	0.41358	0.01135	2220.0	89.1	2225.0	108.2	2231.3	61.2	C
DS102-1-76	0.98	0.08	0.0055	0.7701	0.0586	0.07239	0.00181			579.8	44.1	450.6	11.3	D
DS102-1-77	0.20	0.07	0.0035	0.2631	0.0148	0.02853	0.00059			237.1	13.3	181.4	3.8	D
DS102-1-78	0.65	0.05	0.0025	0.3011	0.0156	0.04218	0.00082			267.2	13.8	266.3	5.2	C
DS102-1-79	0.49	0.07	0.0051	0.1058	0.0082	0.01110	0.00027			102.1	7.9	71.2	1.7	D
DS102-1-80	1.04	0.06	0.0041	0.3037	0.0224	0.03798	0.00087			269.3	19.8	240.3	5.5	D
DS102-1-81	0.62	0.08	0.0132	0.1430	0.0236	0.01240	0.00057			135.7	22.4	79.5	3.7	D
DS102-1-82	0.86	0.82	0.0943	55.9205	7.8566	0.49282	0.04010	4597.0	802.0	4103.7	576.6	2582.9	210.2	D
DS102-1-83	0.85	0.05	0.0046	0.0797	0.0078	0.01172	0.00032			77.8	7.6	75.1	2.1	C
DS102-1-84	0.42	0.06	0.0089	0.1128	0.0162	0.01276	0.00049			108.5	15.6	81.8	3.1	D
DS102-1-85	0.71	0.06	0.0072	0.0909	0.0113	0.01093	0.00037			88.3	11.0	70.1	2.4	D
DS102-1-86	0.43	0.05	0.0038	0.0717	0.0056	0.01018	0.00025			70.3	5.5	65.3	1.6	C
DS102-1-87	0.91	0.13	0.0125	0.2153	0.0229	0.01244	0.00047			198.0	21.0	79.7	3.0	D
DS102-1-88	0.92	0.05	0.0038	0.2106	0.0164	0.02942	0.00073			194.1	15.1	186.9	4.7	C
DS102-1-89	0.72	0.07	0.0084	0.1035	0.0135	0.01121	0.00041			100.0	13.0	71.9	2.6	D
DS102-1-90	0.42	0.09	0.0133	0.1576	0.0238	0.01232	0.00057			148.6	22.4	79.0	3.6	D
DS102-1-91	0.49	0.06	0.0050	0.2670	0.0249	0.03474	0.00097			240.3	22.4	220.1	6.2	C
DS102-1-92	1.10	0.07	0.0049	0.3186	0.0254	0.03551	0.00095			280.8	22.4	224.9	6.0	D
91500-01	0.35	0.0729	0.0041	1.7910	0.1162	0.17816	0.00584	1012.0	56.6	1042.2	67.6	1056.9	34.7	C
91500-02	0.32	0.0738	0.0043	1.7619	0.1092	0.17318	0.00392	1036.0	59.7	1031.5	63.9	1029.6	23.3	C
91500-03	0.34	0.0708	0.0042	1.7723	0.1127	0.18162	0.00423	951.0	56.3	1035.3	65.8	1075.8	25.1	C
91500-04	0.35	0.0749	0.0041	1.8940	0.1099	0.18347	0.00351	1065.0	58.3	1078.9	62.6	1085.9	20.8	C
91500-05	0.35	0.0754	0.0040	1.9084	0.1099	0.18365	0.00410	1079.0	57.3	1084.0	62.4	1086.9	24.3	C
91500-06	0.34	0.0772	0.0042	1.9008	0.1109	0.17853	0.00384	1127.0	61.1	1081.3	63.1	1058.9	22.8	C
91500-07	0.34	0.0728	0.0040	1.8132	0.1084	0.18074	0.00406	1008.0	55.9	1050.2	62.8	1071.0	24.0	C
91500-08	0.33	0.0739	0.0042	1.8492	0.1115	0.18151	0.00357	1039.0	59.2	1063.1	64.1	1075.2	21.2	C
91500-09	0.34	0.0743	0.0042	1.8264	0.1136	0.17831	0.00448	1050.0	59.8	1054.9	65.6	1057.7	26.6	C
91500-10	0.34	0.0727	0.0039	1.8392	0.1036	0.18351	0.00316	1006.0	53.9	1059.5	59.7	1086.1	18.7	C
91500-11	0.34	0.08	0.0043	1.9134	0.1095	0.17690	0.00320	1159.0	62.9	1085.7	62.1	1050.0	19.0	C
91500-12	0.34	0.07	0.0041	1.7746	0.1103	0.17545	0.00479	1024.0	57.2	1044.3	64.9	1054.2	28.8	C
91500-13	0.34	0.08	0.0041	1.8726	0.1110	0.18042	0.00393	1076.0	59.3	1071.4	63.5	1069.2	23.3	C
91500-14	0.35	0.08	0.0040	1.8612	0.1090	0.17960	0.00422	1073.0	57.5	1067.4	62.5	1064.8	25.0	C
91500-15	0.33	0.15	0.0066	3.7935	0.1872	0.17757	0.00435	2402.0	102.9	1591.3	78.5	1053.7	25.8	D
OD3-01	0.92	0.0481	0.0121	0.0322	0.0083	0.00486	0.00027			32.2	8.3	31.3	1.7	C
OD3-02	1.14	0.0468	0.0068	0.0310	0.0046	0.00480	0.00016			31.0	4.6	30.9	1.1	C
OD3-03	1.28	0.0524	0.0076	0.0349	0.0052	0.00484	0.00017			34.9	5.2	31.1	1.1	C
OD3-04	1.22	0.0548	0.0082	0.0364	0.0056	0.00482	0.00016			36.3	5.6	31.0	1.1	C
OD3-05	1.27	0.0445	0.0069	0.0296	0.0047	0.00482	0.00017			29.6	4.7	31.0	1.1	C
OD3-06	1.25	0.0479	0.0072	0.0316	0.0048	0.00477	0.00017			31.5	4.8	30.7	1.1	C
OD3-07	0.98	0.0484	0.0082	0.0328	0.0057	0.00492	0.00019			32.8	5.7	31.6	1.2	C
OD3-08	0.95	0.0528	0.0092	0.0350	0.0062	0.00481	0.00019			34.9	6.2	30.9	1.2	C
OD3-09	1.19	0.0435	0.0069	0.0288	0.0047	0.00480	0.00018			28.8	4.7	30.9	1.1	C
OD3-10	1.27	0.0590	0.0078	0.0403	0.0055	0.00495	0.00016			40.1	5.4	31.9	1.0	D
OD3-11	1.15	0.05	0.0063	0.0322	0.0045	0.00514	0.00015			32.2	4.5	33.1	1.0	C
OD3-12	1.13	0.05	0.0066	0.0318	0.0048	0.00506	0.00019			31.8	4.8	32.5	1.2	C
OD3-13	1.09	0.05	0.0083	0.0334	0.0060	0.00504	0.00020			33.4	5.9	32.4	1.3	C
OD3-14	1.11	0.05	0.0080	0.0321	0.0057	0.00506	0.00020			32.0	5.7	32.6	1.3	C
OD3-15	1.11	0.04	0.0079	0.0294	0.0055	0.00491	0.00020			29.4	5.5	31.6	1.3	C

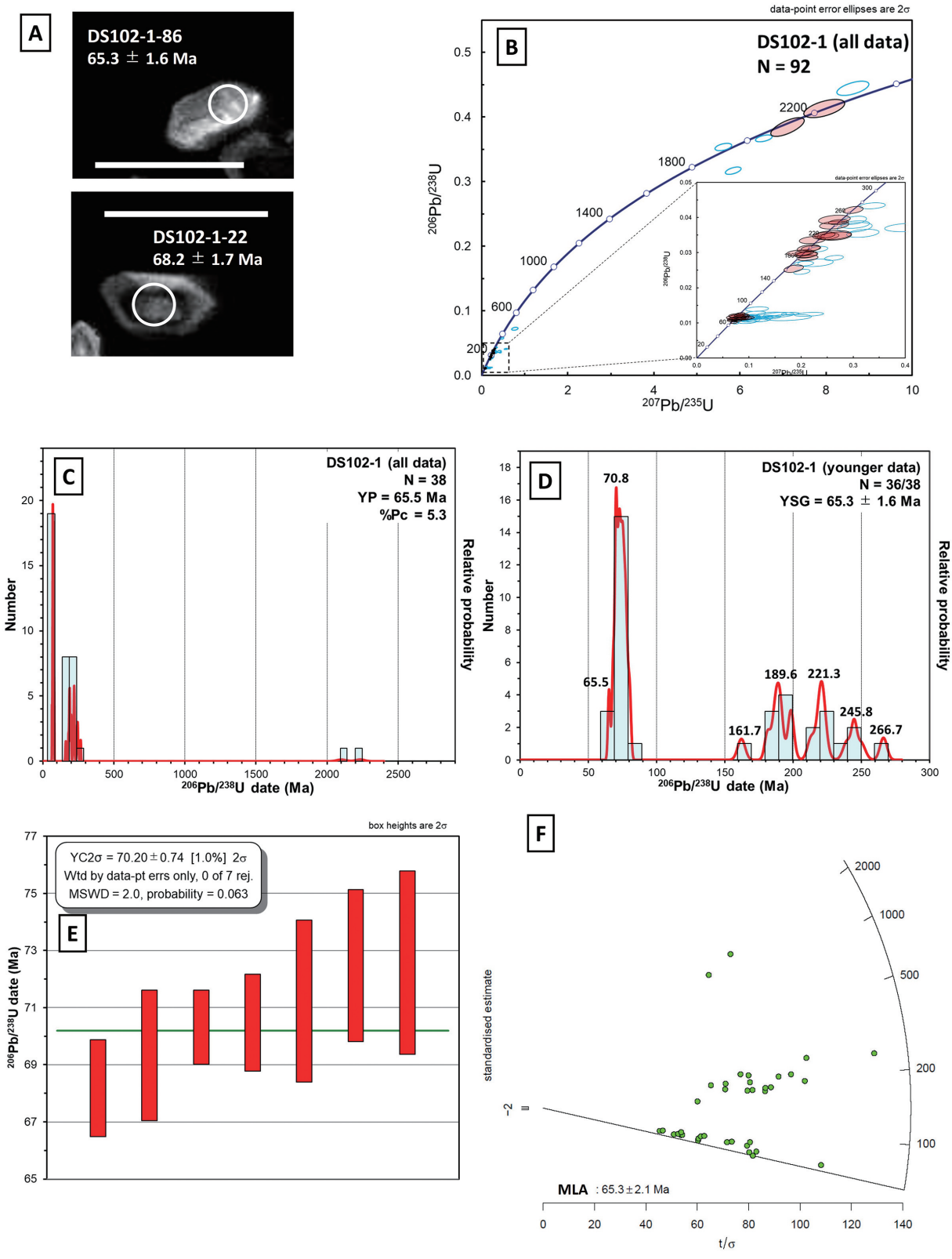

FIGURE 5. Analytical data of detrital zircons from sandstone of the lower part of the Sarao Alternation Member (sample DS102-1). **A**, Cathodoluminescence images of zircons (white scale bar = 100 μm). **B**, Concordia diagram for all data. **C**, Probability density plot with a histogram for all $^{206}Pb/^{238}U$ dates from concordant grains. **D**, Probability density plot with a histogram for younger $^{206}Pb/^{238}U$ dates. **E**, The weighted mean date (YC2σ) for the youngest cluster. **F**, Radial plots and MLA estimates.

TABLE 4. U–Pb isotopes and dates of zircons from sample DS20. Abbreviations: C: concordant data, D: discordant data.

Spot No.	Th/U	$^{207}Pb/^{206}Pb$	Uncertainty 2SD	$^{207}Pb/^{235}U$	Uncertainty 2SD	$^{206}Pb/^{238}U$	Uncertainty 2SD	^{206}Pb-^{207}Pb (Ma)	Uncertainty 2SD	^{235}U-^{207}Pb (Ma)	Uncertainty 2SD	^{238}U-^{206}Pb (Ma)	Uncertainty 2SD	Memo
DS20-01	0.66	0.1154	0.0038	4.9869	0.1830	0.31336	0.00507	1887.0	62.1	1817.0	66.7	1757.2	28.4	D
DS20-02	1.08	0.0805	0.0107	0.1254	0.0172	0.01130	0.00042			119.9	16.5	72.4	2.7	D
DS20-03	0.56	0.0476	0.0060	0.0731	0.0094	0.01113	0.00032			71.6	9.2	71.4	2.1	C
DS20-04	1.60	0.0387	0.0086	0.1776	0.0402	0.03330	0.00142			166.0	37.6	211.2	9.0	D
DS20-05	0.37	0.1170	0.0037	5.7047	0.2000	0.35373	0.00562	1911.0	59.7	1932.0	67.7	1952.4	31.0	C
DS20-06	0.84	0.0642	0.0111	0.0999	0.0177	0.01129	0.00048			96.7	17.2	72.4	3.1	D
DS20-07	0.86	0.0373	0.0072	0.0556	0.0110	0.01081	0.00040			55.0	10.9	69.3	2.6	D
DS20-08	1.26	0.0485	0.0076	0.2344	0.0379	0.03508	0.00127			213.8	34.6	222.3	8.0	C
DS20-09	0.57	0.0628	0.0078	0.0985	0.0127	0.01138	0.00038			95.4	12.3	72.9	2.4	D
DS20-10	0.88	0.0626	0.0158	0.0950	0.0247	0.01101	0.00065			92.2	23.9	70.6	4.2	C
DS20-11	0.55	0.0526	0.0122	0.0819	0.0195	0.01129	0.00057			80.0	19.0	72.4	3.7	C
DS20-12	0.71	0.0330	0.0100	0.0511	0.0158	0.01125	0.00057			50.6	15.6	72.1	3.7	D
DS20-13	0.77	0.0510	0.0063	0.2472	0.0317	0.03519	0.00128			224.3	28.8	223.0	8.1	C
DS20-14	0.34	0.0495	0.0099	0.0783	0.0161	0.01148	0.00054			76.6	15.7	73.6	3.5	C
DS20-15	0.71	0.0484	0.0063	0.0710	0.0096	0.01064	0.00039			69.6	9.4	68.2	2.5	C
DS20-16	0.56	0.0407	0.0086	0.0646	0.0140	0.01152	0.00053			63.6	13.8	73.9	3.4	C
DS20-17	0.73	0.0451	0.0077	0.0689	0.0120	0.01107	0.00046			67.6	11.8	71.0	3.0	C
DS20-18	0.52	0.0412	0.0131	0.0672	0.0217	0.01182	0.00067			66.1	21.4	75.8	4.3	C
DS20-19	0.78	0.0541	0.0068	0.0829	0.0107	0.01112	0.00032			80.8	10.5	71.3	2.1	C
DS20-20	0.46	0.0539	0.0049	0.2157	0.0202	0.02904	0.00062			198.3	18.6	184.5	4.0	C
DS20-21	0.41	0.0512	0.0085	0.0816	0.0141	0.01156	0.00051			79.7	13.7	74.1	3.2	C
DS20-22	0.53	0.0627	0.0156	0.1022	0.0262	0.01183	0.00075			98.8	25.4	75.8	4.8	C
DS20-23	0.35	0.0341	0.0064	0.0860	0.0166	0.01828	0.00076			83.7	16.1	116.8	4.9	D
DS20-24	0.49	0.0384	0.0135	0.0656	0.0235	0.01240	0.00085			64.5	23.1	79.5	5.4	C
DS20-25	0.67	0.0506	0.0094	0.0809	0.0154	0.01159	0.00054			78.9	15.1	74.3	3.5	C
DS20-26	0.59	0.0820	0.0203	0.1327	0.0342	0.01174	0.00082			126.5	32.6	75.2	5.2	D
DS20-27	0.88	0.0553	0.0084	0.0884	0.0139	0.01159	0.00051			86.0	13.5	74.3	3.3	C
DS20-28	0.70	0.0909	0.0374	0.1272	0.0538	0.01014	0.00098			121.6	51.4	65.1	6.3	C
DS20-29	0.84	0.0786	0.0195	0.1380	0.0352	0.01273	0.00077			131.3	33.5	81.6	4.9	D
DS20-30	0.70	0.1226	0.0150	0.2137	0.0276	0.01265	0.00052			196.7	25.4	81.0	3.3	D
DS20-31	0.67	0.0587	0.0152	0.0956	0.0253	0.01180	0.00065			92.7	24.5	75.6	4.1	C
DS20-32	0.69	0.0485	0.0039	0.0770	0.0063	0.01152	0.00024			75.3	6.2	73.8	1.5	C
DS20-33	0.57	0.0479	0.0136	0.0779	0.0225	0.01180	0.00063			76.2	22.0	75.6	4.0	C
DS20-34	0.60	0.0510	0.0114	0.0887	0.0203	0.01261	0.00061			86.3	19.7	80.8	3.9	C
DS20-35	0.90	0.0508	0.0133	0.0799	0.0214	0.01141	0.00063			78.0	20.9	73.1	4.0	C
DS20-36	0.68	0.0529	0.0093	0.0824	0.0148	0.01129	0.00045			80.4	14.4	72.4	2.9	C
DS20-37	0.66	0.0437	0.0064	0.0697	0.0105	0.01158	0.00036			68.4	10.3	74.2	2.3	C
DS20-38	1.23	0.0636	0.0131	0.1042	0.0221	0.01189	0.00059			100.7	21.4	76.2	3.8	D
DS20-39	0.52	0.0466	0.0122	0.0716	0.0191	0.01113	0.00059			70.2	18.7	71.4	3.8	C
DS20-40	0.71	0.0507	0.0036	0.2726	0.0204	0.03902	0.00086			244.7	18.4	246.7	5.4	C
DS20-41	0.63	0.0540	0.0063	0.2128	0.0255	0.02859	0.00084			195.9	23.5	181.7	5.4	C
DS20-42	0.47	0.0511	0.0065	0.0777	0.0101	0.01102	0.00034			76.0	9.9	70.7	2.2	C
DS20-43	0.51	0.0470	0.0176	0.0813	0.0309	0.01255	0.00079			79.4	30.2	80.4	5.0	C
DS20-44	0.57	0.0550	0.0147	0.0792	0.0216	0.01044	0.00056			77.4	21.1	67.0	3.6	C
DS20-45	0.58	0.0457	0.0066	0.0784	0.0116	0.01244	0.00040			76.6	11.4	79.7	2.6	C
DS20-46	0.85	0.0635	0.0286	0.0943	0.0429	0.01077	0.00076			91.5	41.7	69.1	4.9	C
DS20-47	0.52	0.0382	0.0164	0.0591	0.0256	0.01124	0.00061			58.3	25.2	72.0	3.9	C
DS20-48	0.46	0.0467	0.0060	0.1857	0.0244	0.02887	0.00083			172.9	22.7	183.4	5.3	C
DS20-49	0.55	0.0492	0.0177	0.0758	0.0275	0.01117	0.00061			74.2	26.9	71.6	3.9	C
DS20-50	0.57	0.0510	0.0040	0.0802	0.0066	0.01141	0.00026			78.3	6.5	73.1	1.7	C
DS20-51	0.56	0.0337	0.0153	0.1026	0.0468	0.02211	0.00116			99.2	45.3	141.0	7.4	C
DS20-52	0.49	0.0526	0.0064	0.2246	0.0280	0.03096	0.00091			205.7	25.6	196.5	5.8	C
DS20-53	1.50	0.0583	0.0081	0.2822	0.0404	0.03513	0.00121			252.4	36.1	222.6	7.7	C
DS20-54	0.47	0.0541	0.0054	0.2123	0.0219	0.02845	0.00073			195.5	20.1	180.8	4.6	C
DS20-55	1.03	0.0749	0.0077	0.1166	0.0124	0.01129	0.00033			112.0	11.9	72.4	2.1	D
DS20-56	0.79	0.0479	0.0137	0.0691	0.0201	0.01045	0.00059			67.9	19.8	67.0	3.8	C
DS20-57	0.51	0.0590	0.0062	0.3353	0.0366	0.04120	0.00113			293.6	32.1	260.3	7.1	C
DS20-58	0.52	0.0353	0.0093	0.0573	0.0153	0.01179	0.00054			56.6	15.1	75.5	3.4	D
DS20-59	0.52	0.0554	0.0102	0.0848	0.0159	0.01110	0.00046			82.6	15.5	71.1	3.0	C
DS20-60	0.67	0.0620	0.0155	0.0902	0.0231	0.01056	0.00060			87.7	22.5	67.7	3.8	C
DS20-61	0.82	0.0622	0.0116	0.0943	0.0181	0.01100	0.00050			91.5	17.5	70.5	3.2	C
DS20-62	0.34	0.0477	0.0054	0.0714	0.0083	0.01085	0.00030			70.0	8.2	69.6	1.9	C
DS20-63	0.41	0.0447	0.0078	0.0655	0.0116	0.01063	0.00040			64.4	11.5	68.2	2.5	C
DS20-64	0.55	0.0490	0.0170	0.0709	0.0251	0.01049	0.00072			69.5	24.6	67.3	4.6	C
DS20-65	0.66	0.0557	0.0053	0.0792	0.0079	0.01031	0.00028			77.4	7.7	66.1	1.8	D
DS20-66	0.47	0.0541	0.0112	0.0783	0.0166	0.01049	0.00049			76.5	16.2	67.3	3.1	C

continued on next page

Spot No.	Th/U	$^{207}Pb/^{206}Pb$	Uncertainty 2SD	$^{207}Pb/^{235}U$	Uncertainty 2SD	$^{206}Pb/^{238}U$	Uncertainty 2SD	^{206}Pb-^{207}Pb (Ma)	Uncertainty 2SD	^{235}U-^{207}Pb (Ma)	Uncertainty 2SD	^{238}U-^{206}Pb (Ma)	Uncertainty 2SD	Memo
DS20-67	0.64	0.0383	0.0053	0.0586	0.0083	0.01109	0.00034			57.8	8.2	71.1	2.2	D
DS20-68	0.47	0.0455	0.0035	0.0655	0.0053	0.01046	0.00025			64.5	5.2	67.1	1.6	C
DS20-69	0.59	0.0505	0.0103	0.0795	0.0166	0.01141	0.00051			77.6	16.2	73.1	3.3	C
DS20-70	0.82	0.0620	0.0151	0.0945	0.0236	0.01106	0.00061			91.7	22.9	70.9	3.9	C
DS20-71	0.46	0.0484	0.0052	0.0800	0.0088	0.01198	0.00034			78.1	8.6	76.7	2.2	C
91500-01	0.34	0.0739	0.0050	1.7956	0.1289	0.17625	0.00394	1039.0	70.9	1043.8	74.9	1046.4	23.4	C
91500-02	0.34	0.0740	0.0049	1.8134	0.1280	0.17770	0.00417	1042.0	69.4	1050.3	74.1	1054.4	24.7	C
91500-03	0.35	0.0802	0.0055	1.9736	0.1482	0.17840	0.00556	1203.0	82.2	1106.5	83.1	1058.3	33.0	C
91500-04	0.34	0.0774	0.0050	1.8891	0.1273	0.17709	0.00331	1131.0	73.2	1077.2	72.6	1051.0	19.7	C
91500-05	0.35	0.0721	0.0049	1.7911	0.1336	0.18005	0.00543	991.0	67.6	1042.2	77.7	1067.2	32.2	C
91500-06	0.34	0.0747	0.0054	1.8895	0.1506	0.18358	0.00636	1060.0	76.1	1077.4	85.9	1086.5	37.6	C
91500-07	0.32	0.0807	0.0053	1.9399	0.1341	0.17441	0.00373	1214.0	79.8	1094.9	75.7	1036.4	22.2	C
91500-08	0.35	0.0832	0.0049	2.0527	0.1283	0.17896	0.00351	1274.0	75.6	1133.1	70.8	1061.3	20.8	D
91500-09	0.31	0.0743	0.0047	1.8179	0.1220	0.17752	0.00404	1049.0	66.3	1051.9	70.6	1053.4	23.9	C
91500-10	0.35	0.0711	0.0049	1.7770	0.1281	0.18125	0.00418	961.0	65.6	1037.1	74.7	1073.8	24.7	C
91500-11	0.35	0.0761	0.0046	1.8765	0.1212	0.17877	0.00375	1099.0	67.1	1072.8	69.3	1060.3	22.2	C
91500-12	0.34	0.0803	0.0050	1.9865	0.1317	0.17950	0.00387	1204.0	75.5	1110.9	73.6	1064.3	23.0	C
91500-13	0.34	0.0750	0.0049	1.8122	0.1240	0.17531	0.00382	1068.0	69.3	1049.8	71.8	1041.3	22.7	C
91500-14	0.34	0.0739	0.0049	1.8061	0.1287	0.17721	0.00433	1040.0	69.6	1047.6	74.6	1051.7	25.7	C
OD3-01	1.46	0.0427	0.0088	0.0328	0.0069	0.00557	0.00023			32.7	6.9	35.8	1.5	C
OD3-02	0.81	0.0514	0.0151	0.0364	0.0109	0.00514	0.00031			36.3	10.9	33.1	2.0	C
OD3-03	0.96	0.0558	0.0155	0.0392	0.0111	0.00510	0.00031			39.1	11.1	32.8	2.0	C
OD3-04	0.98	0.0464	0.0136	0.0332	0.0099	0.00518	0.00029			33.1	9.9	33.3	1.9	C
OD3-05	1.22	0.0406	0.0088	0.0280	0.0062	0.00500	0.00024			28.1	6.2	32.2	1.6	C
OD3-06	1.19	0.0437	0.0103	0.0297	0.0072	0.00493	0.00026			29.7	7.2	31.7	1.7	C
OD3-07	1.18	0.0419	0.0116	0.0285	0.0080	0.00493	0.00024			28.5	8.0	31.7	1.6	C
OD3-08	1.06	0.0375	0.0115	0.0262	0.0081	0.00506	0.00027			26.2	8.1	32.5	1.8	C
OD3-09	0.98	0.0521	0.0177	0.0379	0.0131	0.00527	0.00032			37.8	13.0	33.9	2.1	C
OD3-10	1.25	0.0464	0.0153	0.0314	0.0105	0.00492	0.00025			31.4	10.5	31.6	1.6	C
OD3-11	1.16	0.0531	0.0111	0.0363	0.0078	0.00496	0.00023			36.2	7.8	31.9	1.5	C
OD3-12	1.19	0.0466	0.0110	0.0315	0.0076	0.00490	0.00023			31.5	7.6	31.5	1.5	C
OD3-13	1.06	0.0506	0.0124	0.0352	0.0088	0.00504	0.00026			35.1	8.8	32.4	1.7	C
OD3-14	0.75	0.0486	0.0195	0.0322	0.0131	0.00481	0.00034			32.2	13.1	30.9	2.2	C

Ma (1.2%), 172–296 Ma (78.6%), 311–377 Ma (4.7%), 462–471 Ma (2.4%), 514 Ma (1.2%), 969 Ma (1.2%), and 1764–2161 Ma (7.1%) (Fig. 9C, 9D). %Pc was 8.3. The YSG was 106.7 ± 2.7 Ma, YC1σ (2 dates) was 107.5 ± 1.1 Ma (1σ). YC2σ (3 dates) was 109.3 ± 1.7 Ma (2σ; MSWD = 3.8, probability = 0.022; Fig. 9E), and the MLA was 107.2 ± 3.9 Ma (2σ) (Fig. 9F).

The Hinosan Mesozoic Formation

Siltstone of the Hinosan Mesozoic Formation (sample KD01)

The zircons from sample KD01 were commonly abraded and had anhedral to subhedral shapes (Fig. 10A). Most grains were colorless and exhibited oscillatory zoning, and three grains showed metamorphic rims in CL images. We obtained 97 U–Pb data sets from 97 zircon grains collected from this sample. The weighted mean of $^{206}Pb/^{238}U$ dates for 91500 zircon, analyzed alongside this sample, was 1054.2 ± 6.3 Ma (2σ). Its best estimate is approximately 0.77% younger than that of the recommended age. The weighted mean of $^{206}Pb/^{238}U$ dates for OD-3 zircon was 31.54 ± 0.3 Ma (2σ), with the best estimate being approximately 4.5% younger than that of the recommended age. Of the zircon grains analyzed from KD01, 61 grains yielded concordant results (Table 8; Fig. 10B). The $^{206}Pb/^{238}U$ dates obtained from concordant data sets formed four date groups and three single dates: 159–163 Ma (3 grains; 4.9% of 61 concordant grains), 174–229 Ma (32.8%), 246–280 Ma (14.8%), 398 Ma (1.6%), 415 Ma (1.6%), 1788–2304 Ma (42.7%), and 2966 Ma (1.6%) (Fig. 10C, 10D). %Pc was 44.3. The YSG was 159.8 ± 5.4 Ma, YC1σ (2 dates) was 162.7 ± 1.3 Ma (1σ). YC2σ (3 dates) was 162.7 ± 2.6 Ma (2σ; MSWD = 0.75, probability = 0.47; Fig. 10E), and the MLA was 163 ± 3 Ma (2σ) (Fig. 10F).

DISCUSSION

Depositional dates and characteristics of the studied strata

Metrics of the detrital zircon maximum depositional date (MDD)

When estimating the maximum depositional age of clastic rocks or the eruption age of volcanic rocks, the statistically most robust estimator is the maximum likelihood age (MLA: Vermeesch, 2021). However, if the age difference between the youngest and the second-youngest grains in a rock sample greatly exceeds their respective analytical uncertainties, the MLA solution collapses to the YSG (Vermeesch, 2021; Schwartz et al., 2022).

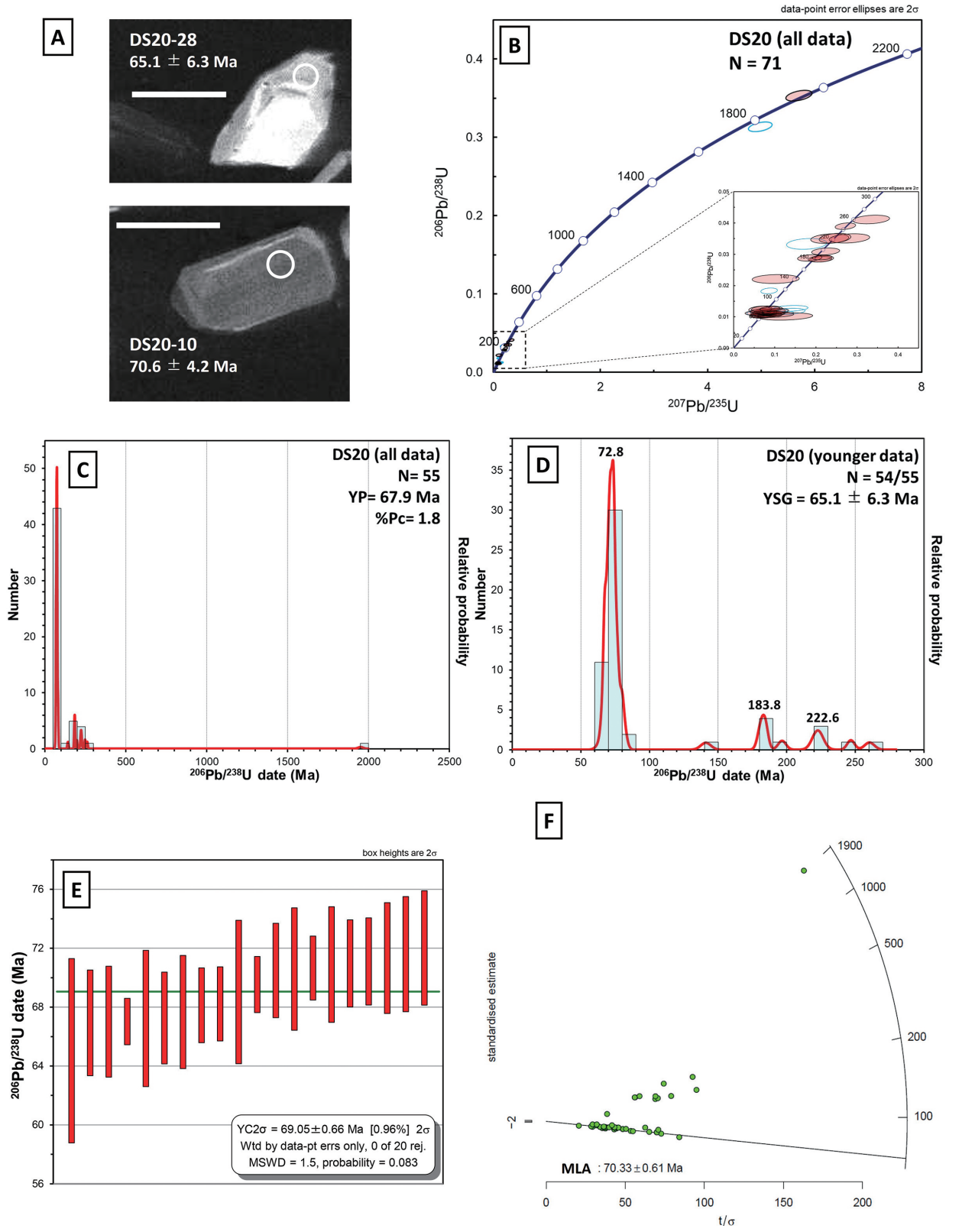

FIGURE 6. Analytical data of detrital zircons from sandstone of the upper part of the Sarao Alternation Member (sample DS20). **A**, Cathodoluminescence images of zircons (white scale bar = 100 μm). **B**, Concordia diagram for all data. **C**, Probability density plot with a histogram for all $^{206}Pb/^{238}U$ dates from concordant grains. **D**, Probability density plot with a histogram for younger $^{206}Pb/^{238}U$ dates. **E**, The weighted mean date (YC2σ) for the youngest cluster. **F**, Radial plots and MLA estimates.

TABLE 5. U–Pb isotopes and dates of zircons from sample KM01. Abbreviations: C: concordant data, D: discordant data.

Spot No.	Th/U	$^{207}Pb/^{206}Pb$	Uncertainty 2SD	$^{207}Pb/^{235}U$	Uncertainty 2SD	$^{206}Pb/^{238}U$	Uncertainty 2SD	^{206}Pb–^{207}Pb (Ma)	Uncertainty 2SD	^{235}U-^{207}Pb (Ma)	Uncertainty 2SD	^{238}U-^{206}Pb (Ma)	Uncertainty 2SD	Memo
KM01-001	0.26	0.0363	0.0114	0.1793	0.0577	0.03584	0.00223			167.5	53.8	227.0	14.1	D
KM01-002	0.26	0.1254	0.0037	5.6533	0.1857	0.32689	0.00485	2035.0	59.6	1924.2	63.2	1823.3	27.1	D
KM01-003	0.15	0.1154	0.0029	5.2744	0.1528	0.33158	0.00452	1886.0	48.2	1864.7	54.0	1846.0	25.2	C
KM01-004	0.63	0.0492	0.0038	0.2227	0.0178	0.03285	0.00066			204.2	16.3	208.3	4.2	C
KM01-005	1.21	0.0607	0.0080	0.5119	0.0697	0.06121	0.00211			419.7	57.1	383.0	13.2	C
KM01-006	0.19	0.1140	0.0019	5.1206	0.1052	0.32580	0.00406	1864.0	30.5	1839.5	37.8	1818.0	22.6	C
KM01-007	0.64	0.1096	0.0047	4.8323	0.2253	0.31974	0.00608	1793.0	76.3	1790.5	83.5	1788.5	34.0	C
KM01-008	0.70	0.1141	0.0034	2.1856	0.0729	0.13889	0.00213	1867.0	55.3	1176.4	39.2	838.4	12.9	D
KM01-009	0.54	0.0515	0.0129	0.0849	0.0218	0.01196	0.00066			82.7	21.2	76.6	4.2	C
KM01-010	0.61	0.0790	0.0138	0.1251	0.0227	0.01149	0.00056			119.7	21.7	73.6	3.6	D
KM01-011	0.61	0.1282	0.0039	2.1208	0.0726	0.11998	0.00188			1155.6	39.5	730.4	11.5	D
KM01-012	0.33	0.1147	0.0032	4.9805	0.1593	0.31479	0.00479	1876.0	52.8	1816.0	58.1	1764.2	26.8	D
KM01-013	0.84	0.1730	0.0216	0.2788	0.0375	0.01169	0.00059			249.7	33.6	74.9	3.8	D
KM01-014	0.51	0.0468	0.0057	0.0731	0.0092	0.01134	0.00035			71.7	9.0	72.7	2.2	C
KM01-015	1.01	0.0489	0.0080	0.0726	0.0122	0.01075	0.00041			71.1	12.0	68.9	2.7	C
KM01-016	0.21	0.0770	0.0026	1.7556	0.0685	0.16533	0.00326	1122.0	37.7	1029.2	40.1	986.3	19.5	D
KM01-017	0.76	0.0555	0.0071	0.2237	0.0296	0.02924	0.00098			204.9	27.1	185.8	6.3	C
KM01-018	0.60	0.0473	0.0053	0.2530	0.0291	0.03884	0.00113			229.0	26.4	245.6	7.2	C
KM01-019	0.20	0.1158	0.0022	5.1042	0.1366	0.31975	0.00593	1892.0	36.5	1836.7	49.2	1788.5	33.2	D
KM01-020	0.76	0.0615	0.0141	0.0938	0.0222	0.01106	0.00064			91.0	21.5	70.9	4.1	C
KM01-021	0.96	0.0597	0.0082	0.0878	0.0126	0.01067	0.00040			85.4	12.2	68.4	2.6	D
KM01-022	0.46	0.1148	0.0041	5.1644	0.2153	0.32631	0.00704	1877.0	66.9	1846.7	77.0	1820.5	39.3	C
KM01-023	0.49	0.1143	0.0036	4.4008	0.1651	0.27923	0.00581	1869.0	58.4	1712.4	64.3	1587.5	33.0	D
KM01-024	0.52	0.0597	0.0116	0.0847	0.0171	0.01030	0.00051			82.6	16.6	66.0	3.3	C
KM01-025	1.36	0.0505	0.0089	0.1776	0.0324	0.02552	0.00110			166.0	30.2	162.4	7.0	C
KM01-026	0.58	0.0652	0.0033	1.1453	0.0630	0.12745	0.00284			775.0	42.6	773.3	17.2	C
KM01-027	0.81	0.0598	0.0111	0.0899	0.0172	0.01091	0.00052			87.4	16.7	69.9	3.3	C
KM01-028	0.75	0.1134	0.0037	4.7604	0.2163	0.30453	0.00950	1855.0	61.3	1777.9	80.8	1713.7	53.5	D
KM01-029	0.67	0.0825	0.0222	0.1182	0.0330	0.01038	0.00078			113.4	31.7	66.6	5.0	D
KM01-030	0.48	0.0575	0.0080	0.2117	0.0308	0.02672	0.00116			195.0	28.3	170.0	7.4	C
KM01-031	0.37	0.0515	0.0050	0.2764	0.0287	0.03893	0.00142			247.8	25.7	246.2	9.0	C
KM01-032	0.56	0.0505	0.0057	0.0781	0.0094	0.01121	0.00043			76.3	9.2	71.9	2.8	C
KM01-033	0.55	0.0528	0.0038	0.2559	0.0205	0.03518	0.00119			231.3	18.5	222.9	7.5	C
KM01-034	0.79	0.0526	0.0066	0.0747	0.0097	0.01029	0.00033			73.1	9.5	66.0	2.1	C
KM01-035	0.37	0.0563	0.0081	0.1005	0.0149	0.01294	0.00048			97.2	14.5	82.9	3.1	C
KM01-036	0.85	0.0529	0.0070	0.0793	0.0109	0.01087	0.00037			77.5	10.6	69.7	2.4	C
KM01-037	0.49	0.0494	0.0058	0.0774	0.0094	0.01138	0.00035			75.7	9.2	72.9	2.2	C
KM01-038	0.59	0.0415	0.0077	0.0616	0.0117	0.01075	0.00043			60.7	11.5	68.9	2.8	C
KM01-039	0.81	0.0536	0.0072	0.2061	0.0285	0.02788	0.00096			190.3	26.3	177.2	6.1	C
KM01-040	0.53	0.0443	0.0118	0.0698	0.0190	0.01143	0.00064			68.5	18.7	73.2	4.1	C
KM01-041	0.41	0.0501	0.0061	0.0801	0.0101	0.01160	0.00037			78.2	9.9	74.3	2.4	C
KM01-042	0.48	0.0451	0.0055	0.0689	0.0087	0.01108	0.00034			67.6	8.6	71.0	2.2	C
KM01-043	0.72	0.0472	0.0103	0.0849	0.0190	0.01303	0.00063			82.7	18.5	83.4	4.0	C
KM01-044	1.38	0.0464	0.0065	0.2312	0.0335	0.03617	0.00124			211.2	30.6	229.0	7.8	C
KM01-045	0.61	0.0467	0.0104	0.0737	0.0168	0.01145	0.00056			72.2	16.5	73.4	3.6	C
KM01-046	0.50	0.0435	0.0043	0.0689	0.0071	0.01147	0.00031			67.6	6.9	73.5	2.0	C
KM01-047	0.33	0.0495	0.0065	0.0772	0.0105	0.01132	0.00038			75.5	10.3	72.6	2.4	C
KM01-048	0.47	0.0446	0.0085	0.0644	0.0126	0.01047	0.00044			63.3	12.4	67.2	2.8	C
KM01-049	0.81	0.0470	0.0162	0.0664	0.0232	0.01023	0.00065			65.2	22.8	65.6	4.2	C
KM01-050	0.50	0.0497	0.0048	0.1972	0.0198	0.02880	0.00081			182.8	18.4	183.1	5.1	C
KM01-051	0.45	0.0451	0.0045	0.0709	0.0074	0.01139	0.00032			69.5	7.2	73.0	2.0	C
KM01-052	0.44	0.0446	0.0243	0.0832	0.0458	0.01352	0.00115			81.1	44.6	86.6	7.4	C
KM01-053	0.24	0.0466	0.0033	0.1954	0.0147	0.03044	0.00073			181.2	13.6	193.3	4.7	C
KM01-054	0.43	0.0530	0.0059	0.1993	0.0231	0.02729	0.00084			184.5	21.4	173.6	5.4	C
KM01-055	0.67	0.0621	0.0092	0.0975	0.0148	0.01138	0.00042			94.4	14.4	72.9	2.7	D
KM01-056	0.35	0.6100	0.2753	34.9240	18.8154	0.41522	0.12219	4533.0	2045.6	3636.4	1959.1	2238.7	658.8	D
KM01-057	0.55	0.0468	0.0124	0.0696	0.0189	0.01080	0.00061			68.3	18.5	69.2	3.9	C
KM01-058	0.41	0.1213	0.0035	4.2969	0.1332	0.25695	0.00316	1976.0	56.2	1692.7	52.5	1474.2	18.1	D
KM01-059	0.31	0.0497	0.0047	0.2657	0.0256	0.03877	0.00089			239.2	23.1	245.2	5.6	C
KM01-060	0.46	0.0506	0.0060	0.0824	0.0101	0.01181	0.00036			80.4	9.8	75.7	2.3	C
KM01-061	0.04	0.1263	0.0021	5.9652	0.1456	0.34251	0.00601	2048.0	34.8	1970.7	48.1	1898.7	33.3	D
KM01-062	1.18	0.1595	0.0032	7.9905	0.2168	0.36336	0.00659	2451.0	49.5	2229.9	60.5	1998.1	36.2	D
KM01-063	0.36	0.1311	0.0033	6.8703	0.2164	0.37999	0.00712	2114.0	53.5	2094.8	66.0	2076.2	38.9	C
KM01-064	0.49	0.0506	0.0048	0.0774	0.0076	0.01109	0.00030			75.6	7.4	71.1	1.9	C
KM01-065	0.45	0.0451	0.0056	0.0727	0.0092	0.01168	0.00036			71.2	9.1	74.9	2.3	C
KM01-066	0.53	0.0495	0.0052	0.0753	0.0082	0.01102	0.00031			73.7	8.0	70.7	2.0	C

continued on next page

Spot No.	Th/U	$^{207}Pb/^{206}Pb$	Uncertainty 2SD	$^{207}Pb/^{235}U$	Uncertainty 2SD	$^{206}Pb/^{238}U$	Uncertainty 2SD	^{206}Pb-^{207}Pb (Ma)	Uncertainty 2SD	^{235}U-^{207}Pb (Ma)	Uncertainty 2SD	^{238}U-^{206}Pb (Ma)	Uncertainty 2SD	Memo
KM01-067	0.46	0.0497	0.0038	0.2704	0.0215	0.03943	0.00093			243.0	19.4	249.3	5.9	C
KM01-068	0.59	0.0464	0.0041	0.0723	0.0068	0.01129	0.00037			70.8	6.7	72.3	2.3	C
KM01-069	0.50	0.0459	0.0083	0.0725	0.0136	0.01146	0.00053			71.1	13.3	73.4	3.4	C
KM01-070	0.44	0.0537	0.0061	0.2488	0.0296	0.03363	0.00124			225.6	26.8	213.2	7.9	C
KM01-071	0.56	0.0483	0.0062	0.0744	0.0100	0.01117	0.00043			72.8	9.8	71.6	2.7	C
KM01-072	0.44	0.0509	0.0064	0.0858	0.0113	0.01224	0.00047			83.6	11.0	78.4	3.0	C
KM01-073	0.40	0.0561	0.0073	0.0967	0.0131	0.01250	0.00050			93.7	12.7	80.1	3.2	C
KM01-074	0.51	0.0556	0.0075	0.2342	0.0329	0.03058	0.00125			213.7	30.0	194.2	7.9	C
KM01-075	0.54	0.0482	0.0065	0.2548	0.0357	0.03837	0.00151			230.5	32.3	242.7	9.6	C
KM01-076	0.53	0.0780	0.0123	0.1215	0.0199	0.01130	0.00050			116.4	19.0	72.4	3.2	D
KM01-077	0.72	0.0461	0.0058	0.1697	0.0218	0.02669	0.00081			159.1	20.5	169.8	5.1	C
KM01-078	0.96	0.0572	0.0070	0.0849	0.0108	0.01076	0.00034			82.8	10.5	69.0	2.2	D
KM01-079	0.86	0.0423	0.0106	0.0640	0.0163	0.01099	0.00056			63.0	16.1	70.5	3.6	C
KM01-080	0.70	0.0541	0.0066	0.2143	0.0270	0.02872	0.00090			197.2	24.8	182.5	5.7	C
KM01-081	0.35	0.0614	0.0058	0.2418	0.0240	0.02856	0.00085			219.9	21.8	181.6	5.4	D
KM01-082	0.56	0.0472	0.0077	0.0730	0.0123	0.01122	0.00044			71.5	12.1	71.9	2.8	C
KM01-083	0.49	0.0535	0.0060	0.1770	0.0207	0.02399	0.00077			165.5	19.4	152.8	4.9	C
KM01-084	0.48	0.0537	0.0052	0.0859	0.0086	0.01160	0.00034			83.7	8.4	74.4	2.2	C
KM01-085	0.49	0.0547	0.0076	0.2657	0.0381	0.03520	0.00130			239.2	34.3	223.0	8.2	C
KM01-086	0.18	0.1119	0.0031	4.8552	0.1698	0.31473	0.00658	1831.0	51.3	1794.5	62.7	1763.9	36.9	C
KM01-087	0.60	0.0510	0.0048	0.0822	0.0080	0.01169	0.00033			80.2	7.8	74.9	2.1	C
KM01-088	0.04	0.0543	0.0036	0.2773	0.0192	0.03702	0.00084			248.5	17.2	234.3	5.3	C
KM01-089	0.66	0.0483	0.0067	0.2412	0.0345	0.03620	0.00124			219.4	31.3	229.2	7.8	C
KM01-090	0.40	0.0494	0.0040	0.1854	0.0156	0.02721	0.00067			172.7	14.6	173.1	4.2	C
KM01-091	0.09	0.1146	0.0031	5.3710	0.1759	0.33992	0.00632	1874.0	50.5	1880.2	61.6	1886.3	35.1	C
KM01-092	0.59	0.0502	0.0046	0.2449	0.0235	0.03537	0.00094			222.4	21.4	224.1	5.9	C
KM01-093	0.26	0.1136	0.0036	5.1932	0.1935	0.33147	0.00643			1851.4	69.0	1845.5	35.8	C
KM01-094	0.70	0.0455	0.0057	0.0743	0.0095	0.01184	0.00035			72.8	9.3	75.9	2.2	C
KM01-095	0.64	0.0688	0.0156	0.1139	0.0267	0.01202	0.00068			109.6	25.7	77.0	4.4	D
KM01-096	0.68	0.0506	0.0040	0.3115	0.0254	0.04468	0.00099			275.3	22.4	281.8	6.3	C
KM01-097	0.91	0.1150	0.0030	4.5499	0.1383	0.28685	0.00462			1740.1	52.9	1625.8	26.2	D
KM01-098	0.53	0.0167	0.0178	0.0228	0.0244	0.00992	0.00091			22.9	24.5	63.6	5.8	D
KM01-099	1.02	0.0516	0.0055	0.0760	0.0084	0.01069	0.00029			74.4	8.2	68.6	1.9	C
KM01-100	0.43	0.0453	0.0071	0.0698	0.0113	0.01117	0.00039			68.6	11.0	71.6	2.5	C
KM01-101	0.11	0.1296	0.0024	5.7422	0.1383	0.32147	0.00485	2092.0	39.3	1937.7	46.7	1796.9	27.1	D
91500-01	0.34	0.0739	0.0046	1.8181	0.1188	0.17845	0.00365	1039.0	64.5	1051.9	68.7	1058.5	21.6	C
91500-02	0.33	0.0768	0.0049	1.9323	0.1307	0.18249	0.00405	1116.0	71.3	1092.3	73.9	1080.5	24.0	C
91500-03	0.34	0.0735	0.0046	1.8171	0.1210	0.17936	0.00431	1028.0	63.8	1051.6	70.0	1063.5	25.5	C
91500-04	0.34	0.0780	0.0048	1.8655	0.1249	0.17336	0.00433	1149.0	71.4	1068.9	71.6	1030.6	25.7	C
91500-05	0.34	0.0770	0.0049	1.9246	0.1395	0.18136	0.00620	1121.0	71.6	1089.6	79.0	1074.4	36.7	C
91500-06	0.34	0.0755	0.0049	1.8377	0.1263	0.17664	0.00421	1081.0	69.7	1059.0	72.8	1048.6	25.0	C
91500-07	0.33	0.0753	0.0047	1.8640	0.1237	0.17948	0.00434	1078.0	66.6	1068.4	70.9	1064.1	25.7	C
91500-08	0.34	0.0718	0.0047	1.7471	0.1228	0.17640	0.00447	982.0	64.4	1026.0	72.1	1047.3	26.5	C
91500-09	0.34	0.0755	0.0051	1.8622	0.1304	0.17899	0.00363	1081.0	72.4	1067.7	74.7	1061.4	21.6	C
91500-10	0.33	0.0725	0.0046	1.7798	0.1206	0.17796	0.00421	1002.0	63.6	1038.1	70.3	1055.8	25.0	C
91500-11	0.34	0.0735	0.0046	1.8237	0.1283	0.17991	0.00572	1029.0	64.6	1054.0	74.2	1066.5	33.9	C
91500-12	0.34	0.0765	0.0048	1.9049	0.1266	0.18066	0.00417	1108.0	69.0	1082.8	71.9	1070.6	24.7	C
91500-13	0.33	0.0753	0.0049	1.8266	0.1281	0.17601	0.00457	1076.0	70.1	1055.0	74.0	1045.2	27.1	C
91500-14	0.33	0.0701	0.0049	1.7093	0.1256	0.17686	0.00436	932.0	64.5	1012.0	74.3	1049.8	25.9	C
91500-15	0.34	0.0730	0.0047	1.8044	0.1220	0.17917	0.00393	1016.0	65.0	1047.0	70.8	1062.4	23.3	C
OD3-01	1.11	0.0543	0.0121	0.0361	0.0083	0.00482	0.00025			36.0	8.3	31.0	1.6	C
OD3-02	0.74	0.0506	0.0161	0.0360	0.0117	0.00516	0.00035			35.9	11.7	33.2	2.2	C
OD3-03	0.95	0.0514	0.0162	0.0346	0.0111	0.00488	0.00032			34.6	11.1	31.4	2.0	C
OD3-04	1.14	0.0420	0.0094	0.0287	0.0066	0.00495	0.00024			28.7	6.6	31.8	1.5	C
OD3-05	1.14	0.0416	0.0109	0.0270	0.0073	0.00471	0.00027			27.1	7.3	30.3	1.7	C
OD3-06	0.94	0.0536	0.0136	0.0363	0.0094	0.00491	0.00029			36.2	9.4	31.6	1.9	C
OD3-07	0.87	0.0393	0.0140	0.0265	0.0096	0.00489	0.00032			26.5	9.6	31.4	2.1	C
OD3-08	0.88	0.0524	0.0178	0.0340	0.0118	0.00471	0.00031			34.0	11.8	30.3	2.0	C
OD3-09	1.11	0.0543	0.0105	0.0398	0.0079	0.00532	0.00024			39.6	7.9	34.2	1.5	C
OD3-10	0.92	0.0436	0.0151	0.0304	0.0107	0.00506	0.00035			30.4	10.7	32.6	2.2	C
OD3-11	1.05	0.0475	0.0107	0.0351	0.0082	0.00536	0.00029			35.1	8.1	34.5	1.9	C
OD3-12	0.89	0.0476	0.0175	0.0307	0.0115	0.00468	0.00035			30.7	11.5	30.1	2.2	C
OD3-13	1.05	0.0479	0.0104	0.0315	0.0070	0.00477	0.00024			31.5	7.0	30.7	1.5	C
OD3-14	1.01	0.0547	0.0105	0.0377	0.0074	0.00500	0.00023			37.5	7.4	32.1	1.5	C
OD3-15	0.91	0.0520	0.0129	0.0371	0.0094	0.00518	0.00028			37.0	9.4	33.3	1.8	C

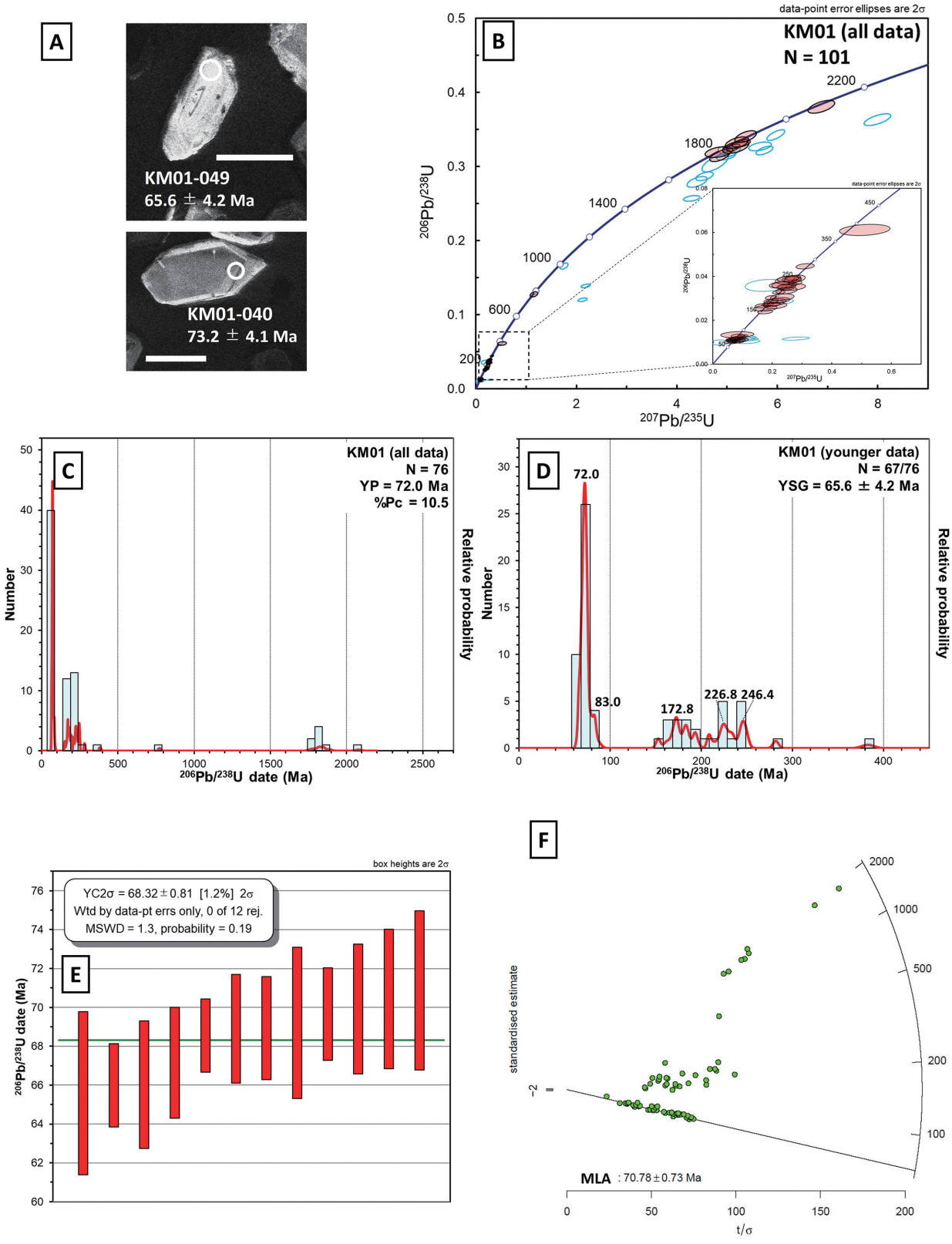

FIGURE 7. Analytical data of detrital zircons from sandstone of the Subara Formation (sample KM01). **A**, Cathodoluminescence images of zircons (white scale bar = 100 μm). **B**, Concordia diagram for all data. **C**, Probability density plot with a histogram for all $^{206}Pb/^{238}U$ dates from concordant grains. **D**, Probability density plot with a histogram for younger $^{206}Pb/^{238}U$ dates. **E**, The weighted mean date (YC2σ) for the youngest cluster. **F**, Radial plots and MLA estimates.

TABLE 6. U–Pb isotopes and dates of zircons from sample UM01-2. Abbreviations: C: concordant data, D: discordant data.

Spot No.	Th/U	$^{207}Pb/^{206}Pb$	Uncertainty 2SD	$^{207}Pb/^{235}U$	Uncertainty 2SD	$^{206}Pb/^{238}U$	Uncertainty 2SD	^{206}Pb–^{207}Pb (Ma)	Uncertainty 2SD	^{235}U–^{207}Pb (Ma)	Uncertainty 2SD	^{238}U–^{206}Pb (Ma)	Uncertainty 2SD	Memo
UM01-2-001	0.37	0.1129	0.0026	5.1906	0.1416	0.33341	0.00465	1847.0	43.3	1851.0	50.5	1854.9	25.9	C
UM01-2-002	0.18	0.1138	0.0030	5.0706	0.1517	0.32318	0.00471	1861.0	48.6	1831.1	54.8	1805.2	26.3	C
UM01-2-003	0.40	0.1139	0.0029	5.0462	0.1489	0.32129	0.00465	1863.0	47.9	1827.1	53.9	1796.0	26.0	C
UM01-2-004	0.16	0.1118	0.0027	4.8698	0.1365	0.31601	0.00445	1829.0	44.3	1797.0	50.4	1770.2	24.9	C
UM01-2-005	1.20	0.1386	0.0036	5.1329	0.1546	0.26868	0.00400	2210.0	57.9	1841.5	55.5	1534.1	22.8	D
UM01-2-006	0.31	0.0568	0.0055	0.3136	0.0314	0.04006	0.00102			277.0	27.8	253.2	6.5	C
UM01-2-007	0.37	0.0542	0.0031	0.2871	0.0172	0.03840	0.00069			256.2	15.4	242.9	4.4	C
UM01-2-008	0.65	0.1372	0.0015	7.2286	0.1224	0.38212	0.00500	2193.0	23.6	2140.0	36.2	2086.2	27.3	D
UM01-2-009	0.52	0.0493	0.0035	0.1985	0.0150	0.02923	0.00071			183.9	13.9	185.7	4.5	C
UM01-2-010	0.37	0.0745	0.0029	0.3388	0.0151	0.03300	0.00069	1054.0	41.3	296.2	13.2	209.3	4.4	D
UM01-2-011	0.66	0.1168	0.0037	3.5232	0.1324	0.21882	0.00450	1908.0	60.0	1532.4	57.6	1275.7	26.2	D
UM01-2-012	1.29	0.0537	0.0036	0.3525	0.0248	0.04758	0.00114			306.6	21.5	299.6	7.2	C
UM01-2-013	0.27	0.0543	0.0043	0.3104	0.0256	0.04146	0.00107			274.5	22.6	261.9	6.8	C
UM01-2-014	0.72	0.0557	0.0037	0.2998	0.0210	0.03903	0.00093			266.2	18.6	246.8	5.9	C
UM01-2-015	0.26	0.1139	0.0036	5.1037	0.1918	0.32513	0.00670	1862.0	58.5	1836.7	69.0	1814.7	37.4	C
UM01-2-016	0.40	0.1215	0.0035	5.0877	0.1796	0.30359	0.00612	1980.0	57.4	1834.0	64.7	1709.1	34.5	D
UM01-2-017	0.33	0.1139	0.0033	5.7099	0.2013	0.36363	0.00748	1863.0	53.3	1932.8	68.1	1999.4	41.1	D
UM01-2-018	0.20	0.1509	0.0044	7.8602	0.2818	0.37784	0.00789	2356.0	68.7	2215.1	79.4	2066.2	43.2	D
UM01-2-019	0.40	0.0555	0.0064	0.3004	0.0361	0.03928	0.00128			266.7	32.0	248.4	8.1	C
UM01-2-020	0.48	0.1213	0.0031	4.8689	0.1580	0.29103	0.00586	1976.0	50.3	1796.8	58.3	1646.7	33.1	D
UM01-2-021	0.78	0.0502	0.0033	0.2051	0.0142	0.02961	0.00071			189.4	13.2	188.1	4.5	C
UM01-2-022	0.22	0.1138	0.0031	5.0449	0.1710	0.32145	0.00654	1862.0	50.5	1826.8	61.9	1796.8	36.6	C
UM01-2-023	0.53	0.0550	0.0043	0.3114	0.0257	0.04109	0.00108			275.2	22.7	259.6	6.8	C
UM01-2-024	1.00	0.0552	0.0045	0.3732	0.0317	0.04900	0.00130			322.0	27.4	308.4	8.2	C
UM01-2-025	0.96	0.1197	0.0038	5.7654	0.3065	0.34922	0.01489	1953.0	62.0	1941.2	103.2	1930.9	82.4	C
UM01-2-026	0.54	0.0699	0.0055	0.4108	0.0372	0.04263	0.00196			349.4	31.6	269.1	12.4	D
UM01-2-027	0.28	0.0514	0.0059	0.2913	0.0362	0.04109	0.00200			259.6	32.2	259.6	12.6	C
UM01-2-028	0.45	0.0554	0.0021	0.5542	0.0316	0.07253	0.00308			447.8	25.5	451.4	19.2	C
UM01-2-029	0.23	0.1163	0.0034	5.4809	0.2826	0.34178	0.01450	1901.0	55.7	1897.5	97.8	1895.2	80.4	C
UM01-2-030	0.44	0.0605	0.0039	0.3829	0.0298	0.04590	0.00203			329.1	25.6	289.3	12.8	D
UM01-2-031	0.14	0.1144	0.0024	5.1090	0.2393	0.32401	0.01357	1870.0	39.2	1837.5	86.1	1809.3	75.8	C
UM01-2-032	0.98	0.0552	0.0045	0.2430	0.0227	0.03195	0.00145			220.9	20.7	202.7	9.2	C
UM01-2-033	0.37	0.1147	0.0029	5.5421	0.2461	0.35059	0.01277	1875.0	47.6	1907.1	84.7	1937.4	70.6	C
UM01-2-034	0.78	0.1375	0.0033	7.9988	0.3493	0.42187	0.01536	2197.0	53.0	2230.8	97.4	2269.0	82.6	C
UM01-2-035	0.69	0.0521	0.0061	0.3176	0.0395	0.04423	0.00194			280.0	34.8	279.0	12.2	C
UM01-2-036	0.41	0.0488	0.0020	0.3018	0.0166	0.04482	0.00165			267.8	14.7	282.7	10.4	D
UM01-2-037	0.23	0.1124	0.0023	4.6086	0.1904	0.29747	0.01073	1838.0	37.0	1750.8	72.3	1678.8	60.5	D
UM01-2-038	0.52	0.0499	0.0044	0.2847	0.0275	0.04135	0.00167			254.4	24.5	261.2	10.5	C
UM01-2-039	0.21	0.1118	0.0027	5.7835	0.2535	0.37522	0.01364	1829.0	44.8	1943.9	85.2	2053.9	74.7	D
UM01-2-040	0.62	0.0450	0.0046	0.1752	0.0185	0.02825	0.00075			163.9	17.3	179.6	4.7	C
UM01-2-041	0.61	0.5477	0.0118	29.3210	0.8327	0.38827	0.00719	4376.0	94.2	3464.2	98.4	2114.8	39.2	D
UM01-2-042	0.79	0.0490	0.0037	0.2021	0.0160	0.02991	0.00068			186.9	14.8	190.0	4.3	C
UM01-2-043	1.25	0.0598	0.0079	0.2421	0.0332	0.02936	0.00102			220.2	30.2	186.5	6.5	D
UM01-2-044	0.84	0.0543	0.0043	0.2193	0.0183	0.02928	0.00070			201.3	16.8	186.0	4.5	C
UM01-2-045	0.44	0.1222	0.0026	5.4324	0.1488	0.32253	0.00549	1988.0	42.7	1889.9	51.8	1802.1	30.7	D
UM01-2-046	0.22	0.0568	0.0052	0.3185	0.0304	0.04068	0.00107			280.7	26.8	257.0	6.8	C
UM01-2-047	0.61	0.0550	0.0026	0.3116	0.0159	0.04108	0.00079			275.4	14.1	259.6	5.0	D
UM01-2-048	0.35	0.0450	0.0031	0.1710	0.0124	0.02757	0.00065			160.3	11.6	175.3	4.1	D
UM01-2-049	0.62	0.0517	0.0077	0.3153	0.0484	0.04420	0.00166			278.2	42.7	278.8	10.5	C
UM01-2-050	0.77	0.0513	0.0038	0.2151	0.0168	0.03038	0.00075			197.8	15.5	192.9	4.8	C
UM01-2-051	0.10	0.1092	0.0020	3.4752	0.0926	0.23084	0.00447	1786.0	32.7	1521.5	40.6	1338.9	25.9	D
UM01-2-052	0.49	0.1135	0.0052	5.2475	0.2693	0.33531	0.00796	1857.0	84.5	1860.3	95.5	1864.1	44.3	C
UM01-2-053	0.46	0.1143	0.0029	5.1143	0.1650	0.32446	0.00656	1870.0	47.0	1838.4	59.3	1811.5	36.6	C
UM01-2-054	0.38	0.0768	0.0046	0.7498	0.0484	0.07077	0.00174	1117.0	66.7	568.1	36.7	440.8	10.8	D
UM01-2-055	0.40	0.0548	0.0041	0.2560	0.0203	0.03388	0.00086			231.4	18.4	214.8	5.4	C
UM01-2-056	1.11	0.1166	0.0024	5.4309	0.1432	0.33791	0.00543	1905.0	39.8	1889.7	49.8	1876.6	30.2	C
UM01-2-057	0.35	0.0870	0.0035	0.4581	0.0201	0.03820	0.00070	1360.0	54.1	382.9	16.8	241.7	4.5	D
UM01-2-058	0.85	0.0536	0.0028	0.2855	0.0159	0.03866	0.00073			255.0	14.2	244.5	4.6	C
UM01-2-059	0.31	0.0519	0.0030	0.2858	0.0175	0.03997	0.00078			255.2	15.6	252.6	4.9	C
UM01-2-060	0.60	0.0530	0.0031	0.2556	0.0157	0.03500	0.00069			231.1	14.2	221.8	4.4	C
UM01-2-061	0.28	0.1108	0.0028	5.1212	0.1535	0.33521	0.00557	1813.0	45.2	1839.6	55.1	1863.6	31.0	C
UM01-2-062	0.42	0.1144	0.0022	5.3707	0.1353	0.34047	0.00541	1871.0	36.6	1880.1	47.4	1888.9	30.0	C
UM01-2-063	0.35	0.1451	0.0022	8.5266	0.1836	0.42605	0.00658	2290.0	34.4	2288.7	49.3	2287.9	35.3	C
UM01-2-064	0.65	0.0528	0.0029	0.2066	0.0116	0.02838	0.00043			190.7	10.7	180.4	2.7	C
UM01-2-065	0.31	0.1236	0.0031	5.3630	0.1494	0.31470	0.00364	2009.0	50.9	1878.9	52.4	1763.8	20.4	D
UM01-2-066	0.23	0.0492	0.0036	0.2630	0.0196	0.03877	0.00070			237.1	17.7	245.2	4.5	C
UM01-2-067	0.35	0.1116	0.0028	4.9317	0.1344	0.32054	0.00363	1826.0	45.3	1807.6	49.3	1792.4	20.3	C
UM01-2-068	0.31	0.1188	0.0034	5.5912	0.1726	0.34136	0.00419	1939.0	54.9	1914.7	59.1	1893.2	23.3	C
UM01-2-069	0.63	0.1172	0.0038	5.3913	0.1884	0.33358	0.00444	1915.0	61.9	1883.4	65.8	1855.7	24.7	C
UM01-2-070	0.29	0.0555	0.0038	0.3021	0.0217	0.03948	0.00072			268.1	19.2	249.6	4.6	C

continued on next page

Spot No.	Th/U	$^{207}Pb/^{206}Pb$	Uncertainty 2SD	$^{207}Pb/^{235}U$	Uncertainty 2SD	$^{206}Pb/^{238}U$	Uncertainty 2SD	^{206}Pb-^{207}Pb (Ma)	Uncertainty 2SD	^{235}U-^{207}Pb (Ma)	Uncertainty 2SD	^{238}U-^{206}Pb (Ma)	Uncertainty 2SD	Memo
UM01-2-071	0.83	0.0498	0.0032	0.1719	0.0114	0.02502	0.00042			161.1	10.7	159.3	2.7	C
UM01-2-072	0.29	0.1307	0.0032	5.0041	0.1521	0.27765	0.00489	2108.0	52.2	1820.0	55.3	1579.5	27.8	D
UM01-2-073	0.48	0.1140	0.0029	5.0628	0.1582	0.32204	0.00569	1865.0	48.1	1829.8	57.2	1799.7	31.8	C
UM01-2-074	0.41	0.0562	0.0044	0.2102	0.0172	0.02715	0.00065			193.7	15.8	172.7	4.1	D
UM01-2-075	0.69	0.0539	0.0054	0.2983	0.0310	0.04012	0.00111			265.1	27.6	253.5	7.0	C
UM01-2-076	0.24	0.1153	0.0031	5.2471	0.1695	0.32993	0.00589	1886.0	50.8	1860.2	60.1	1838.0	32.8	C
UM01-2-077	0.37	0.0529	0.0038	0.3995	0.0300	0.05480	0.00124			341.3	25.6	343.9	7.8	C
UM01-2-078	0.34	0.1151	0.0029	5.1879	0.1585	0.32684	0.00574	1882.0	47.1	1850.6	56.5	1823.1	32.0	C
UM01-2-079	0.54	0.0681	0.0066	0.4201	0.0424	0.04477	0.00130			356.1	35.9	282.4	8.2	D
UM01-2-080	0.87	0.0573	0.0084	0.2504	0.0377	0.03172	0.00114			226.9	34.1	201.3	7.2	C
UM01-2-081	0.60	0.0477	0.0055	0.2567	0.0307	0.03907	0.00110			232.0	27.7	247.1	6.9	C
UM01-2-082	0.24	0.1128	0.0021	5.0477	0.1199	0.32460	0.00477	1845.0	34.4	1827.3	43.4	1812.2	26.6	C
UM01-2-083	0.43	0.1144	0.0030	5.5177	0.1699	0.34993	0.00567	1870.0	49.0	1903.3	58.6	1934.3	31.3	C
UM01-2-084	0.73	0.0473	0.0052	0.2024	0.0230	0.03104	0.00084			187.1	21.3	197.1	5.3	C
UM01-2-085	0.13	0.0565	0.0027	0.3366	0.0174	0.04319	0.00077			294.6	15.3	272.6	4.9	D
UM01-2-086	0.72	0.0514	0.0032	0.2606	0.0170	0.03678	0.00073			235.1	15.3	232.8	4.6	C
UM01-2-087	0.28	0.1190	0.0020	4.6288	0.1057	0.28213	0.00435	1942.0	32.7	1754.4	40.0	1602.1	24.7	D
UM01-2-088	0.46	0.0500	0.0035	0.2514	0.0182	0.03649	0.00079			227.7	16.5	231.0	5.0	C
UM01-2-089	0.78	0.0505	0.0060	0.2077	0.0255	0.02985	0.00091			191.6	23.5	189.6	5.8	C
UM01-2-090	0.55	0.1760	0.0051	11.3240	0.3927	0.46654	0.00874	2616.0	76.3	2550.1	88.4	2468.4	46.2	D
UM01-2-091	0.47	0.0650	0.0075	0.3563	0.0428	0.03974	0.00129			309.4	37.1	251.2	8.2	D
UM01-2-092	0.68	0.0532	0.0062	0.3159	0.0383	0.04305	0.00132			278.7	33.8	271.7	8.3	C
UM01-2-093	0.38	0.1173	0.0032	5.3424	0.1736	0.33029	0.00574	1916.0	52.6	1875.6	60.9	1839.8	32.0	C
UM01-2-094	0.13	0.1149	0.0034	5.5825	0.1926	0.35229	0.00629	1879.0	55.5	1913.3	66.0	1945.5	34.7	C
UM01-2-095	0.85	0.1141	0.0032	5.3238	0.1738	0.33850	0.00589	1866.0	51.5	1872.6	61.1	1879.4	32.7	C
UM01-2-096	0.42	0.0525	0.0033	0.2947	0.0200	0.04068	0.00103			262.3	17.8	257.0	6.5	C
UM01-2-097	0.52	0.1569	0.0051	9.0247	0.3609	0.41710	0.00973	2423.0	78.7	2340.4	93.6	2247.3	52.4	D
UM01-2-098	0.46	0.1420	0.0042	7.8738	0.2922	0.40216	0.00912	2252.0	66.2	2216.6	82.3	2179.0	49.4	C
UM01-2-099	0.32	0.0545	0.0025	0.2503	0.0130	0.03329	0.00079			226.8	11.7	211.1	5.0	D
UM01-2-100	0.66	0.0545	0.0041	0.2249	0.0180	0.02992	0.00081			206.0	16.5	190.0	5.2	C
UM01-2-101	0.46	0.1178	0.0038	3.5467	0.1408	0.21845	0.00502	1923.0	62.2	1537.6	61.0	1273.7	29.3	D
UM01-2-102	0.31	0.1168	0.0040	5.5895	0.2293	0.34694	0.00806	1909.0	64.6	1914.4	78.5	1920.0	44.6	C
UM01-2-103	0.36	0.0493	0.0047	0.1832	0.0182	0.02695	0.00079			170.8	17.0	171.4	5.0	C
UM01-2-104	0.56	0.0550	0.0039	0.2996	0.0221	0.03948	0.00090			266.1	19.6	249.6	5.7	C
UM01-2-105	0.75	0.0551	0.0100	0.2553	0.0478	0.03361	0.00145			230.9	43.2	213.1	9.2	C
UM01-2-106	0.25	0.0508	0.0035	0.2010	0.0145	0.02868	0.00064			186.0	13.4	182.3	4.0	C
UM01-2-107	0.35	0.1253	0.0031	6.8134	0.2079	0.39450	0.00703	2033.0	50.4	2087.4	63.7	2143.7	38.2	D
UM01-2-108	1.09	0.1352	0.0031	7.8186	0.2242	0.41944	0.00735	2167.0	49.2	2210.3	63.4	2258.0	39.6	D
UM01-2-109	0.23	0.1192	0.0078	6.3579	0.4499	0.38672	0.01042	1945.0	127.3	2026.4	143.4	2107.6	56.8	D
UM01-2-110	0.71	0.0500	0.0028	0.2759	0.0164	0.04006	0.00081			247.4	14.7	253.2	5.1	C
UM01-2-111	0.71	0.0498	0.0041	0.1869	0.0160	0.02724	0.00065			174.0	14.9	173.3	4.2	C
91500-01	0.25	0.0776	0.0057	1.8795	0.1443	0.17564	0.00421	1137.0	82.9	1073.9	82.4	1043.1	25.0	C
91500-02	0.25	0.0748	0.0056	1.8264	0.1467	0.17715	0.00495	1063.0	80.0	1054.9	84.7	1051.4	29.4	C
91500-03	0.25	0.0781	0.0058	1.9517	0.1551	0.18126	0.00502	1150.0	85.7	1099.0	87.4	1073.9	29.7	C
91500-04	0.25	0.0729	0.0056	1.8776	0.1675	0.18692	0.00862	1010.0	77.1	1073.2	95.7	1104.7	50.9	C
91500-05	0.25	0.0741	0.0056	1.8933	0.1631	0.18534	0.00757	1044.0	79.2	1078.7	92.9	1096.1	44.8	C
91500-06	0.26	0.0740	0.0056	1.8300	0.1455	0.17940	0.00456	1041.0	78.4	1056.2	84.0	1063.7	27.0	C
91500-07	0.25	0.0744	0.0054	1.8241	0.1405	0.17787	0.00476	1052.0	76.0	1054.1	81.2	1055.3	28.3	C
91500-08	0.26	0.0722	0.0054	1.7762	0.1394	0.17844	0.00435	992.0	74.0	1036.8	81.4	1058.4	25.8	C
91500-09	0.26	0.0821	0.0059	1.9675	0.1486	0.17380	0.00380	1248.0	90.2	1104.4	83.4	1033.0	22.6	D
91500-10	0.25	0.0781	0.0055	1.8545	0.1393	0.17218	0.00429	1150.0	81.5	1065.0	80.0	1024.1	25.5	C
91500-11	0.26	0.0746	0.0057	1.8288	0.1466	0.17791	0.00450	1057.0	80.4	1055.8	84.6	1055.5	26.7	C
91500-12	0.26	0.0780	0.0059	1.9084	0.1520	0.17754	0.00468	1146.0	86.1	1084.0	86.3	1053.5	27.8	C
91500-13	0.25	0.0738	0.0058	1.7940	0.1511	0.17621	0.00519	1038.0	81.9	1043.2	87.9	1046.2	30.8	C
91500-14	0.26	0.0766	0.0058	1.8375	0.1476	0.17393	0.00451	1112.0	84.5	1058.9	85.1	1033.7	26.8	C
OD3-01	0.71	0.0480	0.0132	0.0347	0.0098	0.00524	0.00030			34.7	9.7	33.7	1.9	C
OD3-02	1.22	0.0456	0.0091	0.0296	0.0061	0.00471	0.00021			29.7	6.1	30.3	1.4	C
OD3-03	0.95	0.0437	0.0091	0.0303	0.0064	0.00503	0.00023			30.3	6.4	32.3	1.5	C
OD3-04	0.91	0.0557	0.0118	0.0400	0.0088	0.00521	0.00033			39.8	8.8	33.5	2.1	C
OD3-05	0.84	0.0448	0.0181	0.0318	0.0130	0.00515	0.00040			31.8	13.0	33.1	2.6	C
OD3-06	0.79	0.0519	0.0170	0.0384	0.0129	0.00537	0.00037			38.3	12.8	34.5	2.4	C
OD3-07	0.75	0.0343	0.0147	0.0243	0.0106	0.00514	0.00037			24.4	10.6	33.0	2.4	C
OD3-08	0.71	0.0583	0.0208	0.0399	0.0145	0.00496	0.00037			39.7	14.5	31.9	2.4	C
OD3-09	0.87	0.0469	0.0125	0.0348	0.0095	0.00539	0.00030			34.8	9.5	34.7	1.9	C
OD3-10	1.19	0.0476	0.0087	0.0319	0.0060	0.00486	0.00020			31.8	6.0	31.2	1.3	C
OD3-11	0.85	0.0504	0.0144	0.0359	0.0104	0.00517	0.00030			35.9	10.4	33.3	1.9	C
OD3-12	0.44	0.0550	0.0133	0.0382	0.0095	0.00504	0.00028			38.0	9.4	32.4	1.8	C
OD3-13	0.85	0.0474	0.0099	0.0344	0.0074	0.00528	0.00025			34.4	7.4	33.9	1.6	C
OD3-14	1.12	0.0619	0.0114	0.0483	0.0091	0.00565	0.00026			47.9	9.1	36.3	1.7	D

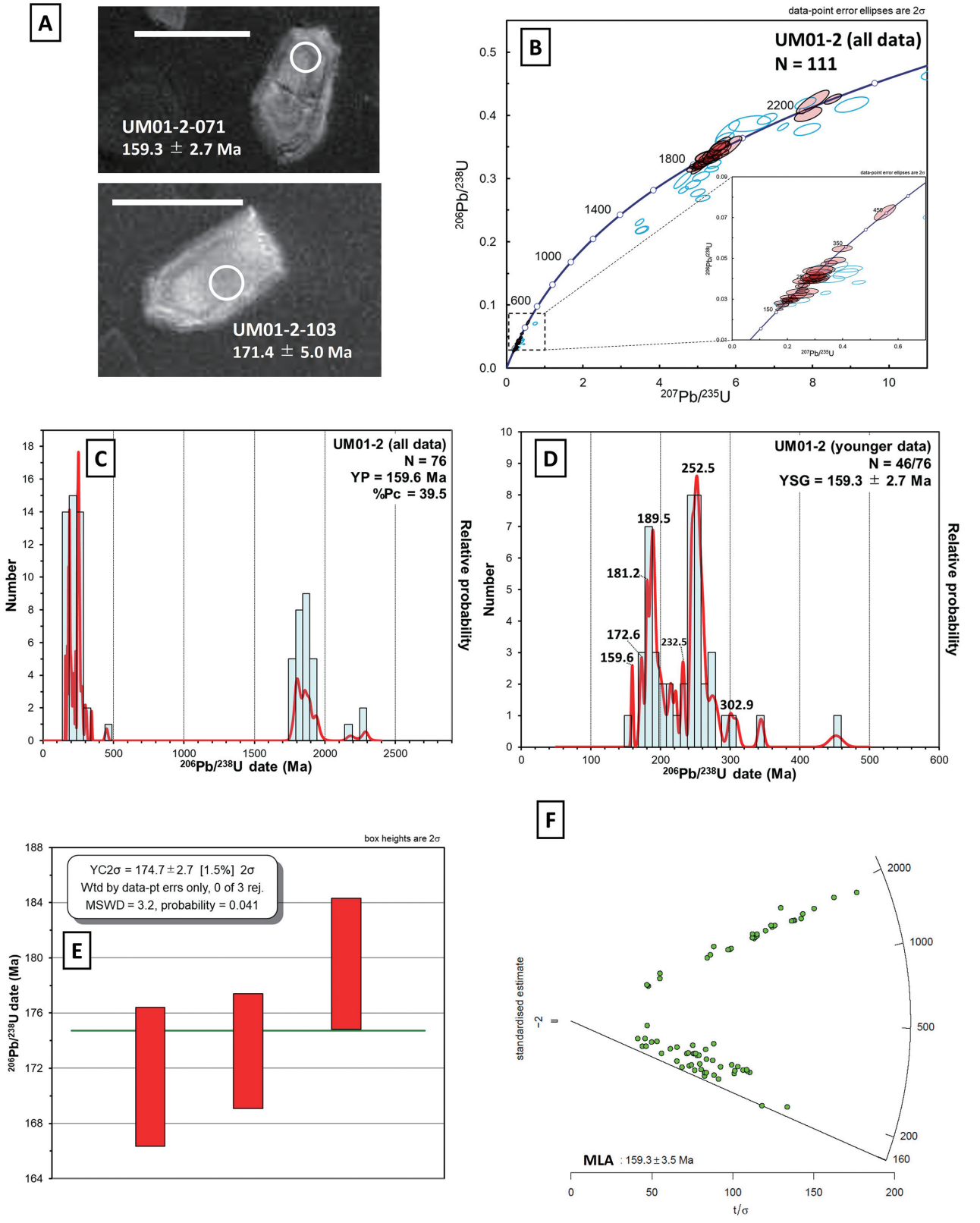

FIGURE 8. Analytical data of detrital zircons from sandstone of the lower part of the Sugo Formation (sample UM01-2). **A**, Cathodoluminescence images of zircons (white scale bar = 100 μm). **B**, Concordia diagram for all data. **C**, Probability density plot with a histogram for all $^{206}Pb/^{238}U$ dates from concordant grains. **D**, Probability density plot with a histogram for younger $^{206}Pb/^{238}U$ dates. **E**, The weighted mean date (YC2σ) for the youngest cluster. **F**, Radial plots and MLA estimates.

TABLE 7. U–Pb isotopes and dates of zircons from sample SG05. Abbreviations: C: concordant data, D: discordant data.

Spot No.	Th/U	$^{207}Pb/^{206}Pb$	Uncertainty 2SD	$^{207}Pb/^{235}U$	Uncertainty 2SD	$^{206}Pb/^{238}U$	Uncertainty 2SD	^{206}Pb-^{207}Pb (Ma)	Uncertainty 2SD	^{235}U-^{207}Pb (Ma)	Uncertainty 2SD	^{238}U-^{206}Pb (Ma)	Uncertainty 2SD	Memo
SG05-001	0.66	0.0503	0.0046	0.2335	0.0220	0.03367	0.00068			213.1	20.1	213.5	4.3	C
SG05-002	0.70	0.0481	0.0054	0.2887	0.0329	0.04357	0.00103			257.5	29.3	274.9	6.5	C
SG05-003	0.56	0.0559	0.0033	0.4475	0.0275	0.05809	0.00085			375.5	23.1	364.0	5.3	C
SG05-004	1.10	0.0668	0.0029	0.8607	0.0389	0.09340	0.00112			630.5	28.5	575.6	6.9	D
SG05-005	0.31	0.0509	0.0037	0.1976	0.0147	0.02817	0.00046			183.1	13.6	179.1	2.9	C
SG05-006	0.47	0.0534	0.0044	0.3005	0.0252	0.04084	0.00077			266.8	22.4	258.0	4.8	C
SG05-007	1.00	0.0500	0.0051	0.1981	0.0206	0.02874	0.00064			183.5	19.1	182.6	4.1	C
SG05-008	0.56	0.0470	0.0063	0.1754	0.0241	0.02708	0.00074			164.1	22.6	172.2	4.7	C
SG05-009	0.48	0.0542	0.0032	0.6213	0.0396	0.08312	0.00211			490.7	31.3	514.7	13.1	C
SG05-010	1.17	0.0524	0.0069	0.2187	0.0299	0.03030	0.00107			200.8	27.5	192.4	6.8	C
SG05-011	0.33	0.1160	0.0022	5.6355	0.1666	0.35237	0.00788	1896.0	36.7	1921.5	56.8	1945.9	43.5	C
SG05-012	0.67	0.0599	0.0072	0.2231	0.0278	0.02701	0.00094			204.5	25.5	171.8	6.0	D
SG05-013	0.66	0.0588	0.0054	0.3359	0.0325	0.04141	0.00126			294.0	28.5	261.6	7.9	D
SG05-014	0.36	0.0527	0.0034	0.2608	0.0182	0.03588	0.00093			235.3	16.4	227.2	5.9	C
SG05-015	0.41	0.0497	0.0031	0.1999	0.0134	0.02916	0.00074			185.0	12.4	185.3	4.7	C
SG05-016	0.83	0.2371	0.0040	16.2379	0.4034	0.49663	0.00899	3101.0	52.8	2890.8	71.8	2599.3	47.0	D
SG05-017	0.67	0.0458	0.0049	0.3158	0.0349	0.05005	0.00132			278.7	30.8	314.8	8.3	D
SG05-018	0.25	0.0476	0.0069	0.2676	0.0395	0.04079	0.00126			240.8	35.5	257.7	8.0	C
SG05-019	0.57	0.0535	0.0048	0.2610	0.0243	0.03540	0.00090			235.4	22.0	224.2	5.7	C
SG05-020	0.35	0.1347	0.0038	7.3981	0.2520	0.39827	0.00780	2161.0	60.2	2160.7	73.6	2161.1	42.3	C
SG05-021	1.07	0.0668	0.0042	0.2658	0.0179	0.02887	0.00066			239.3	16.1	183.5	4.2	D
SG05-022	0.69	0.1125	0.0025	4.8247	0.1414	0.31105	0.00578	1841.0	41.7	1789.1	52.4	1745.9	32.4	D
SG05-023	0.68	0.0859	0.0112	0.4227	0.0573	0.03569	0.00128			358.0	48.6	226.1	8.1	D
SG05-024	0.36	0.0505	0.0030	0.2004	0.0137	0.02877	0.00102			185.5	12.7	182.8	6.5	C
SG05-025	0.73	0.0501	0.0039	0.2291	0.0198	0.03317	0.00123			209.4	18.1	210.4	7.8	C
SG05-026	0.60	0.0524	0.0034	0.3070	0.0227	0.04248	0.00153			271.8	20.1	268.2	9.7	C
SG05-027	0.75	0.0543	0.0078	0.3213	0.0484	0.04293	0.00190			282.9	42.6	270.9	12.0	C
SG05-028	0.28	0.0576	0.0095	0.3340	0.0575	0.04204	0.00199			292.6	50.4	265.5	12.5	C
SG05-029	0.75	0.0484	0.0038	0.1139	0.0098	0.01707	0.00063			109.6	9.5	109.1	4.0	C
SG05-030	0.56	0.2173	0.0061	18.2243	0.6264	0.60816	0.01195	2962.0	83.5	3001.5	103.2	3062.6	60.2	D
SG05-031	0.60	0.0554	0.0051	0.3372	0.0323	0.04416	0.00115			295.0	28.3	278.6	7.2	C
SG05-032	1.04	0.0522	0.0103	0.2785	0.0559	0.03868	0.00149			249.5	50.1	244.6	9.4	C
SG05-033	0.94	0.0557	0.0029	0.4621	0.0261	0.06022	0.00125			385.7	21.8	377.0	7.8	C
SG05-034	0.40	0.0551	0.0163	0.3164	0.0953	0.04169	0.00208			279.2	84.0	263.3	13.1	C
SG05-035	1.03	0.0736	0.0041	0.5088	0.0305	0.05013	0.00110			417.6	25.0	315.3	6.9	D
SG05-036	0.55	0.0721	0.0035	0.5642	0.0300	0.05671	0.00119			454.2	24.1	355.6	7.4	D
SG05-037	0.60	0.0459	0.0059	0.2360	0.0313	0.03733	0.00109			215.1	28.6	236.3	6.9	C
SG05-038	1.12	0.0504	0.0063	0.1883	0.0243	0.02711	0.00082			175.2	22.6	172.4	5.2	C
SG05-039	0.93	0.0533	0.0112	0.3456	0.0739	0.04706	0.00193			301.4	64.5	296.4	12.2	C
SG05-040	0.56	0.0524	0.0053	0.2063	0.0216	0.02854	0.00079			190.4	20.0	181.4	5.0	C
SG05-041	0.37	0.0529	0.0040	0.3100	0.0249	0.04249	0.00104			274.2	22.0	268.2	6.6	C
SG05-042	0.10	0.1215	0.0032	6.1438	0.2029	0.36673	0.00715	1979.0	52.7	1996.4	65.9	2014.0	39.3	C
SG05-043	0.07	0.0531	0.0031	0.2993	0.0188	0.04087	0.00092			265.8	16.7	258.2	5.8	C
SG05-044	0.62	0.0998	0.0046	0.5523	0.0286	0.04013	0.00091			446.5	23.1	253.7	5.7	D
SG05-045	0.32	0.1115	0.0039	4.9530	0.2020	0.32226	0.00669	1824.0	64.0	1811.3	73.9	1800.8	37.4	C
SG05-046	0.49	0.0632	0.0030	0.7238	0.0381	0.08305	0.00182			552.9	29.1	514.3	11.3	D
SG05-047	0.36	0.0403	0.0073	0.1211	0.0224	0.02182	0.00081			116.1	21.5	139.1	5.2	C
SG05-048	0.26	0.1130	0.0042	5.6418	0.2413	0.36221	0.00767	1848.0	68.7	1922.4	82.2	1992.7	42.2	D
SG05-049	0.71	0.0529	0.0043	0.2289	0.0195	0.03138	0.00081			209.3	17.8	199.2	5.2	C
SG05-050	0.64	0.0410	0.0086	0.2306	0.0493	0.04083	0.00168			210.7	45.1	258.0	10.6	C
SG05-051	0.38	0.0584	0.0163	0.2570	0.0736	0.03193	0.00191			232.2	66.5	202.6	12.1	C
SG05-052	0.36	0.0636	0.0044	0.2454	0.0182	0.02796	0.00080			222.8	16.5	177.8	5.1	D
SG05-053	0.36	0.0537	0.0035	0.2709	0.0193	0.03656	0.00101			243.4	17.3	231.5	6.4	C
SG05-054	0.39	0.0587	0.0060	0.2208	0.0236	0.02727	0.00090			202.6	21.7	173.4	5.7	D
SG05-055	0.69	0.0595	0.0037	0.3138	0.0214	0.03824	0.00105			277.1	18.9	241.9	6.7	D
SG05-056	0.93	0.0553	0.0028	0.2801	0.0162	0.03675	0.00096			250.8	14.5	232.7	6.1	C
SG05-057	0.84	0.1164	0.0041	5.3620	0.2323	0.33411	0.00858	1902.0	66.4	1878.7	81.4	1858.3	47.7	C
SG05-058	0.44	0.0520	0.0062	0.2309	0.0285	0.03223	0.00111			210.9	26.0	204.5	7.0	C
SG05-059	0.71	0.0568	0.0033	0.5815	0.0362	0.07431	0.00164			465.4	29.0	462.1	10.2	C
SG05-060	0.78	0.0485	0.0055	0.2099	0.0245	0.03138	0.00090			193.4	22.6	199.2	5.7	C
SG05-061	0.80	0.0506	0.0073	0.2806	0.0413	0.04025	0.00134			251.1	37.0	254.4	8.4	C
SG05-062	0.33	0.1154	0.0108	0.5854	0.0581	0.03679	0.00123			467.9	46.4	232.9	7.8	D
SG05-063	0.57	0.0516	0.0060	0.2315	0.0279	0.03255	0.00097			211.4	25.5	206.5	6.1	C
SG05-064	0.57	0.0517	0.0056	0.2992	0.0337	0.04194	0.00142			265.8	29.9	264.9	8.9	C
SG05-065	0.25	0.1129	0.0037	4.9042	0.2060	0.31492	0.00840	1848.0	60.0	1802.9	75.7	1764.9	47.1	C
SG05-066	0.42	0.1265	0.0039	7.0231	0.2841	0.40270	0.01068	2050.0	62.6	2114.3	85.5	2181.5	57.9	D
SG05-067	0.96	0.0395	0.0062	0.1837	0.0295	0.03378	0.00125			171.3	27.5	214.2	7.9	D
SG05-068	0.43	0.0773	0.0027	0.6857	0.0303	0.06437	0.00172			530.2	23.4	402.2	10.7	D
SG05-069	0.35	0.0554	0.0037	0.2812	0.0203	0.03683	0.00108			251.6	18.2	233.1	6.8	C
SG05-070	0.48	0.0365	0.0069	0.0851	0.0165	0.01690	0.00067			83.0	16.1	108.1	4.3	D
SG05-071	0.95	0.0493	0.0047	0.3359	0.0339	0.04942	0.00159			294.1	29.7	311.0	10.0	C
SG05-072	0.29	0.0526	0.0051	0.2986	0.0298	0.04115	0.00108			265.3	26.5	259.9	6.8	C
SG05-073	0.33	0.0506	0.0065	0.2786	0.0366	0.03995	0.00119			249.5	32.8	252.5	7.5	C

continued on next page

Spot No.	Th/U	$^{207}Pb/^{206}Pb$	Uncertainty 2SD	$^{207}Pb/^{235}U$	Uncertainty 2SD	$^{206}Pb/^{238}U$	Uncertainty 2SD	^{206}Pb-^{207}Pb (Ma)	Uncertainty 2SD	^{235}U-^{207}Pb (Ma)	Uncertainty 2SD	^{238}U-^{206}Pb (Ma)	Uncertainty 2SD	Memo
SG05-074	1.04	0.0549	0.0029	0.5743	0.0328	0.07591	0.00163			460.8	26.3	471.6	10.1	C
SG05-075	0.89	0.0517	0.0031	0.3724	0.0236	0.05221	0.00115			321.4	20.3	328.1	7.2	C
SG05-076	0.33	0.0501	0.0089	0.2954	0.0535	0.04276	0.00149			262.8	47.6	269.9	9.4	C
SG05-077	0.15	0.0525	0.0042	0.2896	0.0241	0.03999	0.00099			258.2	21.5	252.7	6.3	C
SG05-078	0.42	0.0521	0.0045	0.2244	0.0213	0.03123	0.00120			205.5	19.5	198.3	7.6	C
SG05-079	0.56	0.0551	0.0108	0.3365	0.0681	0.04431	0.00235			294.5	59.6	279.5	14.8	C
SG05-080	0.43	0.0528	0.0042	0.3008	0.0264	0.04135	0.00156			267.0	23.4	261.2	9.9	C
SG05-081	0.54	0.0524	0.0044	0.3228	0.0295	0.04468	0.00170			284.1	25.9	281.7	10.7	C
SG05-082	0.57	0.0563	0.0065	0.3287	0.0403	0.04234	0.00179			288.5	35.4	267.3	11.3	C
SG05-083	0.52	0.0514	0.0045	0.1952	0.0187	0.02752	0.00106			181.0	17.4	175.0	6.7	C
SG05-084	0.22	0.1095	0.0027	3.0683	0.0824	0.20331	0.00209	1791.0	44.4	1424.8	38.2	1193.1	12.3	D
SG05-085	0.66	0.0504	0.0035	0.1921	0.0138	0.02768	0.00047			178.5	12.8	176.0	3.0	C
SG05-086	0.42	0.0421	0.0051	0.1018	0.0127	0.01755	0.00044			98.5	12.3	112.1	2.8	C
SG05-087	0.36	0.0565	0.0037	0.3405	0.0231	0.04368	0.00073			297.5	20.2	275.6	4.6	C
SG05-088	0.51	0.0509	0.0050	0.2378	0.0242	0.03391	0.00077			216.6	22.1	215.0	4.9	C
SG05-089	0.29	0.0501	0.0039	0.3022	0.0242	0.04375	0.00080			268.1	21.5	276.0	5.1	C
SG05-090	0.73	0.0520	0.0035	0.2334	0.0160	0.03258	0.00053			213.0	14.6	206.7	3.4	C
SG05-091	0.45	0.1172	0.0028	4.6709	0.1212	0.28905	0.00295	1914.0	45.7	1762.0	45.7	1636.8	16.7	D
SG05-092	0.66	0.0562	0.0063	0.3168	0.0364	0.04091	0.00110			279.4	32.1	258.5	6.9	C
SG05-093	0.72	0.0506	0.0058	0.3108	0.0368	0.04456	0.00118			274.8	32.5	281.1	7.4	C
SG05-094	1.22	0.0644	0.0063	1.4409	0.1448	0.16224	0.00416			906.1	91.1	969.2	24.9	C
SG05-095	0.37	0.1091	0.0043	4.4551	0.1899	0.29621	0.00463	1785.0	70.8	1722.6	73.4	1672.5	26.2	D
SG05-096	0.44	0.0471	0.0038	0.1849	0.0152	0.02845	0.00056			172.2	14.2	180.8	3.6	C
SG05-097	0.73	0.0977	0.0098	0.3907	0.0409	0.02899	0.00089			334.8	35.0	184.2	5.6	D
SG05-098	0.40	0.0495	0.0036	0.1935	0.0147	0.02833	0.00054			179.6	13.6	180.1	3.4	C
SG05-099	0.24	0.0479	0.0034	0.1943	0.0143	0.02940	0.00059			180.3	13.2	186.8	3.8	C
SG05-100	0.47	0.0537	0.0049	0.2433	0.0231	0.03288	0.00077			221.1	21.0	208.5	4.9	C
SG05-101	0.39	0.0480	0.0054	0.1106	0.0127	0.01670	0.00042			106.5	12.2	106.7	2.7	C
SG05-102	0.47	0.0492	0.0052	0.2827	0.0307	0.04165	0.00103			252.8	27.4	263.0	6.5	C
SG05-103	0.26	0.0411	0.0199	0.2332	0.1136	0.04114	0.00228			212.8	103.7	259.9	14.4	C
SG05-104	0.31	0.0522	0.0128	0.1976	0.0493	0.02745	0.00114			183.1	45.7	174.6	7.2	C
SG05-105	0.33	0.0497	0.0071	0.2726	0.0397	0.03981	0.00117			244.7	35.7	251.7	7.4	C
SG05-106	0.49	0.0506	0.0048	0.2170	0.0214	0.03109	0.00073			199.4	19.6	197.4	4.7	C
SG05-107	0.38	0.0592	0.0085	0.3219	0.0491	0.03947	0.00196			283.4	43.2	249.5	12.4	C
SG05-108	0.35	0.0441	0.0089	0.2333	0.0487	0.03836	0.00206			212.9	44.4	242.6	13.0	C
SG05-109	1.24	0.0658	0.0115	0.2728	0.0502	0.03010	0.00168			245.0	45.1	191.1	10.7	D
SG05-110	0.38	0.0551	0.0036	0.3300	0.0254	0.04342	0.00173			289.5	22.2	274.0	10.9	C
SG05-111	0.39	0.0570	0.0029	0.2286	0.0146	0.02908	0.00113			209.0	13.4	184.8	7.2	D
SG05-112	0.32	0.0526	0.0035	0.2946	0.0228	0.04060	0.00161			262.2	20.3	256.6	10.2	C
SG05-113	0.25	0.1248	0.0028	5.8659	0.2554	0.34101	0.01274	2026.0	45.4	1956.1	85.2	1891.5	70.6	D
91500-01	0.31	0.0764	0.0048	1.8874	0.1223	0.17914	0.00325	1106.0	68.8	1076.6	69.8	1062.3	19.3	C
91500-02	0.33	0.0731	0.0047	1.7720	0.1233	0.17586	0.00490	1017.0	64.9	1035.2	72.0	1044.3	29.1	C
91500-03	0.35	0.0775	0.0050	1.9219	0.1316	0.17985	0.00431	1135.0	72.8	1088.7	74.5	1066.2	25.6	C
91500-04	0.34	0.0788	0.0051	1.9883	0.1490	0.18299	0.00685	1168.0	75.8	1111.5	83.3	1083.3	40.5	C
91500-05	0.31	0.0732	0.0052	1.8205	0.1365	0.18036	0.00444	1020.0	72.2	1052.8	78.9	1068.9	26.3	C
91500-06	0.33	0.0770	0.0055	1.9119	0.1461	0.18005	0.00467	1122.0	80.7	1085.2	83.0	1067.3	27.7	C
91500-07	0.33	0.0743	0.0053	1.8587	0.1409	0.18155	0.00476	1049.0	74.6	1066.5	80.9	1075.4	28.2	C
91500-08	0.34	0.0770	0.0049	1.8599	0.1288	0.17525	0.00503	1121.0	70.7	1066.9	73.9	1041.0	29.9	C
91500-09	0.34	0.0720	0.0047	1.7779	0.1246	0.17911	0.00435	986.0	64.8	1037.4	72.7	1062.1	25.8	C
91500-10	0.34	0.0767	0.0052	1.9027	0.1413	0.17994	0.00552	1114.0	75.3	1082.0	80.3	1066.6	32.7	C
91500-11	0.34	0.0727	0.0052	1.8076	0.1361	0.18028	0.00460	1007.0	71.3	1048.2	78.9	1068.5	27.3	C
91500-12	0.32	0.0796	0.0060	1.8987	0.1618	0.17298	0.00676	1188.0	90.0	1080.6	92.1	1028.5	40.2	C
91500-13	0.32	0.0746	0.0049	1.8511	0.1257	0.17999	0.00337	1058.0	69.0	1063.8	72.2	1066.9	20.0	C
91500-14	0.34	0.0707	0.0047	1.7533	0.1222	0.17982	0.00359	950.0	63.4	1028.3	71.7	1066.0	21.3	C
91500-15	0.35	0.0742	0.0048	1.8105	0.1235	0.17707	0.00382	1046.0	67.7	1049.2	71.6	1050.9	22.7	C
91500-16	0.33	0.0739	0.0052	1.8070	0.1480	0.17729	0.00732	1040.0	73.6	1047.9	85.9	1052.1	43.4	C
OD3-01	1.08	0.0323	0.0115	0.0224	0.0080	0.00503	0.00023			22.5	8.1	32.3	1.5	D
OD3-02	0.93	0.0425	0.0116	0.0295	0.0082	0.00504	0.00025			29.6	8.2	32.4	1.6	C
OD3-03	1.34	0.0506	0.0111	0.0361	0.0080	0.00518	0.00020			36.0	8.0	33.3	1.3	C
OD3-04	1.31	0.0509	0.0110	0.0352	0.0078	0.00501	0.00025			35.1	7.8	32.2	1.6	C
OD3-05	1.36	0.0521	0.0113	0.0356	0.0078	0.00496	0.00020			35.6	7.8	31.9	1.3	C
OD3-06	1.36	0.0429	0.0109	0.0308	0.0080	0.00522	0.00022			30.8	8.0	33.5	1.4	C
OD3-07	1.33	0.0460	0.0097	0.0334	0.0072	0.00526	0.00023			33.4	7.2	33.8	1.5	C
OD3-08	1.32	0.0425	0.0085	0.0295	0.0060	0.00503	0.00022			29.5	6.0	32.3	1.4	C
OD3-09	1.34	0.0491	0.0105	0.0337	0.0073	0.00497	0.00021			33.6	7.3	32.0	1.3	C
OD3-10	1.26	0.0414	0.0112	0.0286	0.0079	0.00501	0.00025			28.6	7.9	32.2	1.6	C
OD3-11	1.38	0.0477	0.0097	0.0318	0.0066	0.00483	0.00017			31.8	6.5	31.1	1.1	C
OD3-12	1.37	0.0422	0.0071	0.0292	0.0051	0.00502	0.00023			29.2	5.1	32.3	1.5	C
OD3-13	1.35	0.0442	0.0065	0.0317	0.0048	0.00520	0.00016			31.6	4.8	33.4	1.0	C
OD3-14	1.30	0.0497	0.0076	0.0354	0.0055	0.00516	0.00017			35.3	5.5	33.2	1.1	C
OD3-15	1.29	0.0473	0.0087	0.0339	0.0063	0.00521	0.00017			33.9	6.3	33.5	1.1	C
OD3-16	1.35	0.0478	0.0077	0.0344	0.0058	0.00523	0.00026			34.4	5.8	33.6	1.7	C

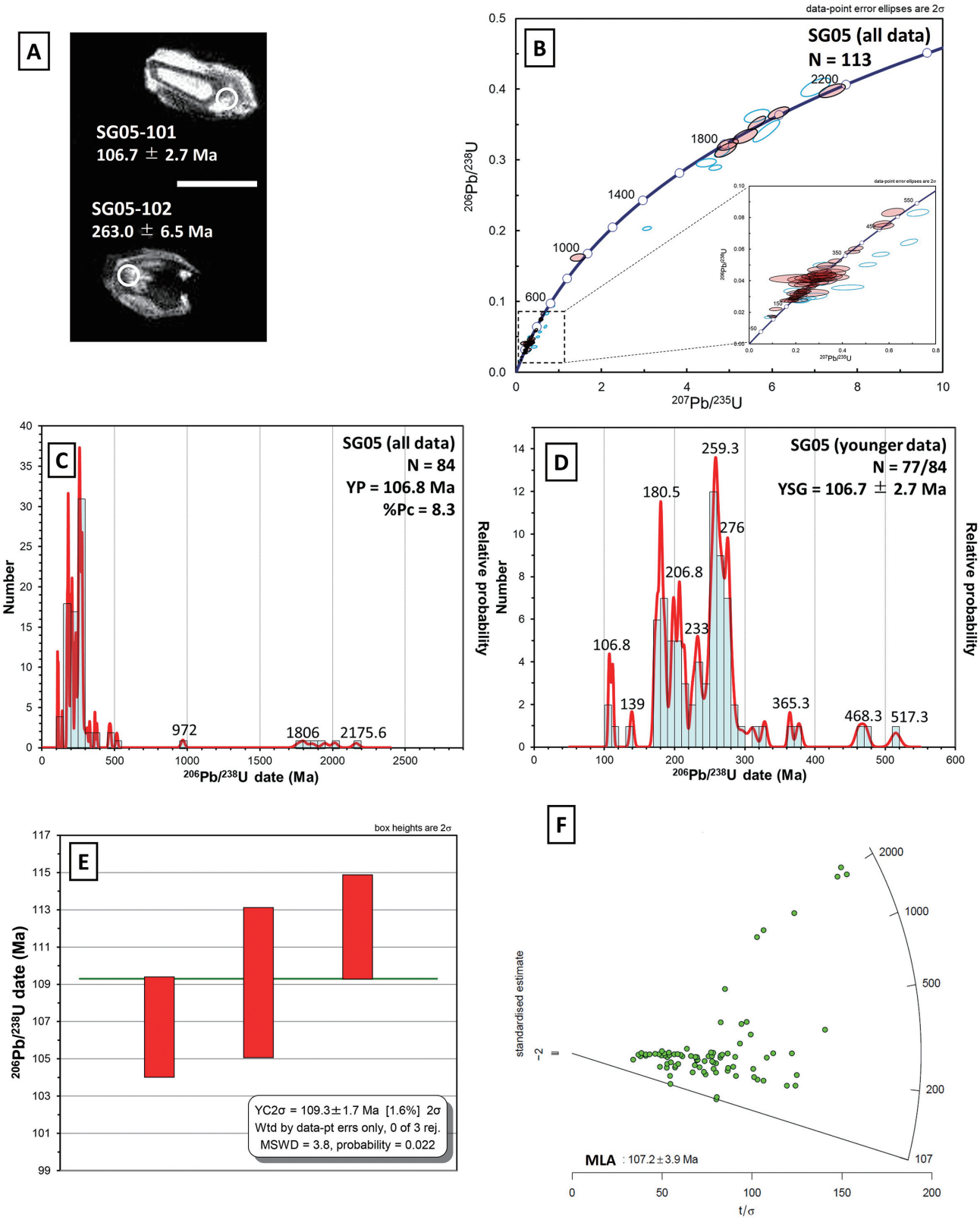

FIGURE 9. Analytical data of detrital zircons from sandstone of the upper part of the Sugo Formation (sample SG05). **A**, Cathodoluminescence images of zircons (white scale bar = 100 μm). **B**, Concordia diagram for all data. **C**, Probability density plot with a histogram for all $^{206}Pb/^{238}U$ dates from concordant grains. **D**, Probability density plot with a histogram for younger $^{206}Pb/^{238}U$ dates. **E**, The weighted mean date (YC2σ) for the youngest cluster. **F**, Radial plots and MLA estimates.

TABLE 8. U–Pb isotopes and dates of zircons from sample KD01. Abbreviations: C: concordant data, D: discordant data.

Spot No.	Th/U	$^{207}Pb/^{206}Pb$	Uncertainty 2SD	$^{207}Pb/^{235}U$	Uncertainty 2SD	$^{206}Pb/^{238}U$	Uncertainty 2SD	^{206}Pb-^{207}Pb (Ma)	Uncertainty 2SD	^{235}U-^{207}Pb (Ma)	Uncertainty 2SD	^{238}U-^{206}Pb (Ma)	Uncertainty 2SD	Memo
KD01-001	1.04	0.0523	0.0042	0.2464	0.0206	0.03414	0.00083			223.6	18.7	216.4	5.2	C
KD01-002	0.30	0.1156	0.0024	5.3265	0.1464	0.33426	0.00587	1889.0	39.9	1873.1	51.5	1859.0	32.7	C
KD01-003	1.42	0.0724	0.0060	0.2939	0.0258	0.02944	0.00080			261.6	22.9	187.0	5.1	D
KD01-004	0.28	0.1146	0.0024	4.7395	0.1292	0.29996	0.00525	1874.0	39.2	1774.2	48.4	1691.1	29.6	D
KD01-005	0.33	0.1134	0.0024	5.0616	0.1419	0.32382	0.00592	1855.0	39.4	1829.6	51.3	1808.4	33.0	C
KD01-006	0.35	0.0511	0.0019	0.2122	0.0088	0.03011	0.00056			195.4	8.1	191.2	3.5	C
KD01-007	0.30	0.0507	0.0025	0.1798	0.0100	0.02573	0.00062			167.9	9.4	163.8	3.9	C
KD01-008	0.65	0.0520	0.0063	0.2920	0.0365	0.04075	0.00140			260.1	32.5	257.4	8.9	C
KD01-009	0.25	0.1149	0.0026	5.4269	0.1711	0.34259	0.00761	1879.0	42.0	1889.1	59.6	1899.1	42.2	C
KD01-010	0.23	0.1918	0.0037	11.8197	0.3464	0.44692	0.00986	2758.0	53.3	2590.1	75.9	2381.5	52.5	D
KD01-011	0.87	0.0551	0.0040	0.2689	0.0207	0.03541	0.00095			241.8	18.6	224.3	6.0	C
KD01-012	1.19	0.0499	0.0043	0.2043	0.0185	0.02972	0.00085			188.8	17.1	188.8	5.4	C
KD01-013	0.74	0.1230	0.0032	4.6075	0.1543	0.27177	0.00575	2000.0	51.9	1750.6	58.6	1549.8	32.8	D
KD01-014	0.82	0.0550	0.0030	0.2235	0.0132	0.02947	0.00069			204.8	12.1	187.2	4.4	D
KD01-015	0.59	0.0527	0.0048	0.1996	0.0191	0.02747	0.00077			184.8	17.7	174.7	4.9	C
KD01-016	0.10	0.1168	0.0027	5.8797	0.1828	0.36516	0.00758	1908.0	44.2	1958.2	60.9	2006.6	41.7	D
KD01-017	0.53	0.0518	0.0024	0.2595	0.0135	0.03630	0.00081			234.3	12.2	229.9	5.2	C
KD01-018	0.80	0.0620	0.0040	0.2218	0.0152	0.02595	0.00065			203.4	14.0	165.1	4.1	D
KD01-019	0.78	0.2142	0.0049	17.2614	0.5332	0.58438	0.01226	2938.0	66.6	2949.4	91.1	2966.6	62.2	C
KD01-020	0.84	0.0518	0.0058	0.2381	0.0276	0.03334	0.00103			216.9	25.1	211.4	6.5	C
KD01-021	0.76	0.0540	0.0027	0.4738	0.0247	0.06370	0.00095			393.8	20.6	398.1	6.0	C
KD01-022	0.76	0.1516	0.0027	8.8365	0.1872	0.42262	0.00470	2365.0	42.6	2321.2	49.2	2272.3	25.3	D
KD01-023	0.30	0.1184	0.0028	5.5556	0.1495	0.34035	0.00414	1933.0	46.4	1909.2	51.4	1888.3	23.0	C
KD01-024	0.84	0.0504	0.0054	0.2388	0.0264	0.03436	0.00087			217.4	24.0	217.8	5.5	C
KD01-025	0.76	0.0633	0.0039	0.2901	0.0187	0.03323	0.00060			258.6	16.7	210.8	3.8	D
KD01-026	0.67	0.0539	0.0025	0.2622	0.0125	0.03530	0.00050			236.5	11.3	223.6	3.2	D
KD01-027	0.50	0.0584	0.0051	0.2823	0.0253	0.03504	0.00079			252.5	22.6	222.0	5.0	D
KD01-028	0.76	0.0549	0.0066	0.1941	0.0239	0.02565	0.00073			180.2	22.2	163.3	4.6	C
KD01-029	0.87	0.0541	0.0029	0.2102	0.0119	0.02819	0.00044			193.7	10.9	179.2	2.8	D
KD01-030	0.14	0.1193	0.0027	5.6367	0.1428	0.34258	0.00388	1947.0	44.1	1921.7	48.7	1899.1	21.5	C
KD01-031	0.39	0.0729	0.0055	0.3800	0.0300	0.03780	0.00082			327.1	25.8	239.2	5.2	D
KD01-032	0.40	0.0631	0.0027	0.6612	0.0296	0.07595	0.00107			515.3	23.0	471.9	6.6	D
KD01-033	0.34	0.0492	0.0052	0.3019	0.0330	0.04449	0.00110			267.9	29.3	280.6	6.9	C
KD01-034	0.78	0.0529	0.0027	0.2848	0.0150	0.03904	0.00058			254.5	13.4	246.9	3.7	C
KD01-035	0.43	0.0480	0.0044	0.1917	0.0189	0.02895	0.00096			178.1	17.5	184.0	6.1	C
KD01-036	0.73	0.0483	0.0031	0.1826	0.0128	0.02741	0.00082			170.3	12.0	174.3	5.2	C
KD01-037	1.11	0.0500	0.0031	0.2144	0.0148	0.03110	0.00093			197.2	13.6	197.4	5.9	C
KD01-038	0.42	0.0513	0.0037	0.2796	0.0220	0.03955	0.00123			250.4	19.7	250.1	7.8	C
KD01-039	0.75	0.0553	0.0047	0.2729	0.0247	0.03577	0.00118			245.0	22.2	226.5	7.4	C
KD01-040	0.29	0.1122	0.0018	4.6284	0.1460	0.29917	0.00810	1836.0	29.7	1754.3	55.3	1687.2	45.7	D
KD01-041	0.25	0.1223	0.0022	6.1388	0.2009	0.36397	0.00992	1991.0	36.1	1995.7	65.3	2001.0	54.5	C
KD01-042	0.53	0.1413	0.0024	8.1235	0.2597	0.41701	0.01135	2243.0	37.6	2244.8	71.8	2246.9	61.2	C
KD01-043	0.19	0.1361	0.0046	7.1467	0.3004	0.38074	0.00933	2179.0	74.4	2129.8	89.5	2079.7	51.0	C
KD01-044	0.29	0.1146	0.0045	5.4766	0.2545	0.34668	0.00875	1874.0	73.1	1896.9	88.1	1918.7	48.4	C
KD01-045	0.33	0.1130	0.0040	5.0527	0.2199	0.32435	0.00801	1848.0	66.2	1828.1	79.6	1810.9	44.7	C
KD01-046	0.31	0.1158	0.0042	5.3261	0.2346	0.33366	0.00828	1892.0	68.9	1873.0	82.5	1856.1	46.0	C
KD01-047	0.26	0.1173	0.0044	5.7171	0.2557	0.35345	0.00881	1916.0	71.1	1933.9	86.5	1951.0	48.7	C
KD01-048	0.49	0.1182	0.0042	5.3946	0.2319	0.33110	0.00816	1929.0	68.0	1883.9	81.0	1843.7	45.4	C
KD01-049	0.69	0.1466	0.0050	8.6849	0.3624	0.42961	0.01051	2307.0	78.0	2305.4	96.2	2304.0	56.4	C
KD01-050	0.35	0.1152	0.0040	4.7230	0.2012	0.29737	0.00730	1883.0	65.6	1771.3	75.5	1678.3	41.2	D
KD01-051	0.60	0.0776	0.0032	0.4699	0.0205	0.04390	0.00061			391.1	17.0	277.0	3.9	D
KD01-052	0.69	0.0503	0.0026	0.2031	0.0109	0.02926	0.00042			187.7	10.0	185.9	2.7	C
KD01-053	0.52	0.0539	0.0031	0.2251	0.0134	0.03030	0.00047			206.1	12.3	192.4	3.0	D
KD01-054	0.29	0.1247	0.0030	5.8165	0.1532	0.33834	0.00381	2025.0	48.2	1948.8	51.3	1878.7	21.2	D
KD01-055	0.14	0.1110	0.0028	4.9738	0.1360	0.32509	0.00369	1816.0	45.2	1814.8	49.6	1814.6	20.6	C
KD01-056	0.06	0.1161	0.0042	5.2901	0.2071	0.33046	0.00476	1898.0	69.1	1867.2	73.1	1840.6	26.5	C
KD01-057	0.45	0.0541	0.0072	0.3189	0.0432	0.04274	0.00128			281.0	38.1	269.8	8.1	C
KD01-058	0.23	0.1192	0.0026	4.7677	0.1169	0.29002	0.00312	1945.0	42.8	1779.2	43.6	1641.7	17.7	D
KD01-059	0.62	0.0532	0.0039	0.2949	0.0229	0.04018	0.00100			262.4	20.4	253.9	6.3	C
KD01-060	1.00	0.0582	0.0047	0.3389	0.0290	0.04226	0.00112			296.4	25.3	266.8	7.1	D
KD01-061	0.57	0.1251	0.0026	5.3930	0.1543	0.31278	0.00614	2030.0	42.3	1883.7	53.9	1754.4	34.4	D
KD01-062	0.22	0.1158	0.0029	5.5379	0.1795	0.34682	0.00700	1893.0	48.0	1906.4	61.8	1919.4	38.7	C
KD01-063	0.52	0.1258	0.0025	6.7635	0.1863	0.38987	0.00759	2041.0	39.8	2080.9	57.3	2122.2	41.3	D
KD01-064	0.43	0.1131	0.0028	5.2672	0.1675	0.33774	0.00677	1850.0	45.7	1863.5	59.3	1875.8	37.6	C
KD01-065	0.26	0.1136	0.0025	5.2701	0.1560	0.33632	0.00663	1859.0	41.0	1864.0	55.2	1868.9	36.9	C
KD01-066	0.88	0.0631	0.0066	0.2983	0.0326	0.03429	0.00104			265.1	28.9	217.3	6.6	D

continued on next page

Spot No.	Th/U	$^{207}Pb/^{206}Pb$	Uncertainty 2SD	$^{207}Pb/^{235}U$	Uncertainty 2SD	$^{206}Pb/^{238}U$	Uncertainty 2SD	^{206}Pb-^{207}Pb (Ma)	Uncertainty 2SD	^{235}U-^{207}Pb (Ma)	Uncertainty 2SD	^{238}U-^{206}Pb (Ma)	Uncertainty 2SD	Memo
KD01-067	0.82	0.0554	0.0026	0.2636	0.0134	0.03448	0.00067			237.5	12.0	218.5	4.3	D
KD01-068	0.24	0.1264	0.0028	6.5563	0.1834	0.37617	0.00652	2049.0	45.0	2053.4	57.4	2058.4	35.7	C
KD01-069	1.14	0.0536	0.0031	0.2052	0.0125	0.02777	0.00058			189.5	11.5	176.6	3.7	C
KD01-070	0.74	0.0540	0.0041	0.2259	0.0181	0.03035	0.00072			206.8	16.6	192.8	4.6	C
KD01-071	0.30	0.1224	0.0028	4.5308	0.1294	0.26840	0.00467	1992.0	45.1	1736.6	49.6	1532.7	26.7	D
KD01-072	1.04	0.0557	0.0051	0.2504	0.0237	0.03259	0.00086			226.9	21.5	206.7	5.5	C
KD01-073	0.26	0.1210	0.0031	5.0612	0.1801	0.30341	0.00738	1971.0	51.2	1829.6	65.1	1708.2	41.5	D
KD01-074	0.77	0.1110	0.0039	4.8953	0.2135	0.31977	0.00824	1817.0	63.9	1801.4	78.6	1788.6	46.1	C
KD01-075	0.73	0.1647	0.0046	11.9038	0.4488	0.52405	0.01322	2505.0	70.2	2596.8	97.9	2716.4	68.5	D
KD01-076	0.42	0.0527	0.0037	0.2372	0.0179	0.03266	0.00091			216.1	16.3	207.2	5.8	C
KD01-077	0.44	0.0497	0.0027	0.2738	0.0165	0.03996	0.00105			245.7	14.8	252.6	6.7	C
KD01-078	0.57	0.0491	0.0032	0.2810	0.0201	0.04150	0.00115			251.5	18.0	262.1	7.2	C
KD01-079	0.21	0.0528	0.0076	0.1828	0.0272	0.02510	0.00085			170.5	25.3	159.8	5.4	C
KD01-080	0.70	0.0578	0.0029	0.2341	0.0124	0.02936	0.00055			213.6	11.3	186.5	3.5	D
KD01-081	0.49	0.0490	0.0028	0.2407	0.0144	0.03563	0.00069			218.9	13.1	225.7	4.3	C
KD01-082	0.84	0.1206	0.0027	5.8555	0.1610	0.35200	0.00561	1966.0	44.0	1954.6	53.7	1944.1	31.0	C
KD01-083	0.51	0.0542	0.0034	0.2930	0.0196	0.03918	0.00081			260.9	17.4	247.7	5.1	C
KD01-084	0.87	0.1397	0.0031	8.1413	0.2247	0.42269	0.00680	2224.0	49.9	2246.8	62.0	2272.7	36.5	C
KD01-085	0.75	0.0516	0.0025	0.2110	0.0110	0.02964	0.00054			194.3	10.1	188.3	3.4	C
KD01-086	0.29	0.1143	0.0013	5.0320	0.0763	0.31918	0.00309	1870.0	21.8	1824.7	27.7	1785.7	17.3	D
KD01-087	0.65	0.0551	0.0031	0.2566	0.0149	0.03375	0.00052			231.9	13.4	213.9	3.3	D
KD01-088	1.26	0.0615	0.0050	0.2490	0.0210	0.02935	0.00063			225.7	19.0	186.5	4.0	D
KD01-089	1.51	0.0547	0.0052	0.2670	0.0260	0.03542	0.00081			240.3	23.4	224.4	5.1	C
KD01-090	0.37	0.1326	0.0016	7.0669	0.1093	0.38657	0.00379	2133.0	25.5	2119.8	32.8	2106.9	20.6	C
KD01-091	0.17	0.1163	0.0022	5.4648	0.1175	0.34085	0.00368	1900.0	35.3	1895.0	40.7	1890.7	20.4	C
KD01-092	0.35	0.1173	0.0020	5.4585	0.1110	0.33758	0.00357	1916.0	33.3	1894.0	38.5	1875.0	19.9	C
KD01-093	0.55	0.0669	0.0020	0.3073	0.0101	0.03332	0.00048			272.1	9.0	211.3	3.1	D
KD01-094	0.67	0.1480	0.0026	9.2454	0.2075	0.45315	0.00626	2323.0	41.1	2362.5	53.0	2409.2	33.3	D
KD01-095	0.40	0.0536	0.0047	0.4911	0.0448	0.06650	0.00154			405.6	37.0	415.0	9.6	C
KD01-096	1.07	0.1603	0.0022	9.6764	0.1863	0.43784	0.00580	2459.0	34.4	2404.4	46.3	2340.9	31.0	D
KD01-097	0.29	0.0652	0.0061	0.3551	0.0343	0.03949	0.00102			308.5	29.8	249.7	6.4	D
91500-01	0.34	0.0833	0.0045	1.9814	0.1151	0.17257	0.00391	1276.0	68.3	1109.2	64.4	1026.3	23.2	D
91500-02	0.35	0.0742	0.0042	1.8224	0.1137	0.17814	0.00472	1047.0	59.2	1053.5	65.7	1056.8	28.0	C
91500-03	0.35	0.0746	0.0043	1.8313	0.1155	0.17793	0.00443	1059.0	61.3	1056.7	66.6	1055.7	26.3	C
91500-04	0.34	0.0773	0.0043	1.8747	0.1095	0.17590	0.00314	1129.0	62.8	1072.2	62.6	1044.5	18.6	C
91500-05	0.35	0.0716	0.0042	1.7594	0.1077	0.17812	0.00319	976.0	57.1	1030.6	63.1	1056.7	18.9	C
91500-06	0.34	0.0749	0.0041	1.8514	0.1165	0.17918	0.00545	1067.0	58.7	1063.9	66.9	1062.5	32.3	C
91500-07	0.34	0.0719	0.0047	1.7811	0.1265	0.17955	0.00509	985.0	64.1	1038.6	73.8	1064.5	30.2	C
91500-08	0.34	0.0763	0.0045	1.8448	0.1128	0.17530	0.00312	1104.0	64.6	1061.5	64.9	1041.2	18.5	C
91500-09	0.35	0.0723	0.0042	1.7787	0.1123	0.17847	0.00430	995.0	58.1	1037.7	65.5	1058.6	25.5	C
91500-10	0.35	0.0770	0.0044	1.9165	0.1186	0.18049	0.00405	1122.0	64.7	1086.8	67.3	1069.7	24.0	C
91500-11	0.35	0.0733	0.0042	1.8674	0.1191	0.18489	0.00518	1021.0	58.5	1069.6	68.2	1093.6	30.6	C
91500-12	0.34	0.0744	0.0044	1.8047	0.1139	0.17585	0.00387	1054.0	62.4	1047.1	66.1	1044.3	23.0	C
91500-13	0.34	0.0713	0.0041	1.7217	0.1045	0.17506	0.00307	967.0	56.2	1016.6	61.7	1039.9	18.3	C
91500-14	0.34	0.0779	0.0042	1.9250	0.1113	0.17923	0.00346	1145.0	62.4	1089.8	63.0	1062.8	20.5	C
OD3-01	0.81	0.0598	0.0132	0.0411	0.0093	0.00498	0.00027			40.9	9.3	32.0	1.7	C
OD3-02	0.88	0.0426	0.0100	0.0291	0.0070	0.00495	0.00025			29.1	7.0	31.8	1.6	C
OD3-03	0.88	0.0558	0.0101	0.0379	0.0071	0.00492	0.00021			37.8	7.0	31.7	1.3	C
OD3-04	0.54	0.1199	0.0309	0.0836	0.0226	0.00506	0.00041			81.5	22.0	32.5	2.6	D
OD3-05	0.93	0.0465	0.0109	0.0326	0.0078	0.00509	0.00024			32.6	7.8	32.7	1.5	C
OD3-06	1.08	0.0531	0.0079	0.0407	0.0063	0.00557	0.00024			40.5	6.3	35.8	1.5	C
OD3-07	1.08	0.0483	0.0068	0.0334	0.0049	0.00501	0.00019			33.3	4.9	32.2	1.2	C
OD3-08	0.95	0.0533	0.0142	0.0358	0.0097	0.00487	0.00026			35.7	9.7	31.3	1.7	C
OD3-09	1.09	0.0478	0.0081	0.0305	0.0053	0.00464	0.00018			30.5	5.3	29.8	1.2	C
OD3-10	0.93	0.0484	0.0078	0.0323	0.0054	0.00484	0.00018			32.3	5.4	31.2	1.2	C
OD3-11	1.29	0.0510	0.0063	0.0332	0.0043	0.00472	0.00017			33.1	4.3	30.3	1.1	C
OD3-12	1.28	0.0510	0.0065	0.0344	0.0045	0.00489	0.00015			34.4	4.5	31.5	1.0	C
OD3-13	1.18	0.0510	0.0075	0.0335	0.0050	0.00476	0.00015			33.4	5.0	30.6	1.0	C
OD3-14	1.39	0.0471	0.0064	0.0324	0.0045	0.00498	0.00015			32.3	4.5	32.0	1.0	C

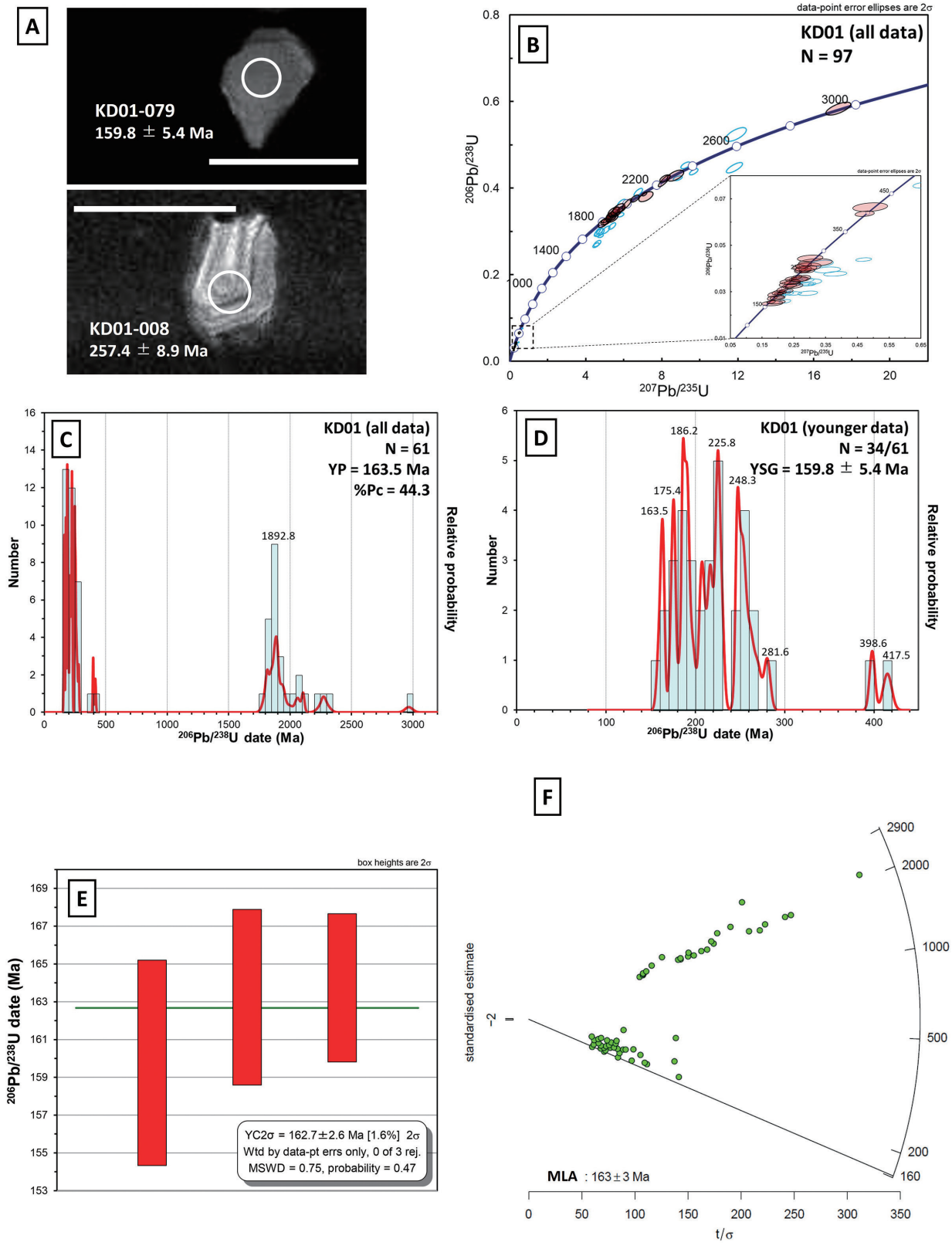

FIGURE 10. Analytical data of detrital zircons from sandstone of the Hinosan Mesozoic Formation (sample KD01). **A**, Cathodoluminescence images of zircons (white scale bar = 100 μm). **B**, Concordia diagram for all data. **C**, Probability density plot with a histogram for all $^{206}Pb/^{238}U$ dates from concordant grains. **D**, Probability density plot with a histogram for younger $^{206}Pb/^{238}U$ data set. **E**, The weighted mean dates (YC2σ) for the youngest cluster. **F**, Radial plots and MLA estimates.

In this study, MLA and YC2σ overlapped within 2σ uncertainty in three of the seven samples (DS08, SG05, KD01). In two samples (DS20 and KM01), MLA and YC2σ differed by 0.01 Myr and 0.92 Myr, respectively, but YC2σ lay closer to MLA than to YSG or YC1σ. In the remaining two samples (DS102-1 and UM01-2), MLA and YC2σ did not overlap within 2σ uncertainty, and the best estimates of MLA coincided with those of YSG. Although an MLA that converges on the YSG is not necessarily inappropriate—because the youngest grain may still represent a statistically meaningful population—such cases do not rule out the possibility that the YSG reflects Pb loss and is therefore younger than the true depositional age (e.g., Dickinson and Gehrels, 2009; Coutts et al., 2019; Vermeesch, 2021).

Consequently, in situations where the MLA collapses to the YSG, the potential for Pb-loss-related age underestimation cannot be excluded. To avoid this bias and obtain a more conservative and geologically reliable estimate of the maximum depositional age, we adopt YC2σ as the preferred MDD in this study.

The Doai Tuff Member of the Asuwa Formation of the Asuwa Group

The Asuwa Formation is divided into the Doai Tuff Member (lower member) and the Sarao Alternation Member (upper member). In this study, we conducted zircon U–Pb dating of the felsic weakly-welded lapilli tuff of the Doai Tuff Member (sample DS08). The concordant $^{206}Pb/^{238}U$ dates range from 66 to 84 Ma. The weighted mean $^{206}Pb/^{238}U$ date of the youngest cluster—the youngest 19 dates whose 2σ uncertainty bars for the $^{206}Pb/^{238}U$ date overlapped—was 71.8 ± 0.87 Ma (2σ; MSWD = 1.2, probability = 0.23) (Table 2; Fig. 4D). Since (1) sample DS08 was collected from an outcrop of weakly-welded lapilli tuff rich in essential materials, and (2) the zircon $^{206}Pb/^{238}U$ dates are tightly clustered within a narrow age range (< 20 Myr), we interpret the weighted mean date of the youngest cluster as a reliable estimate of the depositional age of sample DS08. Considering the occurrence of Maastrichtian pollen fossils from the overlying Sarao Alternation Member (Sazawa et al., 2020), we suggest that the Doai Tuff Member of the Asuwa Formation as a whole is a Maastrichtian (72.2 ± 0.2 Ma to 66.00 Ma; Cohen et al., 2024) geologic unit.

The Sarao Alternation Member of the Asuwa Formation of the Asuwa Group

The MDDs of sample DS102-1 and DS20 of the Sarao Alternation are 70.20 ± 0.74 Ma (2σ) and 69.05 ± 0.66 Ma, respectively, and both fall within the Maastrichtian. Moreover, most of the other MDD estimates from the Sarao Alternation Member also fall within or overlap the Maastrichtian interval.

Sample DS102-1: YSG = 65.3 ± 1.6 Ma, YC1σ = 68.6 ± 0.7 Ma (1σ), YC2σ = 70.20 ± 0.74 Ma (2σ), MLA = 65.3 ± 2.1 Ma

Sample DS20: YSG = 65.1 ± 6.3 Ma, YC1σ = 67.46 ± 0.47 Ma, YC2σ = 69.05 ± 0.66 Ma, MLA = 70.33 ± 0.61 Ma

The Asuwa Formation is a conformable sequence approximately 200 m thick, composed mainly of pyroclastic and epiclastic rocks. Sazawa et al. (2020) reported Maastrichtian pollen fossils from the mudstone of the lower part of the Sarao Alternation Member, and suggested that the felsic tuff in this member may be correlated with the Nohi Rhyolites. In contrast, the Asuwa Flora includes some species that extend into "the Tertiary" (Matsuo, 1962). In addition, among the 38 concordant datasets from sample DS102-1, one grain (DS102-1-86: 65.3 ± 1.6 Ma) yields a best estimate within the Paleogene. Similarly, among the 55 concordant datasets from sample DS20, one grain (DS20-28: 65.1 ± 6.3 Ma) also falls within the Paleogene. However, the $^{206}Pb/^{238}U$ date of DS102-1-86 is significantly younger than the other concordant dates from the same sample, such that it does not overlap with them within 2σ uncertainty. Considering these geochronological results and previous fossil evidence, we suggest that the Sarao Alternation Member was deposited during the Maastrichtian. Nevertheless, the possibility that deposition continued into the Paleogene cannot be entirely ruled out.

The Subara Formation

The MDD of sample KM01 of the Subara Formation is 68.32 ± 0.81 Ma (2σ) and falls within the age range of the Maastrichtian. Like the Sarao Alternation Member, the Subara Formation contains Late Cretaceous Asuwa Flora and tuff layers. The sampling sites for the Subara Formation and the Sarao Alternation Member are located less than 10 km apart, and the samples from both units share several characteristics. First, modal composition analysis shows that sandstone samples from both Formations (KM-01, DS102-1, DS20) are lithic wacke with feldspar contents less than 10%, whereas other samples contain feldspar more than 10% (Table1). Second, the detrital zircon age spectra of the Subara Formation and the Sarao Alternation Member (samples DS20 and DS102-1) are characterized by a high proportion (> 45%) of Late Cretaceous zircons (with few Paleogene grains), along with Jurassic, Triassic, Permian, Neoproterozoic, and Paleoproterozoic components. These similarities are illustrated in Fig. 11 and suggest a common provenance. Based on these shared characteristics, we consider the Subara Formation and the Sarao Alternation Member to be correlative and derived from a common provenance.

The Sugo Formation and the Hinosan Mesozoic Formaiton

Based on the youngest zircon date clusters (YC2σ), the MDDs are as follows: 174.7 ± 2.7 Ma (Early Jurassic Toarcian to Middle Jurassic Aalenian; Cohen et al., 2024) for the lower part of the Sugo Formation (sample UM01-2), 109.3 ± 1.7 Ma (Early Cretaceous Albian) for the upper part (sample SG05), and 162.7 ± 2.6 Ma (Middle Jurassic Callovian to Late Jurassic Oxfordian) for the Hinosan Mesozoic Formation (sample KD01). Among them, sample SG05 of the upper part of the Sugo Formation contains four zircon grains with Early Cretaceous ages (SG05-029, 047, 086, 101; Table 7, Fig. 9). In addition, Omura (1972) reported that the Sugo Formation is overlain by the Asuwa Group, which is interpreted in this study to belong to the Upper Cretaceous. Therefore, the depositional age of sample SG05 of the Sugo Formation is constrained to the Late Albian to Maastrichtian stages of the Cretaceous.

The depositional age of sample UM01-2 from the lower Sugo Formation is constrained to be younger than its MDD of 174.7

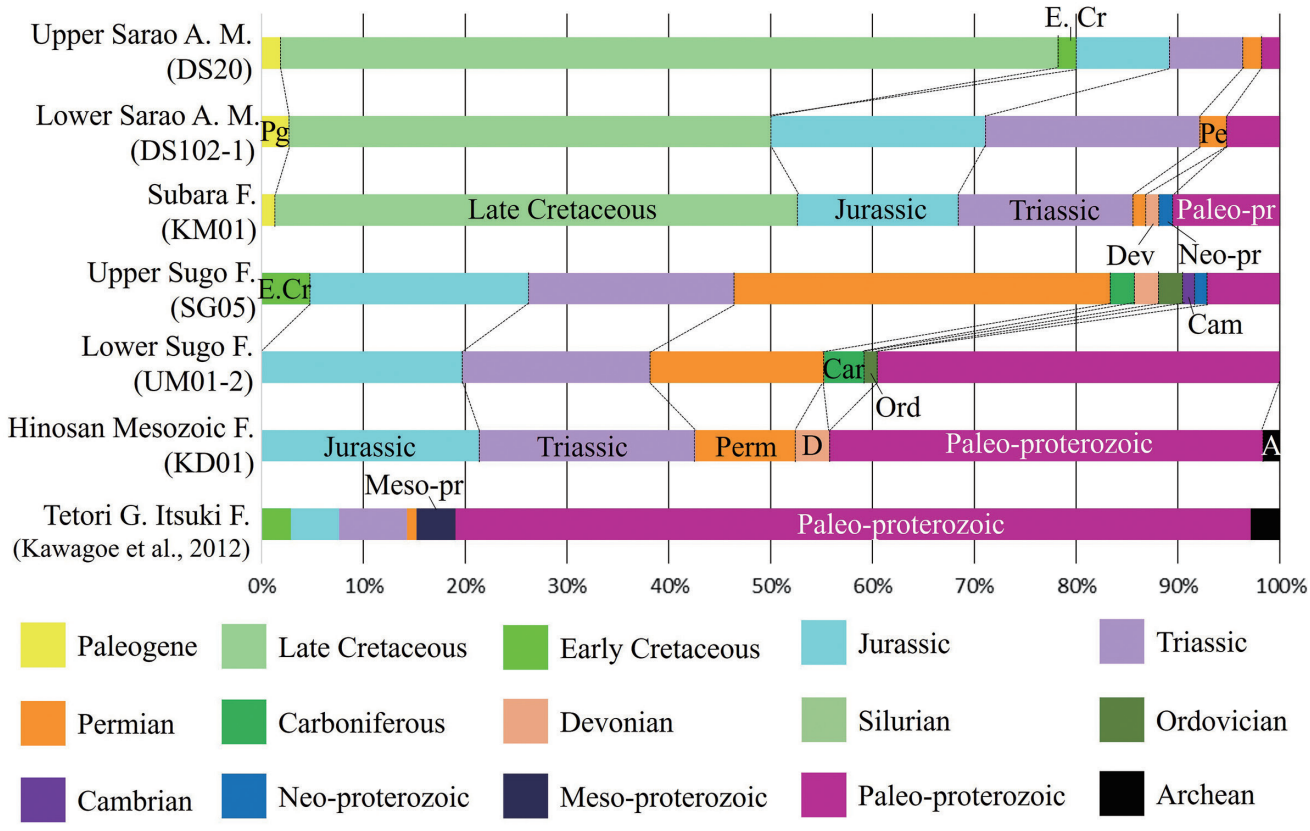

FIGURE 11. Band graphs showing the age composition of detrital zircons from sandstone and siltstone samples. The data of the Itsuki Formation were referred from Kawagoe et al., (2012). G: group, F: formation, A. M.: alternation member.

± 2.7 Ma and older than the deposition of the Asuwa Group. Given that the boundary between the Early and Middle Jurassic is 174.7 ± 0.8 Ma (Cohen et al., 2024), the depositional age of UM01-2 is likely to fall within the Middle Jurassic Aalenian to Late Cretaceous Maastrichtian interval. The depositional age of sample KD01 from the Hinosan Mesozoic Formation is constrained to be younger than its MDD of 162.7 ± 2.6 Ma and older than the deposition of the overlying Nohi Rhyolites (*s.l.*). If the overlying Nohi Rhyolites (*s.l.*) are equivalent to the Nohi Rhyolites (*s.s.*), which are dated to 72–70 Ma, then the depositional age of KD01 is likely to fall within the Middle Jurassic Callovian to Late Cretaceous Maastrichtian interval. The depositional age range of the Tetori Group, which spans the Late Jurassic to Early Cretaceous, is included within the broader age ranges inferred for samples UM01-2 and KD01.

Stratigraphic affiliation of the Sugo Formation and the Hinosan Mesozoic Formation

Comparison of the Sugo and Hinosan Mesozoic Formations with the Asuwa Formation

Since the Hinosan Mesozoic Formation shares similar sandstone lithology and detrital zircon age spectra with the Sugo Formation, we treat it as part of the Sugo Formation in the following discussion. Although some researchers attributed the Sugo Formation to a part of the Asuwa Group or the Asuwa Formation (e.g., Wakita et al., 1992), we identify four key differences that distinguish the Sugo Formation from the Asuwa Formation.

(1) The Sugo Formation is reported to be conformably overlain by the Asuwa Group (Omura, 1972) and lacks evidence for Late Cretaceous volcanic activity. While the Asuwa Formation consists mainly of Late Cretaceous pyroclastic and volcaniclastic rocks, such lithologies are absent in the Sugo Formation, whose youngest detrital zircon age is Early Cretaceous. Moreover, the Sarao Alternation Member within the Asuwa Formation frequently contains tuff and lapilli tuff, whereas tuff layers are rare in the Sugo Formation. If the Sugo Formation were equivalent to the Asuwa Formation, the absence of Late Cretaceous zircons and the scarcity of volcanic products would be difficult to explain. Therefore, based on the absence of Late Cretaceous zircons and tuff layers equivalent to the Doai Tuff Member, we infer that the Sugo Formation is older than the Asuwa Formation.

(2) The Sugo Formation contains few Cretaceous zircons, which are likely close to the age of deposition, but includes numerous Jurassic to Permian zircons, as well as some Carboniferous, Devonian, Silurian, Ordovician, Cambrian,

Paleoproterozoic zircons. Notably, the abundance of Permian zircons is a characteristic feature of the Sugo Formation (Fig.11).

(3) Sandstones of the Sugo Formation are richer in feldspar (11–26%) compared to those from the Sarao Alternation (3–8%) in whole rock volume ratio (Table 1), indicating a significant difference in sediment provenance.

(4) Megafossils are rarely found in the Sugo Formation, and there are no reports of the Asuwa Flora being present.

Taken together, these differences indicate that the Sugo Formation represents a distinct stratigraphic unit and should be separated from the Asuwa Formation.

Comparison of the Sugo Formation with the Tetori and Sasayama Group

Some earlier studies have proposed that the Sugo Formation is part of the Tetori Series (Tetori Group) (Suzuki, 1943; Tsukano, 1969), and the depositional age of the Tetori Group, as constrained in this study, falls within the age range of sample UM01-2 from the lower Sugo Formation. Additionally, neither the Sugo Formation nor the Hinosan Mesozoic Formation contains Late Cretaceous plant fossils, a feature shared with the Tetori Group. In this section, we examine the relationship between the Sugo Formation and the Tetori Group from perspectives other than depositional age.

The Tetori Group (*sensu lato*; *sensu* Sano, 2015) is distributed across Fukui, Ishikawa, Gifu, Toyama, and Niigata prefectures in central Japan, and consists mostly of Late Jurassic to Early Cretaceous marine to terrestrial clastic rocks. In Fukui Prefecture, Kawagoe et al. (2012) reported U–Pb ages of detrital zircon from sandstones, and Nagata et al. (2018) determined the minimum depositional age of the Tetori Group.

First, we compare the detrital zircon age spectra of the Sugo Formation and the Tetori Group (Fig.11). Both units share the feature of containing numerous Paleoproterozoic zircons, particularly in the Lower Cretaceous strata of the Tetori Group in the Itoshiro area in Fukui Prefecture (Kawagoe et al., 2012). Furthermore, the scarcity of Late Jurassic to Early Cretaceous zircons is a common feature of the Sugo Formation and the Tetori Group; the period was referred to as the magmatic hiatus in Korea (158–110 Ma: Sagong et al., 2005) or magmatic gap (158–138 Ma: Lee et al., 2010; 162–110 Ma: Choi et al., 2012). However, the MDD of the upper part of the Sugo Formation is approximately 109 Ma, which is nearly the same age as the Hayashidani Andesite that covered the Tetori Group in the Itoshiro area, northwestern Gifu Prefecture (Nagata et al., 2018). This suggests that the Sugo Formation is, at least in part, younger than the Tetori Group. Additionally, Permian zircons, which are abundant in the Sugo Formation, are rarely found in the Early Cretaceous strata of the Tetori Group (Kawagoe et al., 2012). The Sugo Formation also contains Neoproterozoic and Mesoproterozoic zircons, which are absent in the Tetori Group (Kawagoe et al., 2012). These differences in detrital zircon age spectra clearly distinguish the Sugo Formation from the Tetori Group. Second, we compare the modal composition of sandstones. The sandstone samples from the Sugo Formation are mainly lithic arenite or wacke, rich in rock fragments (17–28% : Table 1). In contrast, a representative sandstone sample from the Tetori Group described by Kawagoe et al. (2012) is feldspathic arenite, poor in rock fragments (3%). These compositional contrasts further support the stratigraphic distinction between the Sugo Formation and the Tetori Group. In summary, the Sugo Formation is, at least partly, younger than the Tetori Group based on zircon dates, and differs significantly in clast composition.

When compared with strata outside Fukui Prefecture, the Sugo Formation may be more closely related in depositional age to other Cretaceous strata such as the Sasayama Group in Hyogo Prefecture (Kusuhashi et al., 2013) or the Shiritakayama and Uchiyama Formations in Toyama Prefecture (Takeuchi et al., 2015). From a tuff sample in the lower part of the lower Sasayama Group (Ohyamashimo Formation), Kusuhashi et al. (2013) reported zircon U–Pb SHRIMP age of 112.1 ± 0.4 Ma (95% confidence interval). In addition, an andesite sample in the lower part of the upper Sasayama Group (Sawada Formation) yields zircon U–Pb SHRIMP age of 106.4 ± 0.4 Ma (95% confidence interval), indicating that the lower Sasayama Group between the two sample horizons was deposited between approximately 112 and 107 Ma, corresponding to the Early Albian stage of the Cretaceous. In addition, welded tuffs from the overlying Arima Group overlying the Sasayama Group yield zircon U–Pb ages of 82.1 ± 0.5 Ma, 82.5 ± 0.6 Ma, and 81.5 ± 0.7 Ma (Sato, 2017), indicating that the Sasayama Group above the andesite horizon (106.4 ± 0.4 Ma) was deposited between approximately 107 and 83 Ma, corresponding to the Late Albian to early Campanian stages of the Cretaceous.

In comparison, sample SG05 from the upper part of the Sugo Formation (YC2σ = 109.3 ± 1.7 Ma) is interpreted to have been deposited between the Late Albian and Maastrichtian stages. Therefore, the Sugo Formation may be contemporaneous with the upper Sasayama Group. However, there are lithological differences: the Sasayama Group contains more felsic to intermediate volcanic materials. To clarify the stratigraphic affinity of the Sugo Formation, further detailed geologic investigations are needed.

Regarding the Shiritakayama and Uchiyama Formations in Toyama Prefecture, their youngest single grain ages (YSG) are around 110 Ma (Takeuchi et al., 2015), and they are overlain by the Oyashirazu Formation, which includes a welded volcanic breccia tuff dated to 109.2 ± 0.8 Ma (2σ). Thus, their depositional ages are close to the MDD of the upper Sugo Formation in this study (sample SG05). However, while the Shiritakayama and Uchiyama Formations are rich in Precambrian zircons, the upper Sugo Formation contains relatively few Precambrian zircons and is dominated by zircons from the Paleozoic. This suggests that, although similar in age, these Formations were derived from different source regions.

Regional volcanism and its implications

In the northern part of central Japan, Early Cretaceous andesitic rocks such as the Hayashidani Andesite (109.3 ± 1.7

Ma; Nagata et al., 2018) and the Oyashirazu Andesite (109.2 ± 0.8 Ma; Takeuchi et al., 2017) are distributed across the Hida and Hida Gaien Belts, where they overlie the Tetori Group. However, in this study, only three zircon grains with dates overlapping these andesites within 2σ uncertainty were identified, all from sample SG05 in the upper Sugo Formation: SG05-101 (106.7 ± 2.7 Ma), SG05-029 (109.1 ± 4.0 Ma), and SG05-086 (112.1 ± 2.8 Ma). This scarcity of zircons matching the ages of the Hayashidani and Oyashirazu andesites suggests two possibilities: either andesitic rocks are generally poor sources of sand-sized detrital zircons, or the strata investigated in this study, which mainly overlie the Higashimata Formation of the Ultra-Tamba Belt, were deposited in areas that received little detrital input from the Hayashidani Andesite.

Felsic pyroclastic and volcanic rocks dated to approximately 70 Ma are widely distributed in central Japan (e.g., Hoshi et al., 2016; Kaneko et al., 2019). In Fukui Prefecture, the Nohi Rhyolite is sporadically distributed in the southern Reihoku district and extensively in the eastern part. Hoshi et al. (2016) proposed that the Nohi Rhyolite represents one of the largest caldera-forming volcanic complexes on Earth, formed rapidly at approximately 70 Ma. We compare zircon U–Pb dates from the Futomiyama Group (Toyama Prefecture), the Oamamiyama Group (northern Gifu Prefecture), and the Doai Tuff Member (this study). All values represent the weighted mean $^{206}Pb/^{238}U$ dates (±2σ) of the youngest cluster (YC):

- Futomiyama Group (Kaneko et al., 2019): Sample FTT02 = 70.2 ± 0.7 Ma,
  sample FUT01 = 70.0 ± 0.5 Ma, sample FUT02 = 70.6 ± 1.1 Ma
- Oamamiyama Group (Nagata et al., 2025): Sample OM02 = 71.47 ± 0.63 Ma
- Doai Tuff Member (this study): Sample DS08 = 71.8 ± 0.87 Ma

The overlapping 2σ uncertainty ranges suggest that these felsic pyroclastic rocks were produced by coeval volcanic activity around 70 Ma, and that the origin of the Doai Tuff Member may be related to the eruption of the Nohi Rhyolites.

The Sarao Alternation Member conformably covers the Doai Tuff Member and contains tuff layers in the upper part. Furthermore, the sandstone samples of the Sarao Alternation Member, taken from both the lower (DS102-1) and upper (DS20) parts, are rich in matrix and rock fragments, particularly volcanic fragments. In addition, the two samples contain abundant (> 45%) Late Cretaceous zircons with some Jurassic, Triassic, Permian, and Paleoproterozoic ones. These similarities suggest that the detrital zircon sources for samples DS102-1 and DS20 were likely the same. The elevated proportion of Maastrichtian zircons, combined with the presence of tuff layers in the upper Sarao Alternation Member, may reflect intensified felsic volcanic activity during its deposition.

CONCLUSIONS

We conducted zircon U–Pb dating on the Upper Cretaceous Asuwa and Subara Formations, and on the previously age-unknown Sugo and Hinosan Mesozoic Formations in Fukui Prefecture, central Japan. We summarized the results of this study and their implications as follows.

(1) A sample of lapilli tuff (DS08) from the Doai Tuff Member, which constitutes the lower part of the Asuwa Formation, yielded a probable formation age of 71.8 ± 0.87 Ma. Two sandstone samples (DS102-1 and DS20) from the Sarao Alternation Member in the upper Asuwa Formation yielded maximum depositional dates (MDDs) of 70.20 ± 0.74 Ma and 69.05 ± 0.66 Ma, respectively. And, a sandstone sample (KM01) from the Subara Formation of the Asuwa Group, yielded an MDD of 68.32 ± 0.81 Ma. These formations correspond to the Maastrichtian Stage of the Upper Cretaceous.

(2) Two sandstone samples (UM01-2 and SG05) from the Sugo Formation yielded MDDs of 174.7 ± 2.7 Ma and 109.3 ± 1.7 Ma, respectively. A sample (KD01) from the undated Hinosan Mesozoic Formation yielded an MDD of 162.7 ± 2.6 Ma. These samples are characteristically rich in rock fragments. Based on the results of zircon ages and lithologic features, the Sugo Formation is a different unit from the Asuwa Group and the Tetori Group.

ACKNOWLEDGMENTS

We are grateful to Associate Professor Takuya Imai of the Fukui Prefectural University (Fukui Prefectural Dinosaur Museum) for his assistance with zircon CL imaging. We also thank Designated Professor Koshi Yamamoto of the Nagoya University Museum for his support during U–Pb age analyses. We sincerely appreciate the constructive comments provided by Dr. Atsushi Yabe of the National Museum of Nature and Science and Dr. Mitsuhiro Nagata of the Department of Earth and Environmental Sciences, College of Humanities and Sciences, Nihon University. This study was partially supported by the Japan–Russia Cooperative Research Program between JSPS (Grant No. 120214804) and RFBR (Grant No. 21-55-50001).

REFERENCES

Choi, T. J., Y. I. Lee and Y. Orihashi. 2012. Mesozoic detrital zircon U–Pb ages of modern river sediments in Korea: implications for migration of arc magmatism in the Mesozoic East Asian continental margin. Terra Nova 24: 156–165.

Cohen, K. M., D. A. T. Harper, D.A.T., and P. L. Gibbard. 2024. ICS International Chronostratigraphic Chart 2024/12. International Commission on Stratigraphy, IUGS. www.stratigraphy.org (visited: 2025/06/30).

Coutts, D. S., W. A. Matthews and S. M. Hubbard. 2019. Assessment of widely used methods to derive depositional ages from detrital zircon populations. Geoscience Frontiers 10: 1421–1435.

Dickinson, W. R., and G. E. Gehrels. 2009. Use of U–Pb ages of detrital zircons to infer maximum depositional ages of strata: A test against a Colorado Plateau Mesozoic database. Earth

and Planetary Science Letters 288: 115–125.

Hattori, I. 2012. Geology of a Few Areas in Fukui PrefectureII:Southeastern Part of Echizen City and Southwestern Part of Ikeda Cho, and Miyama Area of Fukui City. The Memoirs of the Research and Education Center for Regional Environment, University of Fukui 19: 1–12.

Hoshi, H., H. Iwano, T. Danhara and K. Sako. 2016. R5-O-7 U-Pb evidence for rapid formation of the Nohi Rhyolite at about 70 Ma. The 123rd Annual Meeting of the Geological Society of Japan, Abstract: 156.

Iwano, H., Y. Orihashi, T. Hirata, M. Ogasawara, T. Danhara, K. Horie, N. Hasebe, S. Sueoka, A. Tamura, Y. Hayasaka, A. Katsube, H. Ito, K. Tani, J.-I. Kimura, Q. Chang, Y. Kouchi, Y. Haruta and K. Yamamoto. 2013. An inter-laboratory evaluation of OD-3 zircon for use as a secondary U–Pb dating standard. Island Arc 22: 382–394.

Kaneko, K., M. Nagata, Y. Kouchi, K. Yamamoto and S. Otoh. 2019. Zircon U–Pb ages of the Futomiyama Group in Toyama Prefecture, central Japan. Journal of the Geological Society of Japan 125: 781–792.*

Kano, K., H. Yamamoto and T. Nakagawa. 2007. Geology of the Fukui district. With geological sheet map 1:50,000, Fukui, Geological Survey of Japan, AIST, 68 pp.**

Kawagoe, Y., S. Sano, Y. Orihashi, H. Obara, Y. Kouchi and S. Otoh. 2012. New detrital zircon age data from the Tetori Group in the Mana and Itoshiro areas of Fukui Prefecture, Central Japan. Memoir of the Fukui Prefectural Dinosaur Museum 11: 1–18.

Kawai, M. 1956. On the Late Mesozoic movement in the western part of Hida Plateau, Part 1. Journal of the Geological Society of Japan 62: 559–573. *

Kawai, M. 1964. Explanatory text of the geological map of Japan, scale 1 : 50,000, Neo. Geological Survey of Japan, 78pp.

Kobayashi, M. 1954. Geology of of the environs of Nishitani-mura, Ono-gun, Fukui Prefecture. Studies from the Geological and Mineralogical Institute, Tokyo University of Education 3: 35–42.*

Kouchi, Y., Y. Orihashi, H. Obara, T. Fujimoto, Y. Haruta and K. Yamamoto. 2015. Zircon U–Pb dating by 213 nm Nd: YAG laser ablation inductively coupled plasma mass spectrometry: Optimization of the analytical condition to use NIST SRM 610 for Pb/U fractionation correction. Chikyukagaku 49: 19–35.*

Kusuhashi, N., Y. Tsutsumi, H. Saegusa, K. Horie, T. Ikeda, K. Yokoyama and K. Shiraishi. 2013. A new Early Cretaceous eutherian mammal from the Sasayama Group, Hyogo, Japan. Proceedings of the Royal Society, Biological Sciences 280: 20130142.

Lee, Y. I., T. Choi, H. S. Lim and Y. Orihashi. 2010. Detrital zircon geochronology of the Cretaceous Sindong Group, Southeast Korea: Implications for depositional age and Early Cretaceous igneous activity. Island Arc 19: 647–658.

Ludwig, K. R. 2012. User's Manual for Isoplot 3.75–4.15: Geochronological Toolkit for Microsoft Excel. Berkeley Geochronology Center Special Publication 5, 77pp.

Maeda, S. 1961. On the geological history of the Mesozoic Tetori Group in Japan. Journal of the College of Arts and Sciences, Chiba University 3: 369–426.

Matsuo, H. 1954. Proposal of the Upper Cretaceous Asuwa Series in Hokuriku Region (abstract). Journal of the Geological Society of Japan 60: 711.**

Matsuo, H. 1962. A study on the Asuwa Flora (Late Cretaceous age) in the Hokuriku District, Central Japan. The Science Reports of the Kanazawa University 8: 177–250.

Matsuo, H. 1970. On the Ōmichidani Flora (Upper Cretaceous), inner side of Centarl Japan. Transactions and proceedings of the Paleontological Society of Japan. New series 80: 371–389.

Matsuo, H., and S. Kida. 1953. Recovery of Asuwa Flora along the upper stream of the Asuwagawa River, Fukui Prefecture, and on Angiosperm series (abstract). Journal of the Geological Society of Japan 59: 324.**

Moreno, T., S. Wallis, T. Kojima and W. Gibbons (eds.). 2016. The Geology of Japan. The Geological Society, London. 522pp.

Nagata, M., Y. Hayashi, T. Sakashita, Y. Kawagoe, Y. Kouchi, S. Hirasawa, M. Fujita, K. Yamamoto and S. Otoh. 2018. When did the deposition of the Tetori Group terminate? Memoir of the Fukui Prefectural Dinosaur Museum 17: 9–26.

Nagata, M., T. Sakashita, N. Yamada and S. Otoh. 2025. Geochronology of the Oamamiyama Group in Gifu Prefecture. Proceedings of the Institute of Natural Sciences, Nihon University 60: 113–130.*

Nakae, S. 2012. Geology of the Permian Higashimata Complex in the Nanjo Mountains, Fukui Prefecture, Southwest Japan. Bulletin of the Geological Survey of Japan. 63: 269–281.

Nakajima, T., Y. Sawada, T. Nakagawa, A. Hayashi and T. Itaya. 1990. Paleomagnetic results and K-Ar dating on Miocene rocks in the northern part of Fukui Prefecture, Central Japan: with reference to the rotation of Southwest Japan. Journal of Mineralogy, Petrology and Economic Geology 85: 45–59.*

Okada, H. 1968. Classification and nomenclature of sandstones. Journal of the Geological Society of Japan 74: 371–384.*

Okada, H. 1971. Again on classification and nomenclature of sandstones. Journal of the Geological Society of Japan 77: 395–396.**

Omura, K. 1972. The Late Cretaceous deposits of the upper reaches of the Asuwa-gawa and the northern foot of Mt. Hino-san, Fukui Prefecture, central Japan. In Iwai Jun-Ichi Kyoju Taikan Kinen Jigyokai, ed., Professor Jun-Ichi Iwai Memorial Volume, 423–431.*

Sagong, H., S. T. Kwon and J. H. Ree. 2005. Mesozoic episodic magmatism in South Korea and its tectonic implication. Tectonics 24: TC5002 (doi: 10.1029/2004TC001720)

Sakai, Y., S. Sekido and A. Matsuoka. 2018. Stratigraphy of the Lower Cretaceous Tetori Group and stratigraphic implication of plant assemblages in the border area between Ishikawa and Fukui Prefectures, central Japan. Journal of the Geological Society of Japan 124: 171–189.*

Sano, S. 2015. New view of the stratigraphy of the Tetori Group

in central Japan. Memoir of the Fukui Prefectural Dinosaur Museum 14: 25–61.

Sato, D. 2017. Geology of Cretaceous caldera volcanoes and episodic flare-up of felsic magma in Banshu-Ako district, southwest Japan. A dissertation for the degree of Doctor of Science, Kyushu University, 159 p., https://hdl.handle.net/2324/1807139.

Sazawa, T., J. Legrand, A. Yabe, S. Agematsu and K. Sashida. 2020. Geologic age of the Upper Cretaceous Asuwa Formation of Ikeda Town, eastern part of Fukui Prefecture, Japan: A palynostratigraphic approach. Journal of the Geological Society of Japan 126: 215–221.*

Schwartz, T. M., A. K. Souders, J.-E. Lundstern, A. K. Gilmer and R. A. Thompson. 2022. Revised age and regional correlations of Cenozoic strata on Bat Mountain, Death Valley region, California, USA, from zircon U-Pb geochronology of sandstones and ash-fall tuffs. Geosphere 19: 235–257.

Stacey, J. S., and J. D. Kramers. 1975. Approximation of terrestrial lead isotope evolution by a two-stage model. Earth and Planetary Science Letters 26: 207–221.

Suzuki, K. 1943. Geology of the middle reaches of the Asuwagawa River, Fukui Prefecture. Miscellaneous Reports of Research Institute for Natural Resources 3: 75–84.

Takeuchi, M., R. Furukawa. M. H. Nagamori and T. Oikawa. 2017. Geological Map of the Tomari District with Geological Sheet Map at 1:50,000. Geological Survey of Japan, AIST, 121pp.**

Takeuchi, M., M. Ohkawa, K. Kawahara, S. Tomita, H. Yokota, T. Tokiwa and R. Furukawa. 2015. Redefinition of the Cretaceous terrigenous strata in the northeastern Toyama Prefecture based on U–Pb ages of zircon. Journal of the Geological Society of Japan 121: 1–17.*

Tanase, A., T. Sonehara and S. Harayama. 2007. Process for the formation of Horado Cauldron, Okumino Acid Igneous Complex and its bimodal volcanism —Characteristics of late Late Cretaceous to Paleogene igneous activities in central Japan. The 114th Annual Meeting of the Geological Society of Japan, Abstract: 429.

Tsukada, K., S. Yamakita and T. Koike. 1997. Late Triassic conodonts from the Hongo area in the Hida marginal belt. Journal of the Geological Society of Japan 103: 1175–1178.*

Tsukano, Z. 1969. Explanatory text of the geological map of Fukui Prefecture. Fukui, 117 pp.*

Tsukano, Z., and S. Miura. 1959. On the Upper Cretaceous Formation and related some problems in the western part of the Hida Plateau, Japan. Memoirs of the Faculty of Liberal Arts, Fukui University, Series II, Natural Sciences 9: 123–137.

Umeda, M., H. Taga and I. Hattori. 1996. Discovery and its geologic significance of Permian radiolarians from clastic rocks at the northern margin of the Nanjo Massif, Fukui Prefecture, Central Japan. Journal of the Geological Society of Japan, 102: 635–638.*

Vermeesch, P. 2018. IsoplotR: A free and open toolbox for geochronology. Geoscience Frontiers 9: 1479–1493.

Vermeesch, P. 2021. Maximum depositional age estimation revisited. Geoscience Frontiers 12: 843–850.

Wakita, K., S. Harayama, K. Kano, K. Mimura, T. Sakamoto, T. Hiroshima, M. Komazawa and K. Nakajima. 1992. Geological Map, 1:200,000, Gifu. Geological Survey of Japan.*

Wiedenbeck, M., P. Allé, F. Corfu, W. L. Griffin, M. Meier, F. Oberli, A. von Quadt, J. C. Roddick and W. Spiegel. 1995. Three natural zircon standards for U-Th-Pb, Lu-Hf, trace element and REE analyses. Geostandards Newsletter 19: 1–23.

Yamada, T., and S. Sano. 2018. Designation of the type section of the Tetori Group and redefinition of the Kuzuryu Group, distributed in Central Japan. Memoir of the Fukui Prefectural Dinosaur Museum 17: 89–94.

Yamaoka, K., and S. R. Wallis. 2023. Clockwise rotation of SW Japan and timing of Izanagi–Pacific ridge subduction revealed by arc migration. Progress in Earth and Planetary Science 10: 62.

* in Japanese with English abstract

** in Japanese

＜　地名・地層名　＞

Akiyoshi Belt …… 秋吉帯
Arima Group …… 有馬層群
Asuwa Formation …… 足羽層
Asuwa Group …… 足羽層群
Asuwa River …… 足羽川
Doaisarao area…… 土合皿尾地域
Doai Tuff Member …… 土合凝灰岩部層
Echizen City …… 越前市
Fukui Prefecture …… 福井県
Futomiyama Group…… 太美山層群
Gifu Prefecture …… 岐阜県
Hayashidani Andesite …… 林谷安山岩
Heikedake Formation …… 平家岳層
Hida Belt…… 飛騨帯
Hida Gaien Belt …… 飛騨外縁帯
Higashimata Formation …… 東俣層
Hino-San Formation …… 日野山層
Hinosan Mesozoic Formation… 日野山中生層
Ikeda Town …… 池田町
Iritani Alternation …… 入谷互層
Ishikawa Prefecture…… 石川県
Ito-o Formation …… 糸生層
Kayatani …… 萱谷
Kayatani Formation …… 萱谷層
Kumokawa Area …… 雲川地域
Maizuru Belt …… 舞鶴帯
Mino Belt …… 美濃帯
Mobara Formation …… 茂原層
Mt. Hinosan…… 日野山
Nakahirabuki …… 中平吹
Nohi Rhyolites …… 濃飛流紋岩類
Nishikakuma …… 西角間
Oamamiyama Group …… 大雨見山層群
Okumino Acid Igneous Complex
…… 奥美濃酸性岩類
Ohyamashimo Formation …… 大山下層
Ono City …… 大野市
Oyashirazu Formation…… 親不知層
Oyashirazu Andesite …… 親不知安山岩
Renge Belt …… 蓮華帯
Reihoku …… 嶺北
Saruzuka Conglomerate …… 猿塚礫岩
Sasayama Group …… 篠山層群
Sadakata …… 定方
Sarao Alternation Member …… 皿尾互層部層
Shiritakayama Formation …… 尻高山層
Sugo area…… 菅生地域
Sugo Formation …… 菅生層
Subara Formation …… 巣原層
Tetori Group …… 手取層群
Tomari area …… 泊地域
Toyama Prefecture …… 富山県
Tsuji…… 辻
Ubagatake Formation …… 姥ヶ岳層
Uchiyama Formation …… 内山層
Ultra-Tamba Belt…… 超丹波帯
Uomi …… 魚見